Crystal Structure of Mixed Hydrates and Cage Occupancy of Guest Species

YUUKI MATSUMOTO

MARCH 2014

Crystal Structure of Mixed Hydrates and Cage Occupancy of Guest Species

A dissertation submitted to

THE GRADUATE SCHOOL OF ENGINEERING SCIENCE

OSAKA UNIVERSITY

in partial fulfillment of the requirements for the degree of

DOCTOR OF PHILOSOPHY IN ENGINEERING

BY

YUUKI MATSUMOTO

MARCH 2014

Abstract

Clathrate hydrate is suggested to be utilized as gas storage and transportation media and refrigerants because of its dense storage capacity and high dissociation enthalpy, respectively. Generally, clathrate hydrate is thermodynamically stable at high pressures and/or low temperatures, and its stability largely depends on guest species. One of the most efficient ways to moderate the thermodynamic stability conditions of clathrate hydrate is addition of relatively large guest species called thermodynamic promoters to form a mixed hydrate of a target gas with a thermodynamic promoter. Compared to simple hydrate systems, the phase behavior and the cage occupancies of guest species in mixed hydrate systems are much more complicated. In this thesis, thermodynamic promoters were explored toward moderating the thermodynamic stability conditions of a simple hydrate composed of a target gas such as hydrogen, methane, or carbon dioxide. Thermodynamic stability conditions and crystal structure of mixed hydrates were also investigated by means of phase equilibrium measurement and powder X-ray diffractometry. Simultaneously, cage occupancies of guest species in mixed hydrates were clarified by means of Raman spectroscopy. Mixed hydrate systems investigated in the present study were classified according to the cage occupancy; competitive cage occupancy (Competitive-type, **Chapter II**) and compartmental cage occupancy (Compartmental-type, **Chapter III**).

Competitive-type mixed hydrates, where two or more kinds of guest species competitively occupy a certain cage, are summarized in **Chapter II**. Isothermal phase equilibrium relations (pressure-composition) of mixed hydrate systems exhibited some interesting phase behavior such as structural phase transition and azeotropic-like behavior. According to structural phase transition, mixed hydrates construct the most thermodynamically stable crystal structure depending on the cage occupancy of guest species at a given pressure, temperature, and composition. Azeotropic-like behavior indicates that, at a local pressure minimum, guest species compartmentally occupy the appropriate cages in spite of competitive-type mixed hydrate.

Compartmental-type mixed hydrates, where small and large guest species occupy small and large cages selectively, are summarized in **Chapter III**. In general, the thermodynamic stability conditions and crystal structures of mixed hydrates mainly depend on the large guest species. The present results elucidate that the cage occupancy of large guest species in mixed hydrate depends also on small guest species. An unexpected high-stability of the compartmental-type mixed hydrate system at high pressures and high temperatures was discovered, which suggests the competitive large-cage occupancy by large guest species and small guest species.

Table of Contents

Chapter I

General Introduction

I.1. Properties of Clathrate Hydrate

Clathrate hydrate (hereafter simply called "hydrate") is a solid crystalline, which has an ice-like appearance. Hydrate is necessarily composed of host species and guest species, where the former is water (H_2O) molecules and the latter is generally small molecules such as light hydrocarbons and noble gases. Several host molecules construct cage structure (hereafter called "cage") and a cage can normally enclathrate one guest molecule. Generally, a cage enclathrating a guest molecule is more stable than a vacant cage. There are several kinds of hydrate cages. Typical cages are shown in **Figure I-1**. For instance, 5^{12}-cage (S-cage) is a dodecahedron, which is constructed from twelve (^{12}) pentagons (5). The other cages (S'-cage, M-cage, L-cage, and U-cage) are summarized in **Table I-1**. S-cage, S'-cage, and L-cage are nearly spheral but M-cage and U-cage are oval. The other properties of the typical cages are also summarized in **Table I-1**. Some of them are combined to form specific hydrate structures as shown in **Figure I-2**. The unit cell of the structure-I (s-I) hydrate consists of two S-cages and six M-cages. In the same manner, that of the structure-II (s-II) hydrate is formed with sixteen S-cages and eight L-cages. The unit cell of structure-H (s-H) hydrate is composed of three S-cages, two S'-cages, and one U-cage. The properties of s-I, s-II, and s-H hydrates are summarized in **Table I-2** accompanied with those of ice-Ih. Simple hydrate is formed with binary mixture of host species and single guest species. On the other hand, mixed hydrate is formed with more than ternary mixture that is host species and two or more kinds of guest species. Simple hydrates normally belong to s-I or s-II hydrate, and mixed hydrates belong to s-I, s-II, s-H, or the other structures. Crystal structures and thermodynamic stabilities of hydrates depend on the thermodynamic conditions (pressure, temperature, composition, etc.) and the properties of guest species (size, shape, molar volume, molar weight, solubility, polarity, etc.) [1,2]. A lot of guest species have been reported until now. The guest species investigated in the present study are shown in **Figure I-3** in the ascending order of van der Waals diameter. The guest species can be categorized as; (a) occupying S-cages and L-cages of s-II hydrate, (b) occupying S-cages and M-cages of s-I hydrate, (c) occupying M-cages of s-I hydrate, (d) occupying L-cages of s-II hydrate, (e) occupying L-cages of s-II hydrate with help gas, and (f) occupying U-cages of s-H hydrate with help gas ("help gas" is explained below). The guest species categorized as (a) are very small and form s-II hydrates because s-II hydrates have a larger ratio of small cages to large cages than that of s-I hydrates. Some of guest species can multiply occupy L-cages. For instance, hydrogen (H_2) molecules occupy an L-cage doubly, triply, or quadruply [3]. The guest species in (b) such as methane (CH_4) and xenon (Xe) are slightly larger than those of (a), and they occupy both S-cages and M-cages of s-I hydrates. The guest species in (c) are larger than the cavity of S-cage. Therefore, they occupy only M-cages of s-I hydrates. At high pressures,

however, some of them such as ethane (C_2H_6) [4], ethylene (C_2H_4) [5], cyclopropane (*c*-C_3H_6) [6], and tetrafluoromethane (CF_4) [7] are compressed and forced to occupy S-cages. The guest species in (d) are larger than the cavity of M-cage. Therefore, they occupy only L-cages of s-II hydrates. As exceptions, sulfur hexafluoride [8] and propane (C_3H_8) [9], which are in (d), are compressed and forced to occupy M-cage of s-I hydrates at high pressures. The guest species in (e) are slightly large compared to the cavity of L-cage to occupy. Therefore, they cannot form s-II hydrate solely. When the small guest species such as CH_4 are added, large guest species occupy L-cages of s-II hydrates with the help of small guest species occupying S-cages. This is why the small guest species is called "help gas". The guest species in (f) are larger than the cavity of L-cage, so they occupy U-cages of s-H hydrates with the support of help gas occupying S-cages and S'-cages. In the case of s-H hydrates, the ratio of small cages to large cages is larger than that of s-I and s-II hydrates, and S'-cage and U-cage have geometrically unstable faces (squares and hexagons). Therefore, stabilization of cages by help gas occupying S-cages and S'-cages is necessary to form s-H hydrates [10].

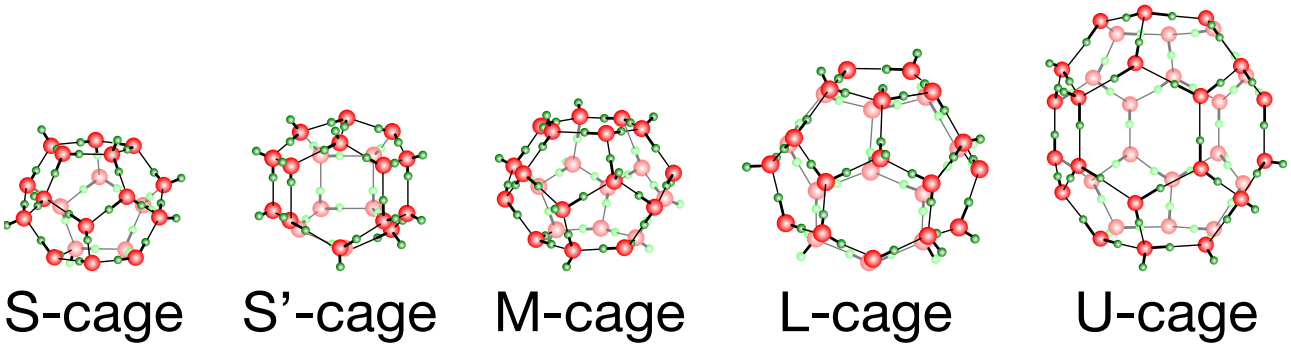

Figure I-1. Schematic illustration of typical hydrate cages.

Table I-1. Summary on properties of typical hydrate cages.

Name	S-cage	S'-cage	M-cage	L-cage	U-cage
Type	5^{12}	$4^3 5^6 6^3$	$5^{12}6^2$	$5^{12}6^4$	$5^{12}6^8$
Kind of polyhedron	dodecahedron	dodecahedron	tetrakaideca-hedron	hexakaideca-hedron	icosahedron
Coordination number	20	20	24	28	36

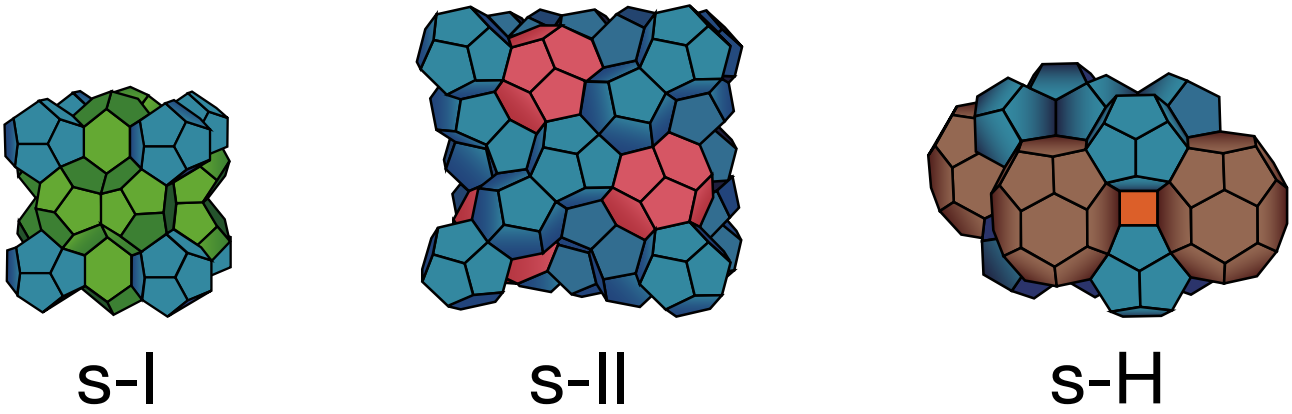

Figure I-2. Schematic illustration of crystal structures of hydrates.

Table I-2. Summary on unit cells of hydrates and ice-Ih.

Solid phase	s-I hydrate		s-II hydrate		s-H hydrate			ice-Ih
Cage	S	M	S	L	S	S'	U	-
Number of cages	2	6	16	8	3	2	1	-
Cage diameter d_1 / nm	0.795	0.860	0.782	0.946	0.782	0.812	1.142	-
Cavity diameter d_2 / nm[a]	0.51	0.59	0.50	0.67	0.49[b]	0.51[b]	0.86[b]	-
Number of water molecules	46		136		34			-
Crystal type	Cubic		Cubic		Hexagonal			Hexagonal
Space group	*Pm3n*		*Fd3m*		*P6/mmm*			$P6_3/mmc$
Lattice constant a / nm	1.20[c]		1.73[c]		1.22[d]			0.451842[e]
Lattice constant c / nm	-		-		1.01[d]			0.735556[e]

[a] The cavity diameters are obtained from the cavity diameter minus the diameter of water (0.28 nm).

[b] From the atomic coordinates measured using single crystal X-ray diffraction on s-H hydrates [11].

[c] From ref. [12].

[d] From ref. [13].

[e] From ref. [14] (at T = 250 K).

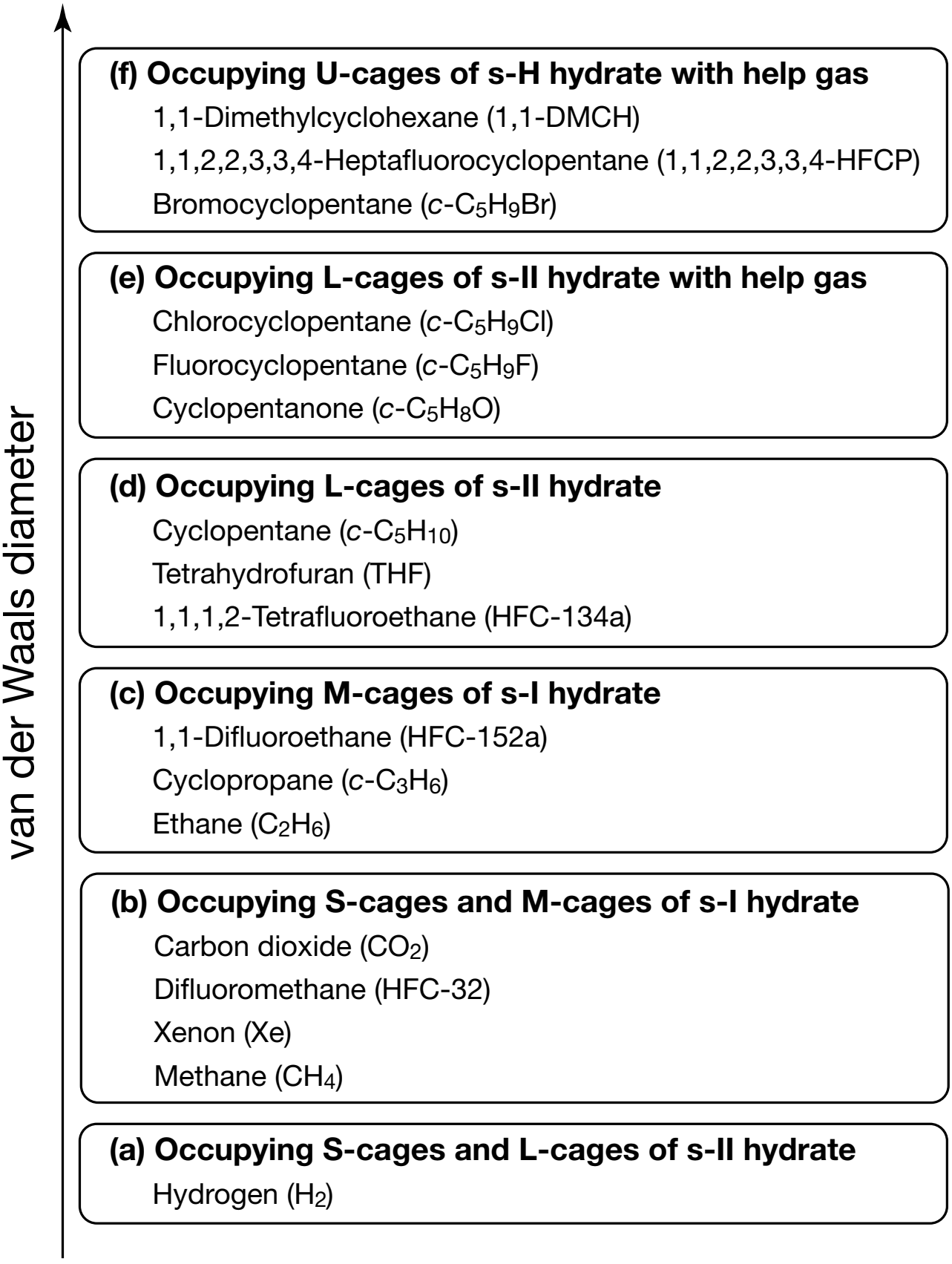

Figure I-3. Relation among size of guest species, hydrate structure, and cage occupancy investigated in the present study.

I.2. History and Applications of Clathrate Hydrate

Davy discovered water-chlorine (Cl_2) crystalline compounds, which were later identified as hydrates, in 1811 [15]. Faraday and Davy clarified that the mole ratio of Cl_2 to water was 0.1 ($Cl_2 \cdot 10H_2O$) [16]. Pauling and Marsh found out that the Cl_2 crystals were composed of host water molecules and guest Cl_2 molecules by means of X-ray diffractometry, that is, the crystals were "clathrate hydrates" [17]. After their studies, the structure models of s-I and s-II hydrates were indicated with a X-ray diffractometer [18]. In 1987, s-H hydrate was discovered by means of ^{2}H and ^{129}Xe NMR spectroscopy and neutron powder diffractometry by Ripmeester *et al*. [10].

In nature, large amounts of natural gas hydrate exist in permafrost and marine sediments as shown in **Figure I-4** [19]. Natural gas hydrate as well as shale gas, tight sand gas, and coal bed methane is non-conventional energy source. Japan is one of the energy-poor countries. However, there are large amounts of natural gas hydrate in deep sea around Japan. The estimated deposit of natural gas hydrate around Japan is approximately a hundred times of the annual consumption of natural gas in Japan [20]. Exploitation of the natural gas hydrate is significantly important for the energy self-sufficiency and the price negotiation of imported natural gas.

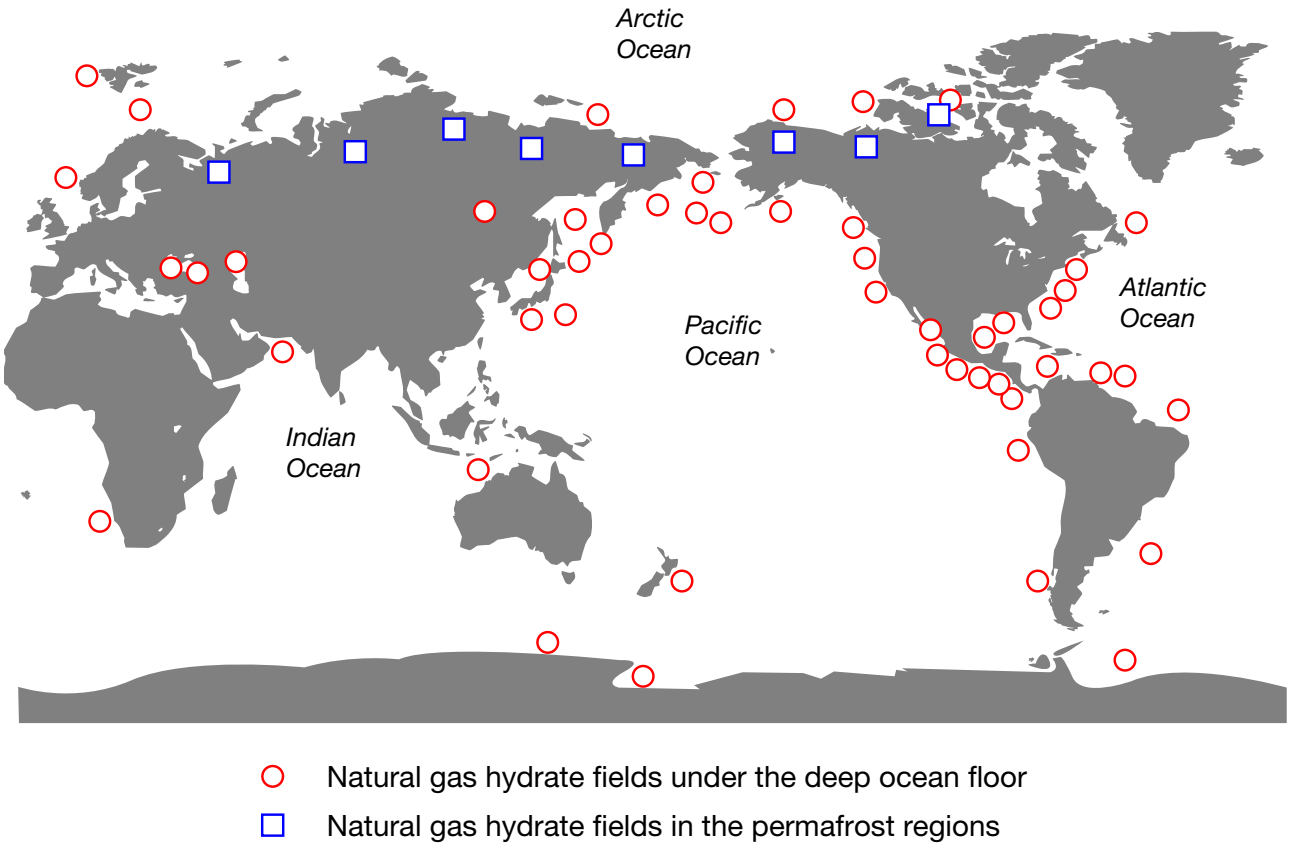

Figure I-4. Distribution of the natural gas hydrate field in the world [19].

In U.S., hydrate has been considered as a nuisance because it forms in the petroleum pipelines and blocks them [21]. This blockage accident occasionally happened. Therefore, main research topic on hydrate has been to explore inhibitors of the hydrate formation. At first, salt and alcohol were investigated as thermodynamic inhibitors that make hydrate thermodynamically unstable as shown in **Figure I-5**. Then, low molecular weight polymers were investigated as kinetic inhibitors that delay hydrate formation. Recently, surfactants have been investigated as anti-agglomerants that inhibit aggregation of hydrate particles.

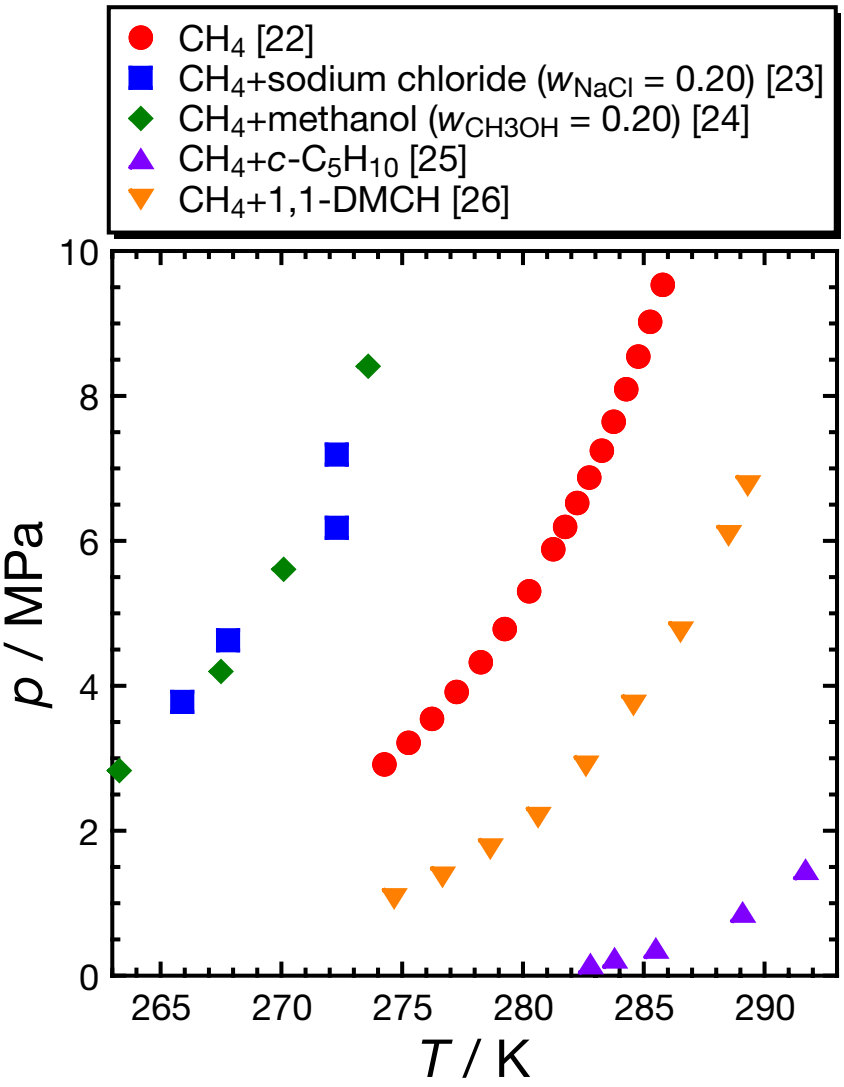

Figure I-5. Phase equilibrium relation for CH_4 hydrate systems with and without additives.

As mentioned before, hydrate can enclathrate large amount of gas. For example, an ideal CH_4 hydrate has approximately 175 times of its volume of CH_4 at standard conditions. This property can give us a potential as the alternative medium for gas storage, transportation, and isolation to gas compression, gas liquefaction, or gas storage in metal hydrides. However, hydrate formation and stabilization requires high pressures and/or low temperatures, which is one of the most severe

problems to be solved. The most effective and simplest solution is an addition of thermodynamic promoter such as cyclopentane (*c*-C_5H_{10}) and tetrahydrofuran (THF), which is larger than the gas molecule and occupies large cages of hydrates. By adding thermodynamic promoters, mixed hydrate forms at more moderate thermodynamic conditions than simple gas hydrate. For example, the thermodynamic stability regions of CH_4+additive mixed hydrates are larger than that of simple CH_4 hydrate as shown in **Figure I-5**. A negative aspect of an addition of thermodynamic promoter is the decrease of the amount of gas enclathration. For the applications of hydrate for gas storage, transportation, and isolation, it is better to achieve both the moderation of hydrate formation condition and the retention of gas enclathration amount.

Hydrogen Hydrate

Originally, it had not seemed that H_2 can form hydrate because of its tiny size. In 1999, H_2 hydrate was firstly reported in the phase diagram for H_2+water system as shown in **Figure I-6** by Dyadin *et al*. [27]. H_2 molecules form s-II hydrates and occupy S-cages singly and L-cages doubly, triply, and quadruply [28]. According to molecular simulation, H_2 molecules can occupy S-cage doubly [29]. However, there is no experimental evidence so far. When it was assumed that H_2 molecules occupy all the S-cages and L-cages singly and quadruply, respectively, the ideal storage capacity of H_2 hydrate is 3.8 wt% of H_2. However, simple H_2 hydrate requires extremely severe thermodynamic conditions for its formation and stabilization, which is the reason why H_2 hydrate is not applied practically yet. In the case of H_2 hydrate, especially, the effect of thermodynamic promoters is significant, compared to the other hydrates such as CH_4 hydrate and carbon dioxide (CO_2) hydrate. For example, s-II H_2+THF hydrate forms at p = 10 MPa and T = 280 K, on the other hand, simple H_2 hydrate forms at p = 150 MPa and T = 270 K [30,31]. In addition, the thermodynamic stability of the H_2+THF hydrate depends on the THF concentrations as shown in **Figure I-7** [32]. Recently, some kinds of quaternary ammonium salts have been reported as new thermodynamic promoters forming semi-clathrate hydrate. H_2+tetra-*n*-butyl ammonium bromide semi-clathrate hydrate has high stability as well as H_2+THF hydrate [31]. In the case of H_2+THF hydrate, however, the storage amount of H_2 decreases down to 1 wt% because THF molecules occupy all of the L-cages of s-II hydrates and there is no L-cage available for H_2 enclathration. Recently, it was reported that H_2 is allowed to occupy L-cage multiply in H_2+THF hydrate by decreasing the THF concentration and using special approach, which is called "tuning effect" [33,34]. Ideally, the amount of H_2 in the tuned H_2+THF hydrate achieves up to 3.8 wt% and the tuned hydrate forms outside the stable region of simple H_2 hydrate. The tuned hydrate is at the metastable state. Therefore, the tuning effect significantly depends on all of the experimental conditions and procedures.

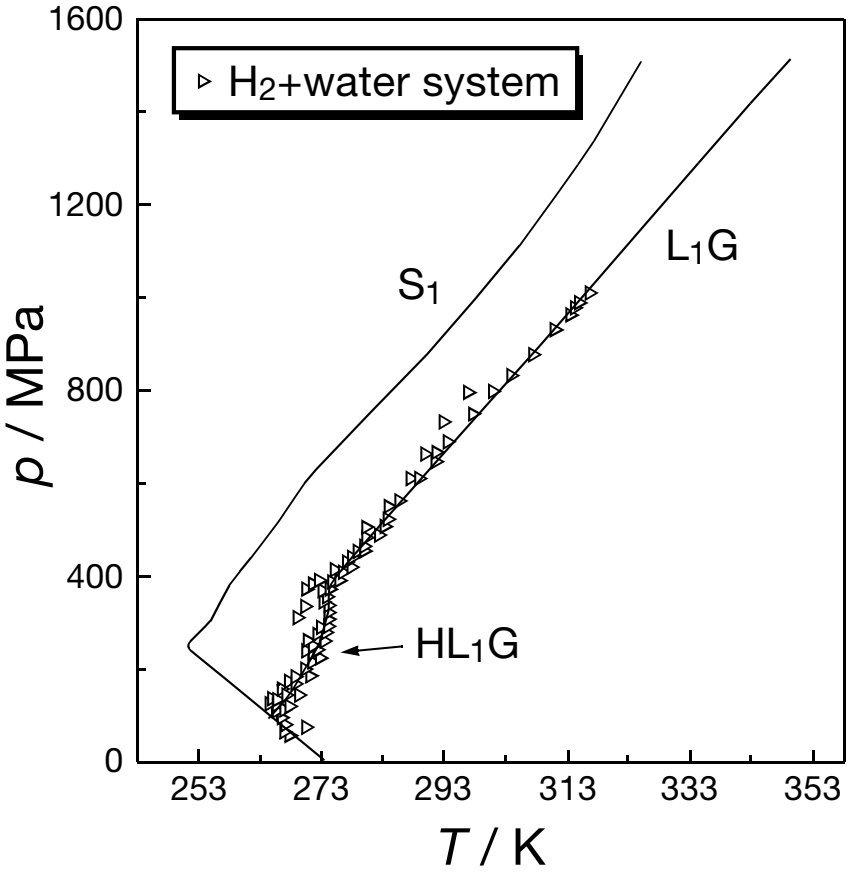

Figure I-6. Phase diagram for H_2+water system [27].

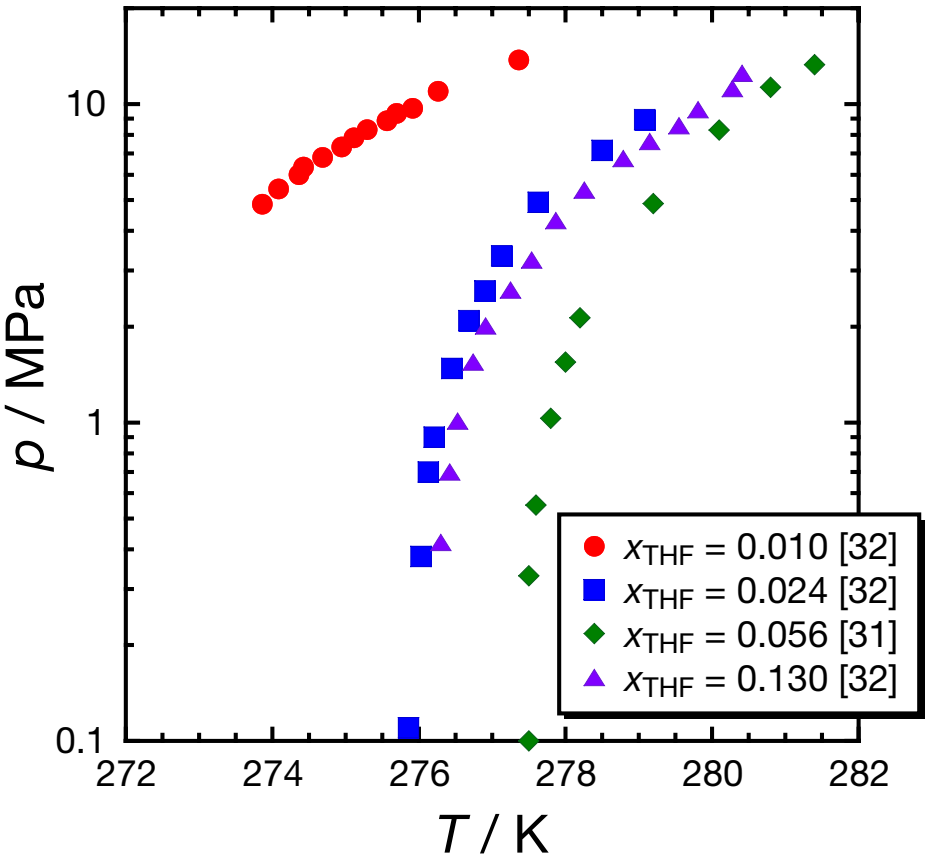

Figure I-7. Phase diagram for H_2+THF+water system [31,32].

Methane Hydrate

CH_4 hydrate has been investigated for a long time. Because CH_4 hydrate is flammable (as shown in **Figure I-8**) in spite of its ice-like appearance, it is called "flammable ice". As mentioned above, natural gas hydrate exists in permafrost field and marine sediment [19]. Complexly, natural gas hydrates include not only CH_4 but also C_2H_6, C_3H_8, *n*-butane, *i*-butane, and other components. It is important to know the thermodynamic stability of many kinds of natural gas hydrate for its exploitation. On the other hand, it is also suggested that CH_4 hydrate is applied for natural gas storage and transportation as shown in **Figure I-9**. Nowadays, natural gas is transported as liquefied natural gas. However, extremely low-temperature is required for its liquefaction (T = 110 K at p = 0.1 MPa). Hydrate is allowed to store and transport natural gases at a condition more moderate than that of liquefied natural gas. Furthermore, it is reported that the dissociation rate of CH_4 hydrate is reduced at a certain temperature region at atmospheric pressure as shown in **Figure I-10** [35], so-called "self-preservation phenomenon". It is much more desirable to use self-preserved CH_4 hydrate for natural gas storage and transportation because the self-preserved CH_4 hydrate is superficially stable at p = 0.1 MPa and T = 263 K.

Figure I-8. Photo of burning CH_4 hydrate.

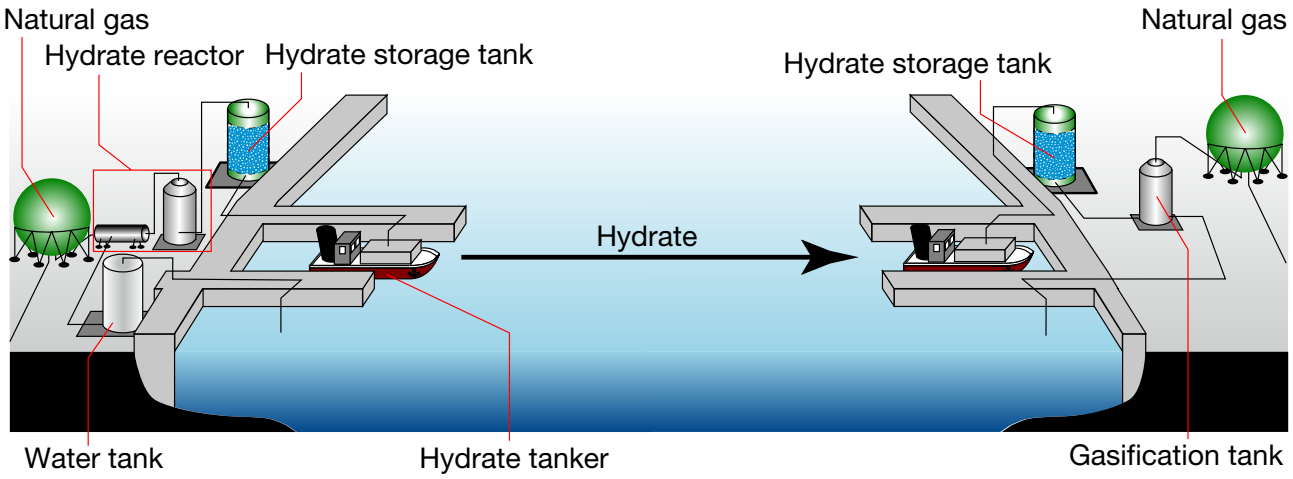

Figure I-9. Schematic illustration of storage and transportation of natural gas using hydrates.

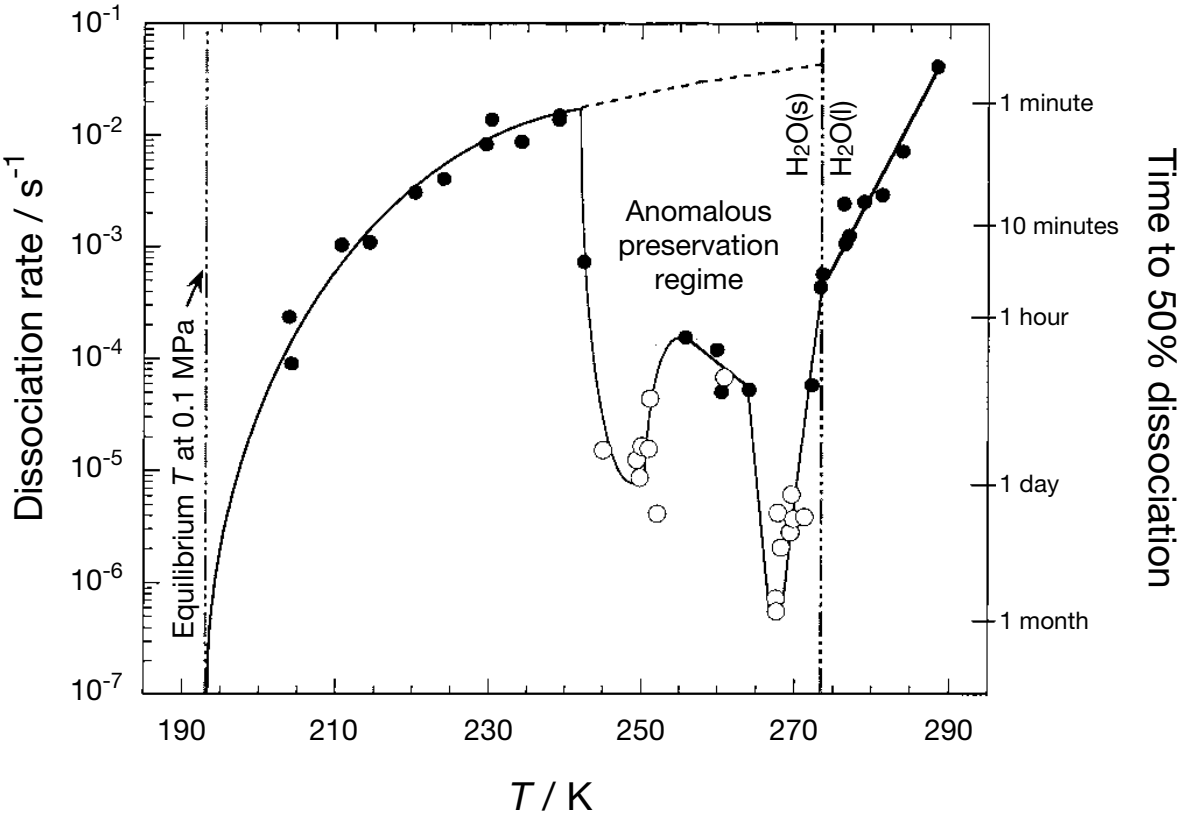

Figure I-10. Dissociation rate of CH_4 hydrate depending on temperature at atmospheric pressure [35].

Carbon Dioxide Hydrate

CO_2 is one of the materials which cause global warming. Avoiding this worldwide problem, it is necessary to reduce CO_2 emission and to promote CO_2 isolation (called "carbon capture and storage (CCS)") and CO_2 utilization. As a method for CO_2 isolation, it is suggested to use CO_2 hydrate. Just leading CO_2 to sea bottom deeper than 6000 m, CO_2 is liquefied at the bottom and at the interface between sea water and liquefied CO_2, CO_2 hydrate is formed as shown in **Figure I-11**

[36]. As a result, liquefied CO_2 can be isolated very densely beneath CO_2 hydrate film. Furthermore, it is suggested that CH_4 enclathrated in natural gas hydrate is replaced with CO_2 by supplying CO_2 into the sand layer including natural gas hydrates as shown in **Figure I-12** [37]. This process is more valuable because CO_2 isolation and CH_4 collection can be achieved simultaneously. As CO_2 utilization, CO_2 is suggested to be used as a refrigerant [38]. Hydrate has some positive aspects for refrigerant. Because the dissociation enthalpy of the gas hydrate is higher than the fusion enthalpy of ice, the hydrate is often employed as thermal energy storage and hydrate-based refrigeration systems [39]. Generally, gas hydrates have the dissociation temperature higher than ice at some pressure, and the dissociation temperature of hydrates can be controlled by changing pressure or adding the other guest species, whereas it is so hard and not effective to control the fusion temperature of ice with pressurization or depressurization. The usage of hydrate slurries can be applied for not only batch cooling system but also continuous one. CO_2 hydrate is more appropriate for refrigerant than hydrocarbon hydrates because the former has the higher dissociation enthalpy than the latters. However, high pressures and low temperatures are still required to form CO_2 hydrates. Thus, it is proposed to moderate the conditions of hydrate formation by use of thermodynamic promoters.

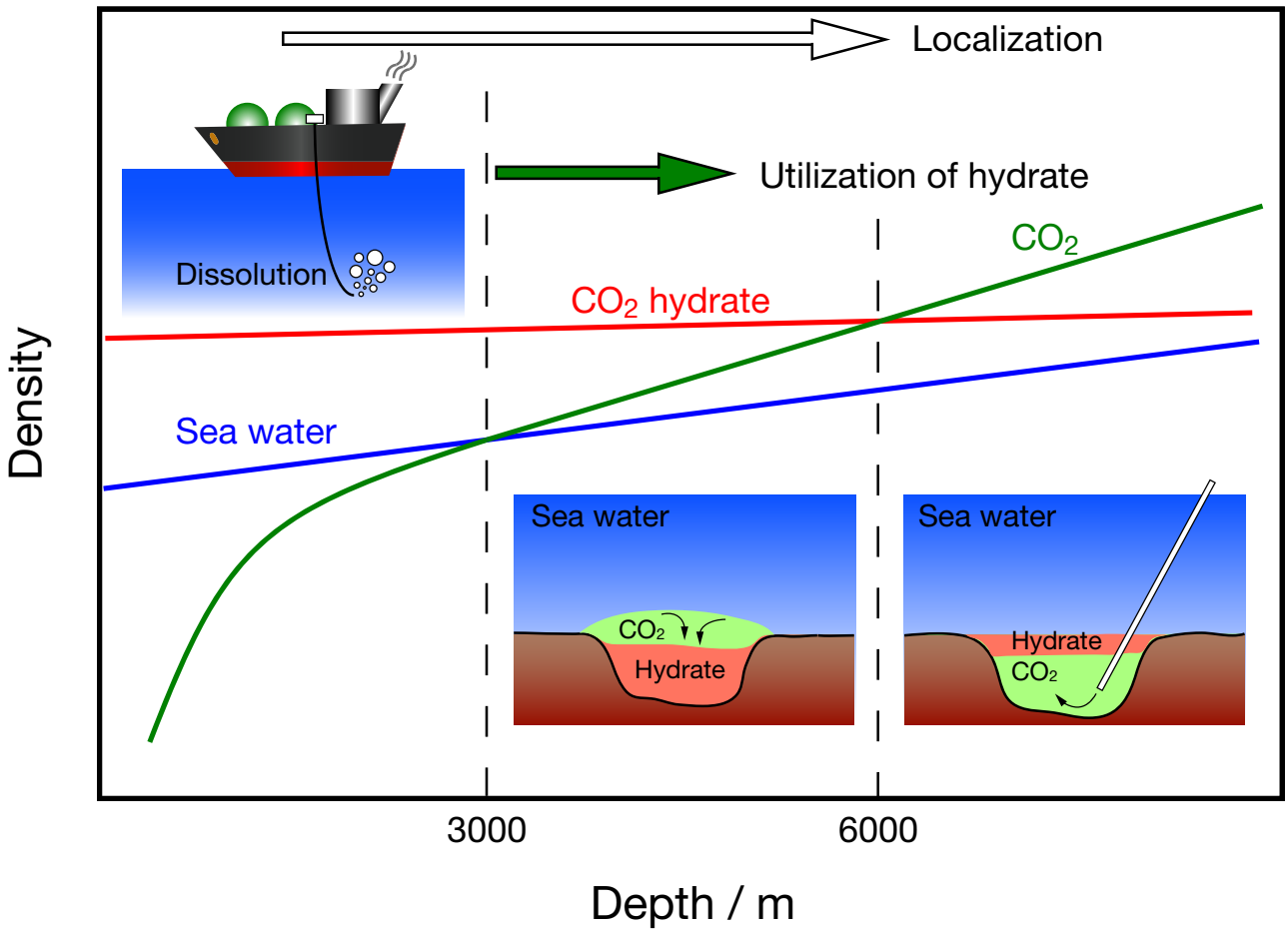

Figure I-11. CO_2 isolation process using hydrates [36].

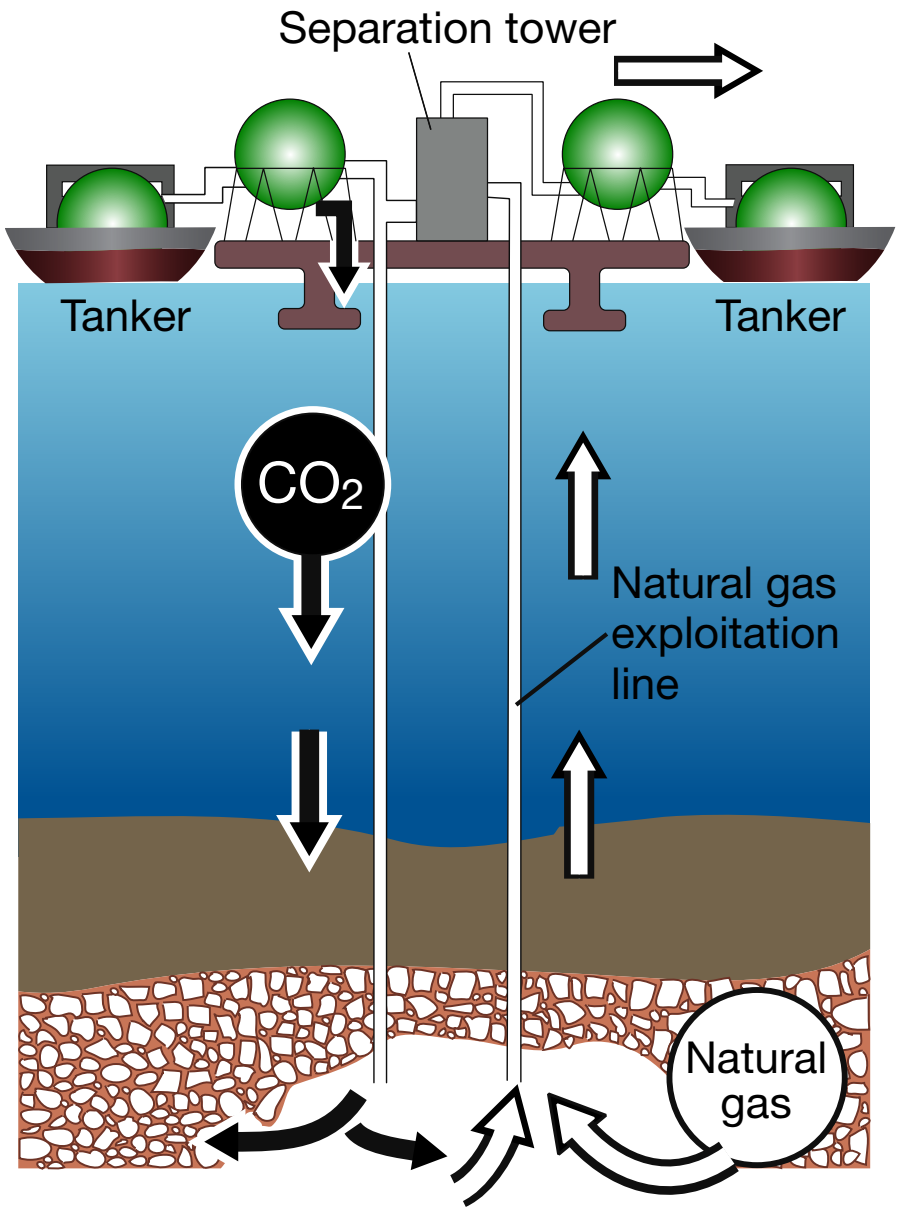

Figure I-12. CH_4/CO_2 replace process using hydrates [37].

Hydrofluorocarbon Hydrate

Hydrofluorocarbons (HFCs) have been used as refrigerants instead of chlorofluorocarbons and hydrochlorofluorocarbons because chloride compounds destroy the ozone layer. HFCs still significantly promote the global warming as similar to CO_2. However, HFC hydrates form under conditions much more moderate than CO_2 hydrate as shown in **Figure I-13**. HFCs generally have global warming potential higher than CO_2, and some of HFCs are flammable. Therefore, it is desirable to use these hydrates as refrigerant in completely closed system.

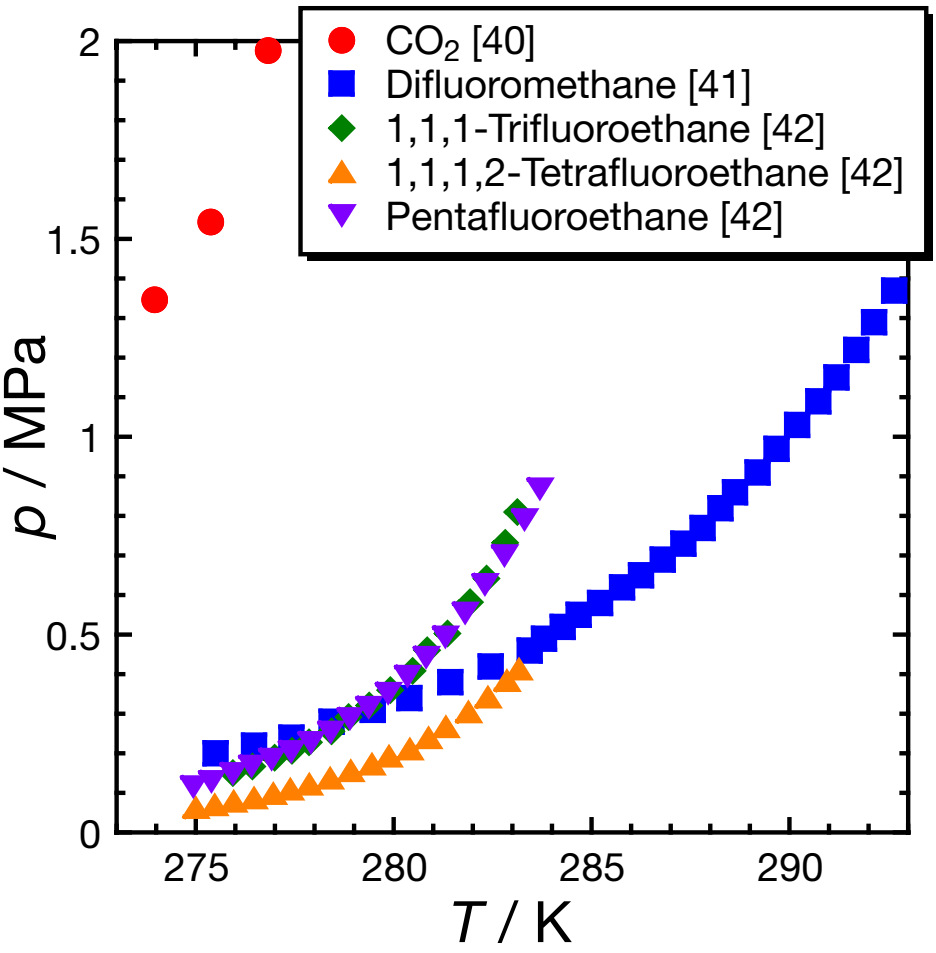

Figure I-13. Phase diagram for simple CO_2 and HFC hydrates.

I.3. Research Purposes of the Present Studies

As mentioned in the previous section, many kinds of utilizations using hydrates have been proposed. However, some problems to be solved still remain. For H_2 storage, it should be satisfied to achieve both the moderation of thermodynamic conditions of H_2 hydrate and the retention of H_2 enclathration amount. Therefore, the mechanism of tuning effect should be clarified to handle it. Or the alternative storage method using hydrate (additive or procedure) should be established. For natural gas storage and transportation, the practical hydrate system should be investigated for feasible natural gas storage and transportation process. For refrigerants, it is important to form CO_2 hydrate or HFC hydrate at a pressure as low as possible for safe, low-cost, and feasible cooling process. What is the comprehensively important for hydrate utilization is to discover remarkable thermodynamic promoters and to use mixed hydrates composed of a target gas and the thermodynamic promoter. Compared to simple hydrate systems, mixed hydrate systems exhibit complicated phase behavior and cage occupancies of guest species. In the present study, small guest

species (H_2, CH_4, CO_2, etc.) and many kinds of the candidates of thermodynamic promoter were adopted. Thermodynamic stabilities of many mixed hydrates were clarified by means of phase equilibrium measurement. The crystal structures of unclarified mixed hydrates were identified by means of powder X-ray diffractometry (PXRD). In addition, cage occupancies of guest species in mixed hydrates were analyzed by means of Raman spectroscopy. Taking into consideration all of the experimental results, phase behavior and structural transitions depending on cage occupancies of guest species in mixed hydrates were comprehensively discussed. According to the cage occupancies, the mixed hydrate systems investigated in this thesis were categorized into two types; competitive-type mixed hydrates are summarized in **Chapter II** and compartmental-type mixed hydrates are in **Chapter III**.

I.4. Nomenclatures

a	Lattice constant [m]
c	Lattice constant [m]
d_1	Cage diameter [m]
d_2	Cavity diameter [m]
p	Pressure [Pa]
T	Temperature [K]
w_{CH3OH}	Mass fraction of methanol in aqueous solution [-]
w_{NaCl}	Mass fraction of sodium chloride in aqueous solution [-]
x_{THF}	Mole fraction of THF in aqueous solution [-]
G	Gas phase
H	Hydrate phase
L_1	Aqueous phase
S_1	Ice phase

I.5. References

[1] E.D. Sloan, C.A. Koh, *Clathrate Hydrates of Natural Gases, 3rd Ed.*; CRC Press, Taylor and Francis Group: Boca Raton, FL, 2008.

[2] K. Tezuka, T. Taguchi, S. Alavi, A.K. Sum, R. Ohmura, "Thermodynamic Stability of Structure H Hydrates Based on the Molecular Properties of Large Guest Molecules", *Energies*, **5**, 459–465 (2012).

[3] T.A. Strobel, C.A. Koh, E.D. Sloan, "Hydrogen Storage Properties of Clathrate Hydrate Materials", *Fluid Phase Equilibria*, **261**, 382–389 (2007).

[4] K. Morita, S. Nakano, K. Ohgaki, "Structure and Stability of Ethane Hydrate Crystal", *Fluid Phase Equilibria*, **169**, 167–175 (2000).

[5] T. Sugahara, K. Morita, K. Ohgaki, "Stability Boundaries and Small Hydrate-Cage Occupancy of Ethylene Hydrate System", *Chemical Engineering Science*, **55**, 6015–6020 (2000).

[6] M. Suzuki, Y. Tanaka, T. Sugahara, K. Ohgaki, "Pressure Dependence of Small-Cage Occupancy in the Cyclopropane Hydrate System", *Chemical Engineering Science*, **56**, 2063–2067 (2001).

[7] K. Sugahara, M. Yoshida, T. Sugahara, K. Ohgaki, "High-Pressure Phase Behavior and Cage Occupancy for the CF_4 Hydrate System", *Journal of Chemical & Engineering Data*, **49**, 326–329 (2004).

[8] K. Sugahara, M. Yoshida, T. Sugahara, K. Ohgaki, "Thermodynamic and Raman Spectroscopic Studies on Pressure-Induced Structural Transition of SF_6 Hydrate", *Journal of Chemical & Engineering Data*, **51**, 301–304 (2006).

[9] Y.A. Dyadin, E.G. Larionov, E.Y. Aladko, F.V. Zhurko, "Clathrate Formation in Propane-Water and Methane-Propane-Water Systems under Pressures of up to 15 kbar", *Doklady Physical Chemistry*, **376**, 23–26 (2001).

[10] J.A. Ripmeester, J.S. Tse, C.I. Ratcliffe, B.M. Powell, "A New Clathrate Hydrate Structure", *Nature*, **325**, 135–136 (1987).

[11] K.A. Udachin, C.I. Ratcliffe, G.D. Enright, J.A. Ripmeester, "Structure H Hydrate: A Single Crystal Diffraction Study of 2,2-Dimethylpentane·5(Xe, H_2S)·34H_2O", *Supramolecular Chemistry*, **8**, 173–176 (1997).

[12] W.R. Parrish, J.M. Prausnitz, “Dissociation Pressures of Gas Hydrates Formed by Gas Mixtures”, *Industrial & Engineering Chemistry Process Design and Development*, **11**, 26–35 (1972).

[13] A.P. Mehta, E.D. Sloan, “Improved Thermodynamic Parameters for Prediction of Structure H Hydrate Equilibria”, *AIChE Journal*, **42**, 2036–2046 (1996).

[14] K. Röttger, A. Endriss, J. Ihringer, S. Doyle, W. F. Kuhs, “Lattice Constants and Thermal Expansion of H_2O and D_2O Ice I*h* between 10 and 265 K”, *Acta Crystallographica Section B*, **50**, 644–648 (1994).

[15] H. Davy, “On a Combination of Oxymuriatic Gas and Oxygen Gas”, *Philosophical Transactions of the Royal Society*, **101**, 155–162 (1811).

[16] M. Faraday, H. Davy, “On Fluid Chlorine”, *Philosophical Transactions of the Royal Society of London*, **113**, 160–165 (1823).

[17] L. Pauling, R.E. Marsh, “The Structure of Chlorine Hydrate”, *Proceedings of National Academy Science*, **38**, 112–118 (1952).

[18] M. Stackelberg, H.R. Müller, “Feste Gashydrate II Struktur und Raumchemie”, *Zeitschrift für Elektrochemie*, **58**, 25–29 (1954).

[19] K.A. Kvenvolden, “Methane Hydrate — A Major Reservoir of Carbon in the Shallow Geosphere?”, *Chemical Geology*, **71**, 41–51 (1988).

[20] M. Satoh, T. Maekawa, Y. Okuda, “Estimation of Amount of Methane and Resources of Natural Gas Hydrates in the World and around Japan”, *Journal of Geological Society Japan*, **102**, 959–971 (1996).

[21] E.G. Hammerschmidt, “Formation of Gas Hydrates in Natural Gas Transmission Lines”, *Industrial and Engineering Chemistry*, **26**, 851–855 (1934).

[22] T. Nakamura, T. Makino, T. Sugahara, K. Ohgaki, "Stability Boundaries of Gas Hydrates Helped by Methane—Structure-H Hydrates of Methylcyclohexane and *cis*-1,2-Dimethylcyclohexane", *Chemical Engineering Science*, **58**, 269–273 (2003).

[23] R. Kobayashi, H.J. Withrow, G.B. Williams, D.L. Katz, "Gas Hydrate Formation with Brine and Ethanol Solutions", *Proceedings of the 30th Annual Convention, Natural Gasoline Association of America*, **1951**, 27–31 (1951).

[24] H.-J. Ng, D.B. Robinson, "Hydrate Formation in Systems Containing Methane, Ethane, Propane, Carbon Dioxide or Hydrogen Sulfide in the Presence of Methanol", *Fluid Phase Equilibria*, **21**, 145–155 (1985).

[25] B. Tohidi, A. Danesh, A.C. Todd, R.W. Burgass, K.K. Østergaard, "Equilibrium Data and Thermodynamic Modelling of Cyclopentane and Neopentane Hydrates", *Fluid Phase Equilibria*, **138**, 241–250 (1997).

[26] T. Hara, S. Hashimoto, T. Sugahara, K. Ohgaki, "Large Pressure Depression of Methane Hydrate by Adding 1,1-Dimethylcyclohexane", *Chemical Engineering Science*, **60**, 3117–3119 (2005).

[27] Y.A. Dyadin, E.G. Larionov, A.Y. Manakov, F.V. Zhurko, E.Y. Aladko, T.V. Mikina, V.Y. Komarov, "Clathrate Hydrates of Hydrogen and Neon", *Mendeleev Communications*, **9**, 209–210 (1999).

[28] T.A. Strobel, E.D. Sloan, C.A. Koh, "Raman Spectroscopic Studies of Hydrogen Clathrate Hydrates", *The Journal of Chemical Physics*, **130**, 014506-1–10 (2009).

[29] W.L. Mao, H.K. Mao, A.F. Goncharov, V.V. Struzhkin, Q.Z. Guo, J.Z. Hu, J.F. Shu, R.J. Hemley, M. Somayazulu, Y.S. Zhao, "Hydrogen Clusters in Clathrate Hydrate", *Science*, **297**, 2247–2249 (2002).

[30] L.J. Florusse, C.J. Peters, J. Schoonman, K.C. Hester, C.A. Koh, S.F. Dec, K.N. Marsh, E.D. Sloan, "Stable Low-Pressure Hydrogen Clusters Stored in a Binary Clathrate Hydrate", *Science*, **306**, 469–471 (2004).

[31] S. Hashimoto, S. Murayama, T. Sugahara, H. Sato, K. Ohgaki, "Thermodynamic and Raman Spectroscopic Studies on H_2+Tetrahydrofuran+Water and H_2+Tetra-*n*-Butyl Ammonium Bromide +Water Mixtures Containing Gas Hydrates", *Chemical Engineering Science*, **61**, 7884–7888 (2006).

[32] S. Hashimoto, T. Sugahara, H. Sato, K. Ohgaki, "Thermodynamic Stability of H_2+Tetrahydrofuran Mixed Gas Hydrate in Nonstoichiometric Aqueous Solutions", *Journal of Chemical & Engineering Data*, **52**, 517–520 (2007).

[33] H. Lee, J.-W. Lee, D.Y. Kim, J. Park, Y.-T. Seo, H. Zeng, I.L. Moudrakovski, C.I. Ratcliffe, J.A. Ripmeester, "Tuning Clathrate Hydrates for Hydrogen Storage", *Nature*, **434**, 743–746 (2005).

[34] T. Sugahara, J.C. Haag, P.S.R. Prasad, A.A. Warntjes, E.D. Sloan, A.K. Sum, C.A. Koh, "Increasing Hydrogen Storage Capacity Using Tetrahydrofuran", *Journal of the American Chemical Society*, **131**, 14616–14617 (2009).

[35] L.A. Stern, S. Circone, S.H. Kirby, W.B. Durham, "Anomalous Preservation of Pure Methane Hydrate at 1 atm", *The Journal of Physical Chemistry B*, **105**, 1756–1762 (2001).

[36] K. Ohgaki, Y. Inoue, "A Proposal for Gas Storage on the Ocean Floor Using Gas Hydrates", *Kagaku Kogaku Ronbunshu*, **17**, 1053–1055 (1991).

[37] K. Ohgaki, K. Takano, M. Moritoki, "Exploitation of CH_4 Hydrates under the Nankai Trough in Combination with CO_2 Storage", *Kagaku Kogaku Ronbunshu*, **20**, 121–123 (1994).

[38] L. Fournaison, A. Delahaye, I. Chatti, J.-P. Petitet, "CO_2 Hydrates in Refrigeration Processes", *Industrial & Engineering Chemistry Research*, **43**, 6521–6526 (2004).

[39] T. Ogawa, T. Ito, K. Watanabe, K. Tahara, R. Hiraoka, J. Ochiai, R. Ohmura, Y. Mori, "Development of a Novel Hydrate-Based Refrigeration System: A Preliminary Overview", *Applied Thermal Engineering*, **26**, 2157–2167 (2006).

[40] K. Ohgaki, Y. Makihara, K. Takano, "Formation of CO_2 Hydrate in Pure and Sea Waters", *Journal of Chemical Engineering of Japan*, **26**, 558–564 (1993).

[41] S. Hashimoto, H. Miyauchi, Y. Inoue, K. Ohgaki, “Thermodynamic and Raman Spectroscopic Studies on Difluoromethane (HFC-32)+Water Binary System”, *Journal of Chemical & Engineering Data*, **55**, 2764–2768 (2010).

[42] S. Hashimoto, T. Makino, Y. Inoue, K. Ohgaki, “Three-Phase Equilibrium Relations and Hydrate Dissociation Enthalpies for Hydrofluorocarbon Hydrate Systems: HFC-134a, -125, and -143a Hydrates”, *Journal of Chemical & Engineering Data*, **55**, 4951–4955 (2010).

Chapter II

Competitive-Type Mixed Hydrates

Section 1

In Situ Raman Spectra of Hydrogen in Large Cages of Hydrogen+Tetrahydrofuran Mixed Hydrates

II.1.1. Abstract

Large-cage occupancy of H_2 in the H_2+THF hydrates has ever been reported only in the *ex situ* spectroscopic measurements with the quenched hydrate sample. In this section, to verify the proof-of-concept for the large-cage occupancy of H_2 competitive with THF, *in situ* Raman spectra of H_2 in the H_2+THF mixed hydrates were detected at p = 74.3 MPa and T = 265 K without the quenching procedure. The Raman spectra revealed that H_2 molecules occupy a part of large cages of the H_2+THF mixed hydrates in a thermodynamically unstable region of simple H_2 hydrate.

II.1.2. Introduction

H_2 and water form s-II hydrate [1,2]. The unit cell of s-II clathrate hydrate consists of sixteen S-cages and eight L-cages, which are singly and multiply occupied by H_2 molecules, respectively [3]. Simple H_2 hydrates potentially offer a clean H_2 storage medium. However, extremely high pressures and/or low temperatures are required for simple H_2 hydrate formation [1–3]. The addition of THF makes H_2+THF mixed hydrates at pressures lower than the equilibrium ones of simple H_2 hydrates [4–9]. In the H_2+THF mixed hydrates prepared with compressed H_2 and THF aqueous solutions, H_2 molecules occupy only S-cages, while THF molecules occupy L-cages [10]. That is, the cage occupancy of H_2+THF mixed hydrates belongs to the compartmental-type. On the other hand, when H_2+THF mixed hydrates are prepared with compressed H_2 and solid mixtures of THF and ice, H_2 molecules metastably occupy not only S-cages but also a part of L-cages [11,12]. The phenomenon has been called the tuning effect [5]. In this case, H_2 storage amount ideally increases to the similar level as that of simple H_2 hydrates. Until now, competitive L-cage occupancies of H_2 and THF have been investigated by means of *ex situ* Raman spectroscopy at atmospheric pressure (p = 0.1 MPa) and liquefied nitrogen (LN_2) temperature (T = 77 K) [11,12]. The hydrate samples

were taken out from high-pressure cells after they were quenched by LN_2. Therefore, some researchers have inferred that the peaks derived from H_2 molecules in L-cages were detected as a result of simple H_2 hydrates generation during the quenching process.

In this section, H_2+THF mixed hydrates were prepared and analyzed in simple H_2 hydrate unstable region (p = 74.3 MPa and T = 265 K).

II.1.3. Experimental

Materials

The materials used in the present study are summarized in **Table II-1-1**. All of them were used without further purification.

Table II-1-1. Information on the materials used in the present study.

Material name	Source	Mole fraction purity
H_2	Neriki Gas Co., Ltd.	> 0.999999
THF	Merck, Ltd.	> 0.999 (Main impurity: water)
Distilled water	Wako Pure Chemicals Ind., Ltd.	> 0.9999

Apparatus

A schematic illustration of the high-pressure optical cell used in the present study is shown in **Figure II-1-1**. The cell has a pair of titanium-free sapphire windows. A laser Raman confocal microprobe spectrophotometer (Jasco, NRS-1000) with a multichannel charge-coupled device (CCD) detector was used accompanied with an argon ion laser (wavelength: 514.5 nm, laser spot diameter: 2 μm). The spectral resolution of the spectrometer was 0.7 cm^{-1}. The system temperature was measured using a RTD thermistor (Eutech, Temp 6, reproducibility: 0.2 K). The system pressure was measured by a pressure gauge (Valcom, VPRH, maximum uncertainty: 0.2 MPa).

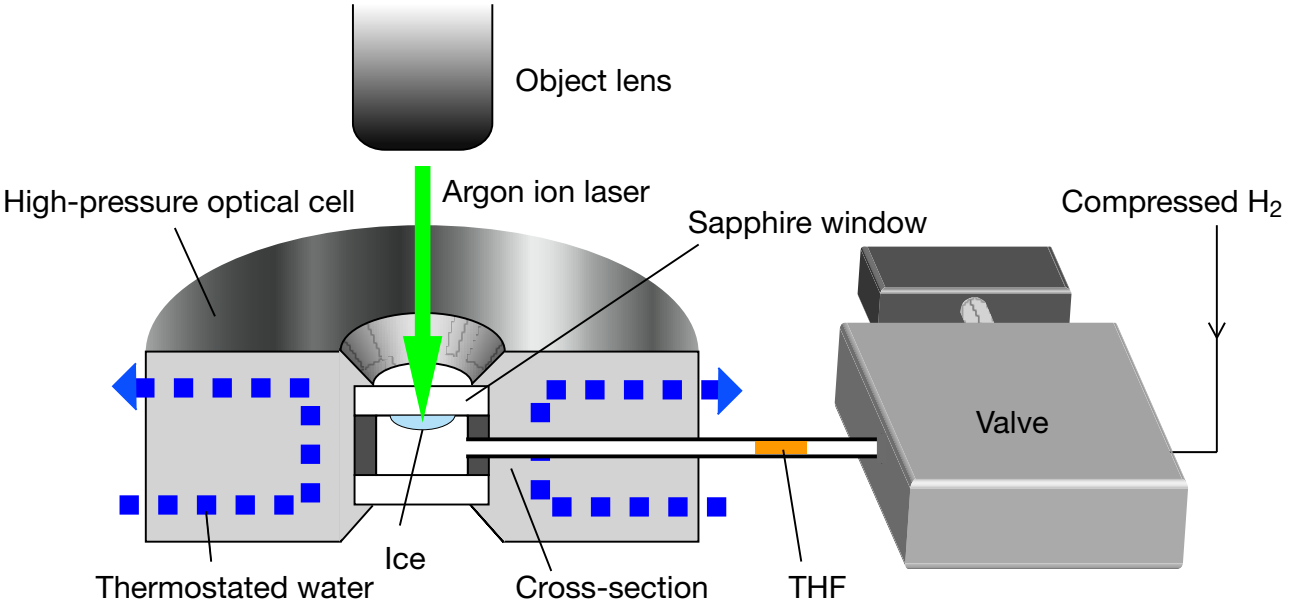

Figure II-1-1. Schematic illustration of the experimental setup and procedure.

Procedure

In the present study, to exclude both effects of the sample quenching and the fluid H_2 in the Raman analysis, I used a different experimental method from the previous reports [10,12]. A schematic illustration of the experimental setup and procedure is shown in **Figure II-1-1**. A small droplet of pure water was directly dropped on a sapphire window of the high-pressure optical cell. It was placed in a temperature-controlled room at T = 263 K, and the droplet was frozen. Then the window with ice was set in the main unit of high-pressure cell, and THF was enclosed within a high-pressure pipe line between the valve and the high-pressure optical cell. Once the valve was opened, THF was sprayed on the ice surface by compressed H_2. At this time, H_2 and THF molecules simultaneously supplied to the ice surface result in the hydrate formation. The approximate amount of the enclosed THF corresponded to the stoichiometric concentration of the simple THF hydrate because the hydrate formation was unable to be detected under a less THF concentration. Though it is difficult to comprehend the exact amount of THF reacted with ice, the THF concentration (on an H_2 free basis) in the H_2+THF mixed hydrate is at least less than the stoichiometric concentration of the simple THF hydrate. The system temperature was controlled at T = 265 K. The hydrate samples were analyzed through a sapphire window by means of *in situ* Raman spectroscopy at p = 74.3 MPa and T = 265 K. The argon ion laser was irradiated to the hydrate crystal and the backscatter was taken in through the same lens. To maximally inhibit the overlap of fluid H_2 on the Raman spectrum, that is, to improve the spatial resolution in the confocal Raman arrangement, the minimal sizes of a slit and an aperture were used. As a compensation of the improved spatial resolution, detected peak intensities are generally sacrificed.

II.1.4. Results and Discussion

Raman peaks corresponding to the intramolecular H–H stretching vibration mode of H_2 in L-cage are strongly affected by surrounding temperature [2]. It has been reported that the peak derived from single H_2 molecule in S-cages (hereafter, peak(S)) is detected at $\Delta\nu$ = 4132 cm^{-1} and the peaks derived from multiple H_2 molecules in L-cages (peaks(L)) are detected at $\Delta\nu$ = 4144 cm^{-1} and 4152 cm^{-1} at T = 77 K [13]. Note that the peak widths and positions are different from those recorded at an extremely low temperature and the peak(S) is broad and seems to be single at ambient temperature. **Figure II-1-2** shows the Raman spectra of the H–H stretching vibration mode of H_2 molecules in the H_2+THF mixed hydrate and fluid H_2 phases. **Figure II-1-2(a)** indicates the Raman spectrum of H_2 in the H_2+THF mixed hydrates prepared with the present experimental method. **Figure II-1-2(a)** also involves the slight contribution of the fluid H_2. It was very difficult, even with the confocal Raman arrangement, to completely exclude the effect of H_2 in fluid phase. **Figure II-1-2(b)** is the spectrum of the H_2+THF mixed hydrate prepared from compressed H_2 and THF aqueous solutions. In this case, no H_2 molecule occupies L-cage even at low THF concentrations [10]. The peak(S) in **Figure II-1-2(a)** has a shoulder at the high wavenumber side, while it does not appear in **Figure II-1-2(b)**. In order to elucidate that the peaks(L) exist in **Figure II-1-2(a)**, a difference spectrum between **Figure II-1-2(a)** and **Figure II-1-2{(b)+(c)}** is shown in **Figure II-1-3(a)**. In this calculation, **Figure II-1-2(b)** and **Figure II-1-2(c)** were normalized by the intensities of the peaks detected at $\Delta\nu$ = 4132 cm^{-1} and 4159 cm^{-1}, respectively. **Figure II-1-3(a)** indicates two peaks assuredly at $\Delta\nu$ = 4140–4160 cm^{-1}. They were fitted by use of Voigt function with the base line correction. The deconvoluted peaks are shown in the dotted ($\Delta\nu$ = 4144 cm^{-1}) and dashed ($\Delta\nu$ = 4152 cm^{-1}) lines. They are in good agreement with the peaks(L) of simple H_2 hydrates [13] as shown in **Figure II-1-3(b)**. This result reveals that H_2 molecules occupy a part of L-cages in the H_2+THF mixed hydrates prepared with the present experimental method. In other words, the competitive L-cage occupancy of H_2 with THF in H_2+THF mixed hydrates surely occurs, and it is not always derived from the simple H_2 hydrate formation. The lower L-cage occupancy of H_2 than previous reports [11,12] results from the present experimental procedure to verify the proof-of-concept, that is, to exclude the effect of fluid H_2 in Raman analysis. Optimizing a preparation procedure and condition would make improvements.

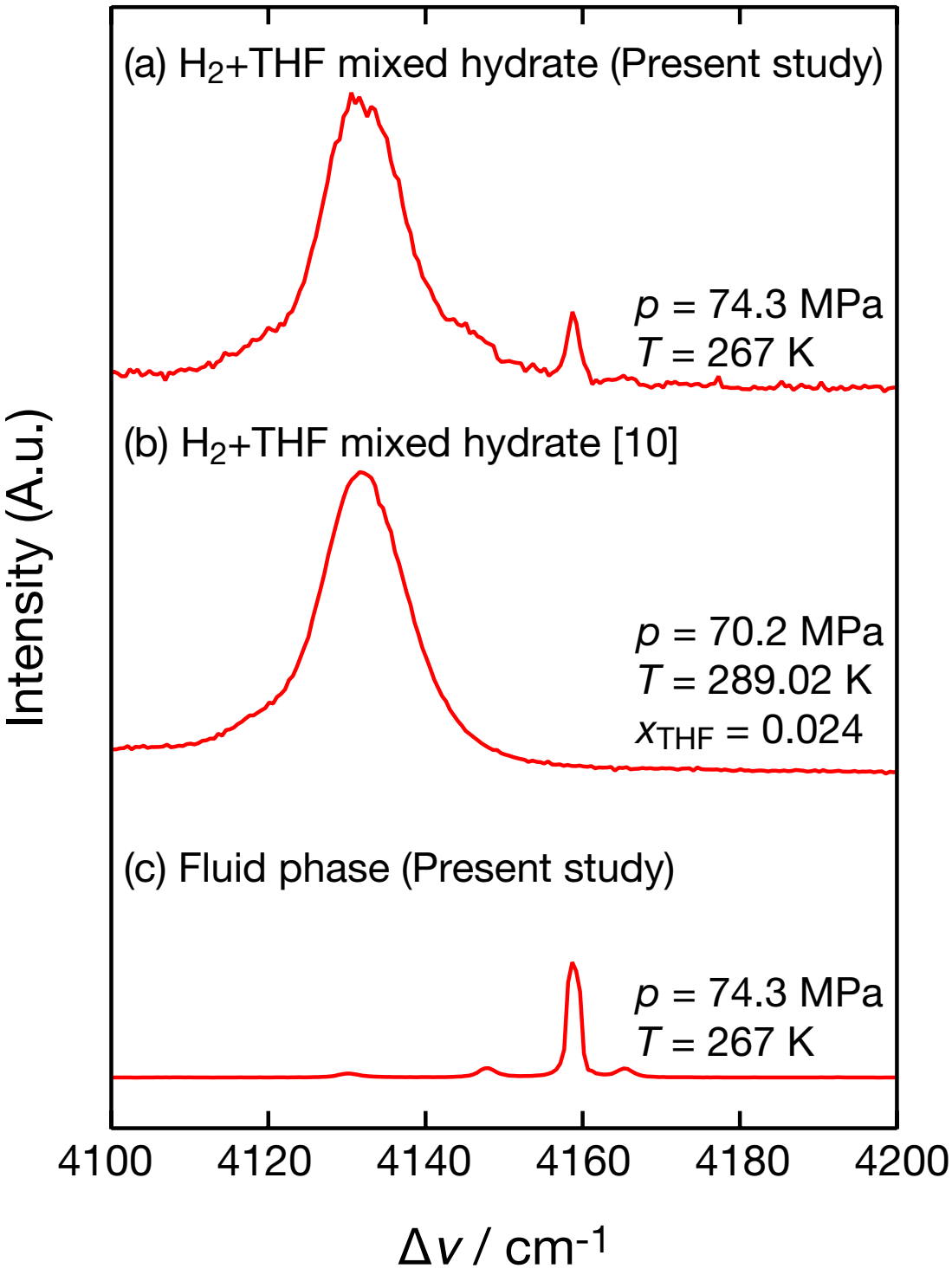

Figure II-1-2. Raman spectra corresponding to the H–H stretching vibration mode of H_2 molecules in the H_2+THF mixed hydrates and fluid phase. Spectrum (a) partially includes fluid H_2.

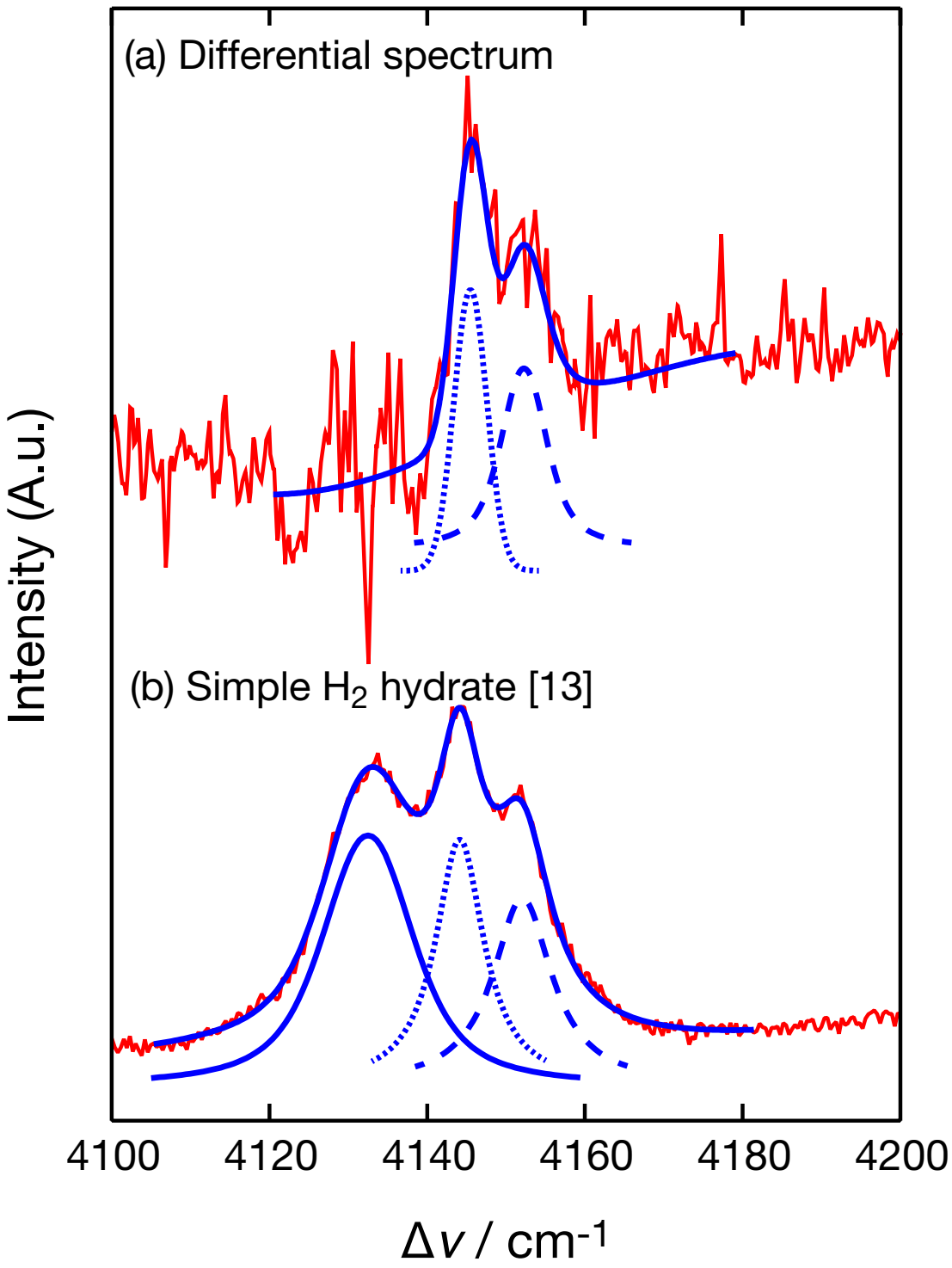

Figure II-1-3. (a) Difference spectrum between **Figure II-1-2(a)** and **Figure II-1-2{(b)+(c)}**, and (b) the Raman spectrum of H_2 in the simple H_2 hydrate [13].

II.1.5. Conclusions

The competitive L-cage occupancy of H_2 molecules in H_2+THF mixed hydrates has been *in situ* observed in a thermodynamically unstable region of the simple H_2 hydrate. The additional Raman peaks, other than the peak derived from single H_2 molecule in S-cage, reveal the competitive L-cage occupancy of H_2 with THF (so-called tuning effect), while the cage occupancy of the H_2+THF mixed hydrates belongs to the compartmental-type on the thermodynamic stability.

II.1.6. Nomenclatures

ν	Wavenumber [m^{-1}]
p	Pressure [Pa]
T	Temperature [K]
x_{THF}	Mole fraction of THF in aqueous solution [-]

II.1.7. References

[1] Y.A. Dyadin, E.G. Larionov, E.Y. Aladko, A.Y. Manakov, F.V. Zhurko, T.V. Mikina, V.Y. Komarov, E.V. Grachev, "Clathrate Formation in Water-Noble Gas (Hydrogen) Systems at High Pressures", *Journal of Structural Chemistry*, **40**, 790–795 (1999).

[2] W.L. Mao, H.K. Mao, A.F. Goncharov, V.V. Struzhkin, Q.Z. Guo, J.Z. Hu, J.F. Shu, R.J. Hemley, M. Somayazulu, Y.S. Zhao, "Hydrogen Clusters in Clathrate Hydrate", *Science*, **297**, 2247–2249 (2002).

[3] K.A. Lokshin, Y. Zhao, D. He, W.L. Mao, H.K. Mao, R.J. Hemley, M.V. Lobanov, M. Greenblatt, "Structure and Dynamics of Hydrogen Molecules in the Novel Clathrate Hydrate by High Pressure Neutron Diffraction", *Physical Review Letters*, **93**, 125503-1–4 (2004).

[4] L.J. Florusse, C.J. Peters, J. Schoonman, K.C. Hester, C.A. Koh, S.F. Dec, K.N. Marsh, E.D. Sloan, "Stable Low-Pressure Hydrogen Clusters Stored in a Binary Clathrate Hydrate", *Science*, **306**, 469–471 (2004).

[5] H. Lee, J.-W. Lee, D.Y. Kim, J. Park, Y.-T. Seo, H. Zeng, I.L. Moudrakovski, C.I. Ratcliffe, J.A. Ripmeester, "Tuning Clathrate Hydrates for Hydrogen Storage", *Nature*, **434**, 743–746 (2005).

[6] S. Hashimoto, S. Murayama, T. Sugahara, H. Sato, K. Ohgaki, "Thermodynamic and Raman Spectroscopic Studies on H_2+Tetrahydrofuran+Water and H_2+Tetra-*n*-Butyl Ammonium Bromide +Water Mixtures Containing Gas Hydrates", *Chemical Engineering Science*, **61**, 7884–7888 (2006).

[7] T.A. Strobel, C.J. Taylor, K.C. Hester, S.F. Dec, C.A. Koh, K.T. Miller, E.D. Sloan, Jr, "Molecular Hydrogen Storage in Binary THF–H_2 Clathrate Hydrates", *The Journal of Physical Chemistry B*, **110**, 17121–17125 (2006).

[8] R. Anderson, A. Chapoy, B. Tohidi, "Phase Relations and Binary Clathrate Hydrate Formation in the System H_2–THF–H_2O", *Langmuir*, **23**, 3440–3444 (2007).

[9] A. Martin, C.J. Peters, "Thermodynamic Modeling of Promoted Structure II Clathrate Hydrates of Hydrogen", *The Journal of Physical Chemistry B*, **113**, 7548–7557 (2009).

[10] S. Hashimoto, T. Sugahara, H. Sato, K. Ohgaki, "Thermodynamic Stability of H_2+Tetrahydrofuran Mixed Gas Hydrate in Nonstoichiometric Aqueous Solutions", *Journal of Chemical & Engineering Data*, **52**, 517–520 (2007).

[11] T. Sugahara, J.C. Haag, P.S.R. Prasad, A.A. Warntjes, E.D. Sloan, A.K. Sum, C.A. Koh, "Increasing Hydrogen Storage Capacity Using Tetrahydrofuran", *Journal of the American Chemical Society*, **131**, 14616–14617 (2009).

[12] T. Sugahara, J.C. Haag, A.A. Warntjes, P.S.R. Prasad, E.D. Sloan, C.A. Koh, A.K. Sum, "Large-Cage Occupancies of Hydrogen in Binary Clathrate Hydrates Dependent on Pressures and Guest Concentrations", *The Journal of Physical Chemistry C*, **114**, 15218–15222 (2010).

[13] S. Amano, T. Tsuda, S. Hashimoto, T. Sugahara, K. Ohgaki, "Competitive Cage-Occupancy of Hydrogen and Argon in Structure-II Hydrates", *Fluid Phase Equilibria*, **298**, 113–116 (2010).

Section 2

Thermodynamic Stabilities of Hydrogen+Methane Binary Gas Hydrates

II.2.1. Abstract

When H_2 is mixed with small amounts of CH_4, the conditions required for clathrate hydrate formation can be significantly reduced when compared to that of simple H_2 hydrate. With growing demand for CH_4 as a commercially viable source of energy, H_2+CH_4 binary hydrates may be more appealing than extensively studied H_2+THF hydrates from an energy density standpoint. Using Raman spectroscopic and PXRD measurements, I show that hydrate structure and storage capacities of H_2+CH_4 mixed hydrates are largely dependent on the composition of the initial gas mixture, total system pressure, and formation period. In some cases, H_2+CH_4 hydrate kinetically forms s-I first, even though the thermodynamically stable phase is s-II.

II.2.2. Introduction

As the amount of easily accessible petroleum-based energy resources continues to decline, the need for alternative energy materials is crucial. Of the recently proposed alternatives, two of the more promising include the use of H_2 and natural gas (e.g. CH_4). Examining the current technologies, many ways exist to store and transport these gases such as, simple compression, liquefaction, metal hydrides, and metal organic frameworks [1]. Alternatively, with the ability to concentrate gases over 175 times their volume at standard conditions, clathrate hydrates, such as those occurring naturally in sediments under the ocean floor and in permafrost regions, have also been considered a promising energy storage medium [2–5]. However, whereas the structure and thermodynamics of natural gas hydrates are relatively well understood, comparatively little is known about H_2+CH_4 mixed hydrates.

H_2 was initially believed to be too small to stabilize hydrate cavities, and it was not until 1999 that the phase diagram of the H_2 hydrate system was reported by Dyadin *et al*. [6]. Since this

pioneering work, several other key discoveries have been made highlighting the structure, cage occupancies, and storage capacities of H_2 hydrates [7–24]. Despite encouraging initial results, the major consensus of much of the previous work has been that due to the extremely high pressures and/or low temperatures (e.g. $p \approx 150$ MPa, $T = 270$ K) required for their stabilization [11], simple H_2 hydrates may be impractical for application.

As a means of easing the extreme thermodynamic requirements, several studies have investigated the possibility of adding small amounts of a second larger guest to better stabilize the hydrate structure [9,10,12–15,17,18,20,21,23,24]. One of the more encouraging binary hydrate systems is H_2+THF mixed hydrate. By simply adding 5.6 mol% THF, mixed hydrate can form at much more moderate conditions than simple H_2 hydrate [13]. Specifically, simple H_2 hydrates form at around $p = 150$ MPa and $T = 270$ K [11], while H_2+THF mixed hydrates form at around $p = 10$ MPa and $T = 280$ K [9,13]. However, the trade off in this scenario is that only a limited amount of H_2 can be enclathrated in the mixed hydrate as stated in **Chapter II Section 1**. For hydrates to become a practical storage medium, it is important to achieve a high energy density at relatively mild conditions. Addressing this issue, Lee *et al*. and Sugahara *et al*. reported a "tuning effect" for the H_2+THF hydrate system in 2005 and 2009, respectively [10,21]. They reported that by reducing the amount of THF added to below 5.6 mol%, H_2 could occupy not only the S-cages but also some of the L-cages. In principle, tuned H_2+THF hydrates could be an interesting energy storage medium. The proof-of-concept for the tuned H_2+THF hydrates was confirmed in **Chapter II Section 1**. However, reproducing the quantitative results on the tuning effect for the H_2+THF system has been a source of controversy [13,14,20,23].

I suggest that, like THF, CH_4 may also serve as a thermodynamic promoter, but unlike THF, CH_4 is small enough that H_2 may compete for occupancy in the larger cages resulting in an overall increase in H_2 enclathration. Furthermore, H_2+CH_4 mixed hydrates are expected to have the higher overall energy density than H_2+THF hydrates because CH_4 serves as an additional source of energy, unlike THF. When compared to H_2+THF mixed hydrate, hydrates incorporating H_2 and CH_4 are comparatively underexplored [15,22,24], with some authors suggesting the H_2+CH_4 system as incapable of forming binary hydrates [15]. In this section, I confirm the formation of binary H_2+CH_4 hydrates and report preliminary results on the thermodynamics of this system, including the effect of initial mole fraction of mixed gas, pressure, and formation period. Hydrate crystal structure and cage occupancies of guest species were obtained from PXRD and Raman spectroscopy, respectively.

II.2.3. Experimental

Apparatus

A high-pressure vessel (Hip, inner volume: ~ 4 mL) was used for hydrate preparation. A gas chromatograph (GC) (Hewlett Packard, 5890 Series II) with a thermal conductivity detector (TCD-GC) was used for decision of gas composition. A powder X-ray diffractometer (Siemens, Kristalloflex 805) with Cu X-ray (generation power: 45 kV, 40 mA) was used for determination of crystal structure of hydrate. A Raman spectrometer (Horiba, Jobin Yvon) with a diode laser (wavelength: 532.268 nm) was used for clarification of cage occupancy of guest species.

Procedure

Hydrates studied in this study were synthesized by pressurizing ice powders incorporating particles less than 180 μm. About 1 g of the ice powder was loaded into a high-pressure cell of internal volume ~ 4 mL followed by immersion in a glycol cooling bath held at 263 K. The cell containing the ice powder was allowed to equilibrate in the bath for more than an hour so that the inner cell temperature would rise from LN_2 temperature to the bath temperature. The cell was then pressurized first with CH_4 followed by H_2 up to the respective desired pressures for each experiment. The partial pressures of each component were calculated using the Peng-Robinson equation of state [25,26] to satisfy the desired composition of the initial mixed gas. As a means of confirming the initial gas composition, an empty cell was simultaneously pressurized in parallel with the same mixed gas and the contents in the empty cell were later analyzed with GC in order to determine any differences between the measured and estimated mole fractions. After pressurization, the cell was left in the glycol bath for a desired formation period. Then the cell was quenched in LN_2 for 15 minutes and vented. The hydrate sample was then analyzed with PXRD and Raman spectrometer at p = 0.1 MPa and T = 83 K. PXRD measurement was performed in the step-scan mode with a dwell time of 2 s and a step size of 0.02°. The PXRD pattern indexing and cell refinement were performed with PowderX [27] and Chekcell [28] programs.

II.2.4. Results and Discussion

Whereas the thermodynamics of binary hydrates including H_2 and larger guest molecules such as THF has been well characterized [9,10,12–14,17,18,20,21,23], comparatively little is known about the thermodynamics of H_2+CH_4 binary hydrate [15,22,24]. From the available studies, the general agreement is that at modest mole fractions of CH_4 [22], s-I is the preferred structure [15,24].

However, it is expected that as the mole fraction of CH_4 decreases, s-II may become more favorable as simple H_2 hydrates naturally form s-II [7]. In the following figures, I show that like other known gas mixtures such as CH_4+C_2H_6 [29–31], the hydrate structure of the H_2+CH_4 mixed system is dependent on at least three variables; initial gas mole fraction, pressure and formation period.

Figures II-2-1 and 2 show Raman spectroscopic evidence of hydrate structural dependence on the initial composition of the gas mixture and total system pressure when held at constant temperature (T = 263 K) and formation period (t = 72 h). At a constant pressure (p = 70 MPa), samples prepared at $y_{CH4} \leq 0.01$ formed no hydrate, $0.03 \leq y_{CH4} \leq 0.05$ formed s-II hydrates, and $y_{CH4} \geq 0.07$ formed s-I hydrates. At a fixed concentration (y_{CH4} = 0.05), the results indicate that s-I hydrates are initially stable starting around p = 50 MPa and it is only when the pressure exceeds $p \approx$ 70 MPa does s-II become the more favorable structure.

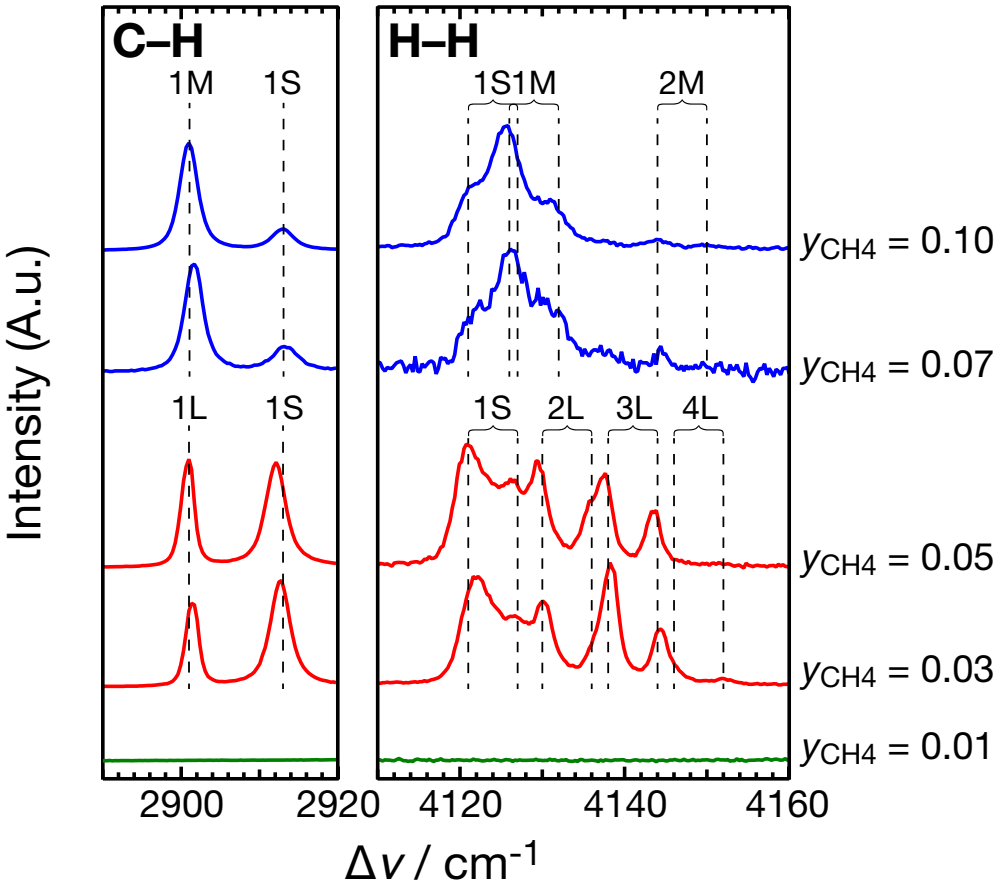

Figure II-2-1. Raman spectra indicating composition dependence at p = 70 MPa and t = 72 h.

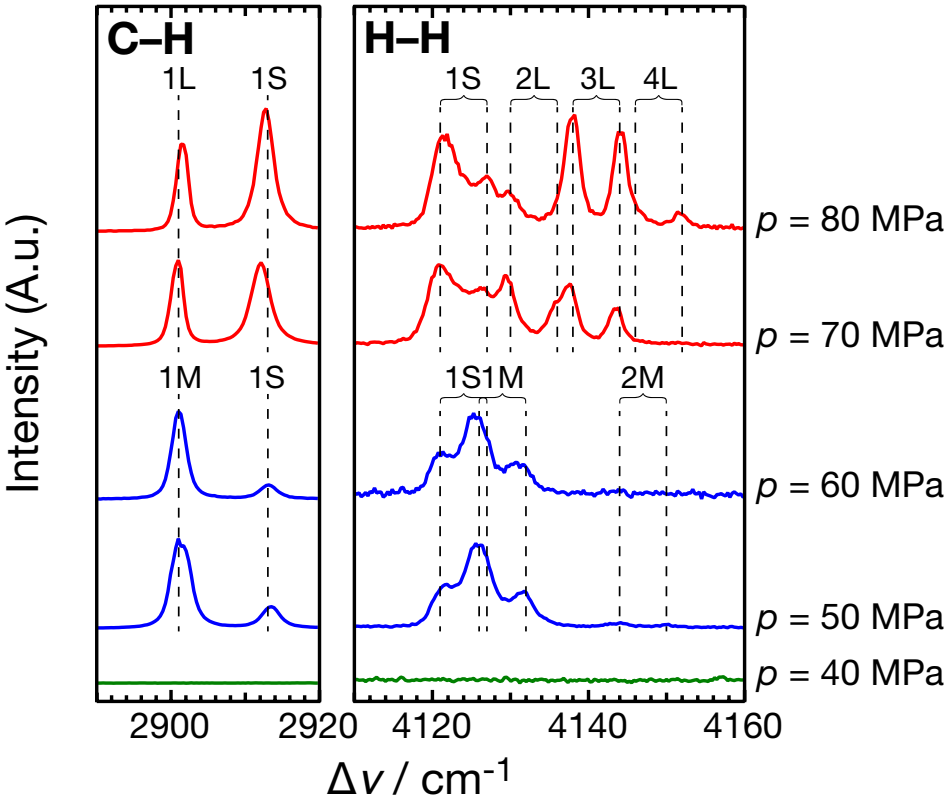

Figure II-2-2. Raman spectra indicating initial pressure dependence at $y_{CH4} = 0.05$ and $t = 72$ h.

Hydrate structure was confirmed directly by PXRD as well as indirectly by the Raman shift. In **Figure II-2-1** at $y_{CH4} \geq 0.07$, the C–H stretching vibration mode region shows two peaks occurring at $\Delta\nu = 2901$ cm^{-1} and 2913 cm^{-1} corresponding with CH_4 occupancy of the M- and S-cages, respectively, in s-I hydrates [24]. Furthermore, the approximate peak area ratio (A_L/A_S) of the two contributions is 3.26, which is similar to the stoichiometry of the s-I hydrate unit cell (two S-cages + six M-cages). Conversely, at $y_{CH4} \leq 0.0$ 5, the approximate peak area ratio (A_L/A_S) of 0.55 confirms the hydrate structure had changed to s-II (sixteen S-cages + eight L-cages).

In contrast to the C–H stretching vibration mode region, where only two peaks are observed (one per cage), in the H–H stretching vibration mode region, multiple peaks per cage are observed due to the multiple clusters and quantum spin of H_2 [19]. H_2 has two kinds of spin isomers, ortho and para [32], occurring in a ratio 3:1 at temperatures near the ice point. For s-I hydrates, the peaks at $\Delta\nu = 4121$ cm^{-1} and 4127 cm^{-1} are derived from H_2 singly occupied in S-cages, the peaks at $\Delta\nu = 4126$ cm^{-1} and 4132 cm^{-1} are from H_2 singly occupied in M-cages, and the peaks at $\Delta\nu = 4144$ cm^{-1} and 4150 cm^{-1} indicate H_2 doubly occupied in M-cages, as previously reported [24]. In the case of s-II hydrate, the peaks at $\Delta\nu = 4121$ cm^{-1} and 4127 cm^{-1} are the same as s-I hydrate, the peaks at $\Delta\nu = 4130$ cm^{-1} and 4136 cm^{-1} are derived from doubly occupied L-cages, the peaks at $\Delta\nu = 4138$ cm^{-1} and 4144 cm^{-1} indicate triply occupied L-cages, and the peaks at $\Delta\nu = 4146$ cm^{-1} and 4152 cm^{-1} indicate quadruply occupied L-cages, in agreement with previous reported data [19].

From the PXRD measurements in **Figure II-2-3**, the space group and lattice constant of a typical s-I H_2+CH_4 hydrate sample were determined to be *Pm3n* with a = 1.187 ± 0.001 nm, and for a typical s-II H_2+CH_4 hydrate, *Fd3m* and a = 1.715 ± 0.003 nm. Interestingly, some of the s-I and s-II hydrate samples showed a significant amount of ice Ih in coexistence with the hydrate phase despite initially being well inside the estimated s-II hydrate phase space (**Figure II-2-4**). This appearance of ice is likely a result of isochoric procedure used in synthesizing the hydrates. Specifically, although the initial gas phase composition is within the thermodynamically stable region for s-II hydrate, due to the larger molecular diameter of CH_4, CH_4 may preferentially become enclathrated, resulting in a depletion of available CH_4 in the gas phase moving the system towards the equilibrium conditions ($H_{II}S_1G$) after a small fraction of conversion.

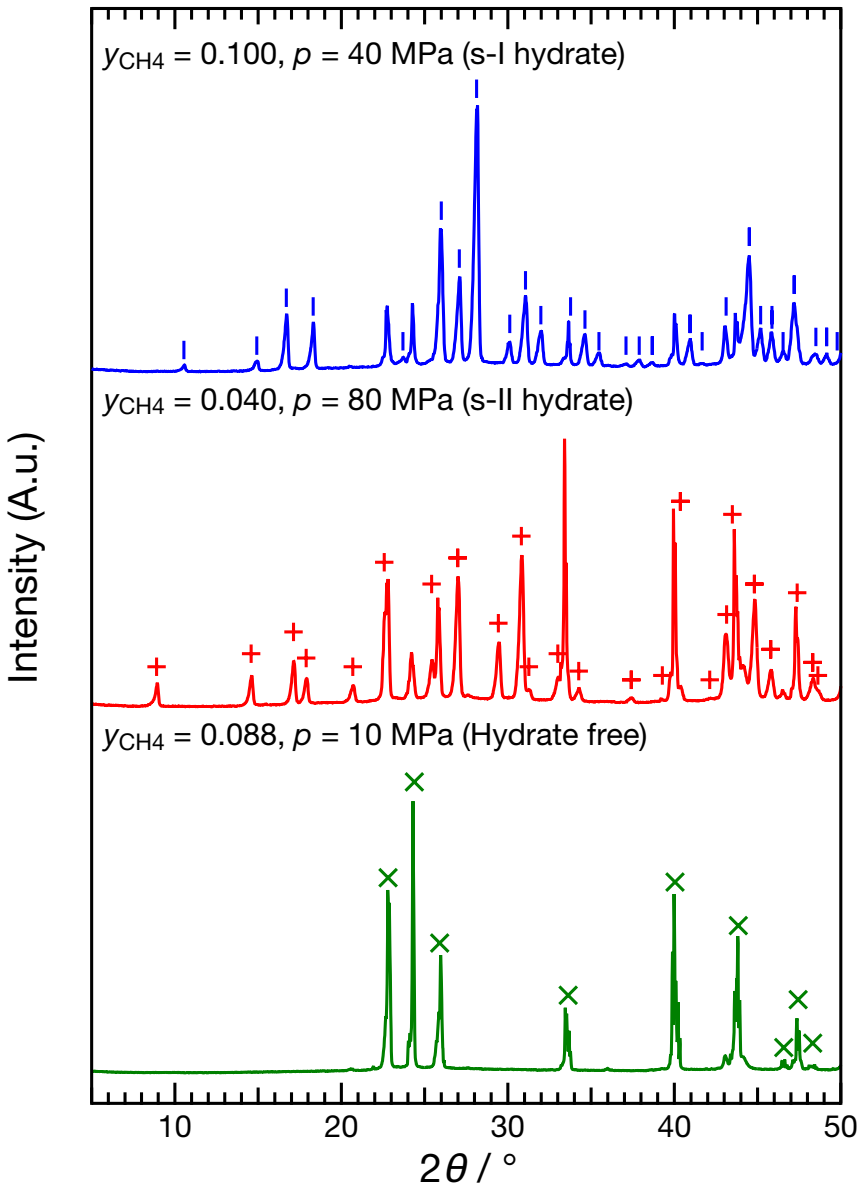

Figure II-2-3. PXRD pattern of three hydrate samples obtained in the present study highlighting the characteristic peaks for s-I, s-II, and hydrate free samples (ice-Ih).

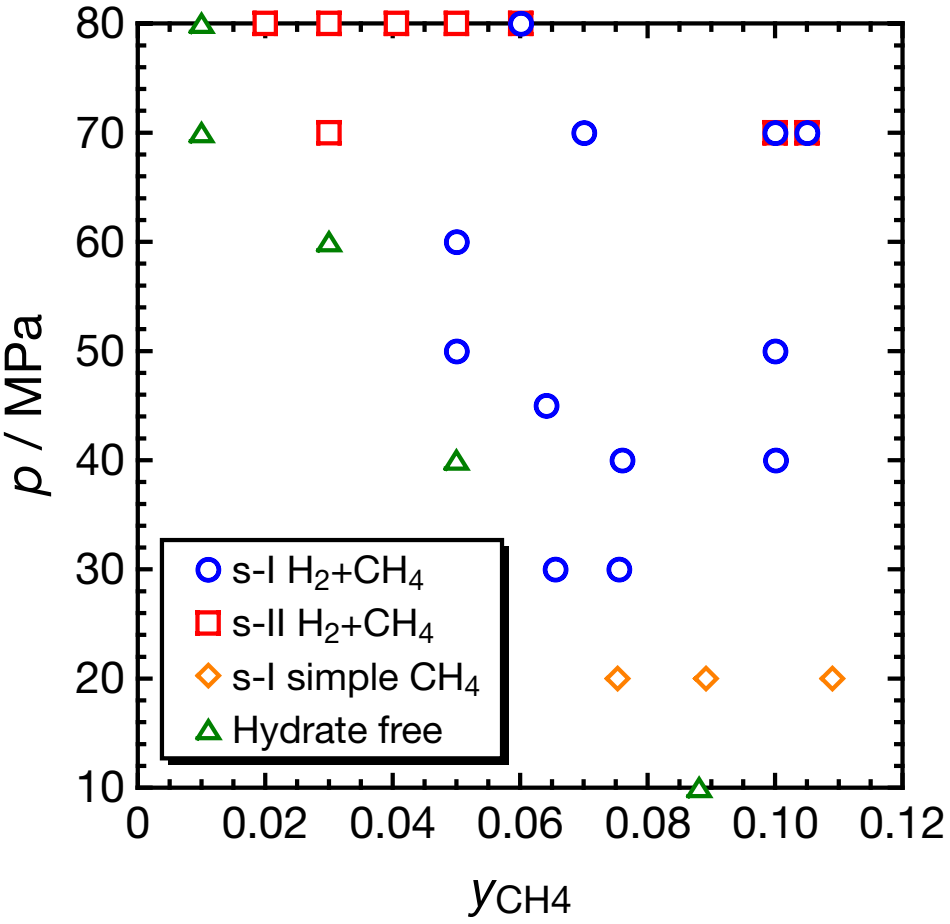

Figure II-2-4. Experimentally observed hydrate structures over a range of pressures and initial gas compositions in H_2+CH_4+water system at t = 72 h and T = 263 K.

From the viewpoint of H_2 storage capacity, s-II hydrate is expected to be more desirable than s-I hydrate due to the ability of the L-cage of s-II hydrate to enclathrate up to four H_2 molecules compared to two H_2 in the M-cage of s-I hydrate [16]. However, from **Figures II-2-1 and 2**, s-II hydrates were observed only in a limited range of conditions. Consequently, a series of additional experiments examining the hydrate structure at a wider range of pressures and CH_4 concentrations were performed to provide a better estimate of the phase space, as shown in **Figure II-2-4**.

Figure II-2-4 shows that at T = 263 K four distinct regions are present in the H_2+CH_4 system in the range of p = 10–80 MPa and y_{CH4} = 0–0.12. Some samples, for example measured at y_{CH4} = 0.10 and p = 70 MPa, showed the co-existence of s-I and s-II hydrates, this implying the system was not yet at equilibrium and maybe a result of the isochoric method. These initial results reveal that from a practical standpoint, although s-II hydrate may have a higher H_2 density, the thermodynamic window for s-II hydrate is small and the requirements necessary for formation, $p \geq$ 70 MPa, remain extreme even after the addition of a CH_4 co-guest molecule. Furthermore, as the pressure decreases around p = 20 MPa, the driving force required to enclathrate H_2 in either structure was too low, resulting in the formation of simple CH_4 hydrate.

In one additional study, the effect of formation period at a fixed mole fraction (y_{CH4} = 0.03) and pressure (p = 70 MPa) was studied (**Figure II-2-5**). Interestingly, although s-II was determined to be the thermodynamically preferred structure at these conditions (as shown above in **Figures II-2-1 and 4**), a metastable s-I hydrate phase was observed as the kinetically favorable structure in the early stages of formation. It was only at t = 5 h that the spectra indicate a change from s-I hydrate to s-II hydrate. To explain this structural change during the formation process, I propose that the ice initially surrounded with CH_4 will quickly convert to a metastable s-I CH_4-rich hydrate seed. Then, the H_2+CH_4 hydrate may then convert to the equilibrium s-II structure with the spectra appearing mostly constant after t = 24 h.

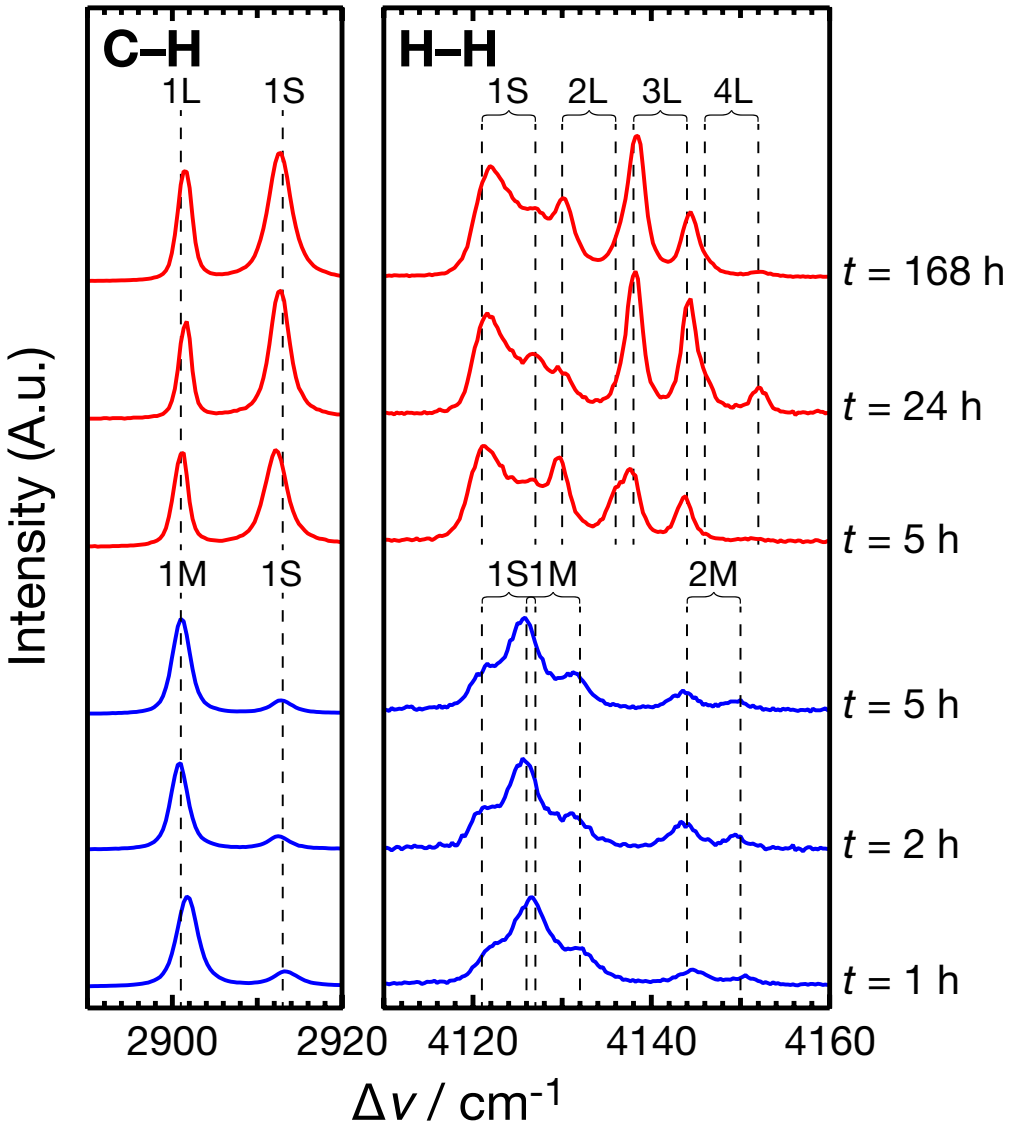

Figure II-2-5. Raman spectral change for each formation period at y_{CH4} = 0.03 and p = 70 MPa.

II.2.5. Conclusions

H_2+CH_4 hydrates prepared at various conditions were analyzed by PXRD and Raman spectroscopy to reveal hydrate structure and cage occupancies of H_2 and CH_4, respectively. The structure of H_2+CH_4 hydrate was determined to be strongly dependent on the mole fraction of mixed gas, total system pressure, and formation period. H_2 and CH_4 were observed to competitively occupy the S-, M-, and L-cages. These hydrates form at more moderate conditions compared to simple H_2 hydrate and H_2+THF tuned hydrate.

II.2.6. Nomenclatures

θ	Diffraction angle [°]
ν	Wavenumber [m^{-1}]
A_L	Raman peak area corresponding CH_4 occupying large cage [-]
A_S	Raman peak area corresponding CH_4 occupying small cage [-]
a	Lattice constant [m]
p	Pressure [Pa]
T	Temperature [K]
t	Formation period [h]
y_{CH4}	Mole fraction of CH_4 in gas phase (water free) [-]
z_{CH4}	Mole fraction of CH_4 in hydrate phase (water free) [-]
G	Gas phase
H_{II}	s-II hydrate phase
S_1	Ice phase

II.2.7. References

[1] N.L. Rosi, J. Eckert, M. Eddaoudi, D.T. Vodak, J. Kim, M. O'Keeffe, O.M. Yaghi, "Hydrogen Storage in Microporous Metal-Organic Frameworks", *Science*, **300**, 1127–1129 (2003).

[2] K.A. Kvenvolden, "Methane Hydrate — A Major Reservoir of Carbon in the Shallow Geosphere?", *Chemical Geology*, **71**, 41–51 (1988).

[3] P. Englezos, "Clathrate Hydrates", *Industrial & Engineering Chemistry Research*, **32**, 1251–1274 (1993).

[4] J.S. Gudmundsson, M. Parlaktuna, A.A. Khokhar, "Storing Natural Gas as Frozen Hydrate", *SPE Production & Facilities*, **9**, 69–73 (1994).

[5] E.D. Sloan, C.A. Koh, *Clathrate Hydrates of Natural Gases, 3rd Ed.*; CRC Press, Taylor and Francis Group: Boca Raton, FL, 2008.

[6] Y.A. Dyadin, E.G. Larionov, A.Y. Manakov, F.V. Zhurko, E.Y. Aladko, T.V. Mikina, V.Y. Komarov, "Clathrate Hydrates of Hydrogen and Neon", *Mendeleev Communications*, **9**, 209–210 (1999).

[7] W.L. Mao, H.K. Mao, A.F. Goncharov, V.V. Struzhkin, Q.Z. Guo, J.Z. Hu, J.F. Shu, R.J. Hemley, M. Somayazulu, Y.S. Zhao, "Hydrogen Clusters in Clathrate Hydrate", *Science*, **297**, 2247–2249 (2002).

[8] K.A. Lokshin, Y. Zhao, D. He, W.L. Mao, H.K. Mao, R.J. Hemley, M.V. Lobanov, M. Greenblatt, "Structure and Dynamics of Hydrogen Molecules in the Novel Clathrate Hydrate by High Pressure Neutron Diffraction", *Physical Review Letters*, **93**, 125503-1–4 (2004).

[9] L.J. Florusse, C.J. Peters, J. Schoonman, K.C. Hester, C.A. Koh, S.F. Dec, K.N. Marsh, E.D. Sloan, "Stable Low-Pressure Hydrogen Clusters Stored in a Binary Clathrate Hydrate", *Science*, **306**, 469–471 (2004).

[10] H. Lee, J.-W. Lee, D.Y. Kim, J. Park, Y.-T. Seo, H. Zeng, I.L. Moudrakovski, C.I. Ratcliffe, J.A. Ripmeester, "Tuning Clathrate Hydrates for Hydrogen Storage", *Nature*, **434**, 743–746 (2005).

[11] K.A. Lokshin, Y. Zhao, "Fast Synthesis Method and Phase Diagram of Hydrogen Clathrate Hydrate", *Applied Physics Letters*, **88**, 131909-1–3 (2006).

[12] T.A. Strobel, C.J. Taylor, K.C. Hester, S.F. Dec, C.A. Koh, K.T. Miller, E.D. Sloan, Jr, "Molecular Hydrogen Storage in Binary THF–H_2 Clathrate Hydrates", *The Journal of Physical Chemistry B*, **110**, 17121–17125 (2006).

[13] S. Hashimoto, S. Murayama, T. Sugahara, H. Sato, K. Ohgaki, "Thermodynamic and Raman Spectroscopic Studies on H_2+Tetrahydrofuran+Water and H_2+Tetra-*n*-Butyl Ammonium Bromide +Water Mixtures Containing Gas Hydrates", *Chemical Engineering Science*, **61**, 7884–7888 (2006).

[14] R. Anderson, A. Chapoy, B. Tohidi, "Phase Relations and Binary Clathrate Hydrate Formation in the System H_2–THF–H_2O", *Langmuir*, **23**, 3440–3444 (2007).

[15] S.S. Skiba, E.G. Larionov, A.Y. Manakov, B.A. Kolesov, V.I. Kosyakov, "Investigation of Hydrate Formation in the System H_2–CH_4–H_2O at a Pressure up to 250 MPa", *The Journal of Physical Chemistry B*, **111**, 11214–11220 (2007).

[16] T.A. Strobel, C.A. Koh, E.D. Sloan, "Hydrogen Storage Properties of Clathrate Hydrate Materials", *Fluid Phase Equilibria*, **261**, 382–389 (2007).

[17] J.-H. Yoon, J. Han, J. Park, S. Choi, S.-H. Yeon, H. Lee, "Spectroscopic Identification, Thermodynamic Stability and Molecular Composition of Hydrogen and 1,4-Dioxane Binary Clathrate Hydrate", *Journal of Physics and Chemistry of Solids*, **69**, 1432–1435 (2008).

[18] A.R.C. Duarte, A. Shariati, L.J. Rovetto, C.J. Peters, "Water Cavities of sH Clathrate Hydrate Stabilized by Molecular Hydrogen: Phase Equilibrium Measurements", *The Journal of Physical Chemistry B*, **112**, 1888–1889 (2008).

[19] T.A. Strobel, E.D. Sloan, C.A. Koh, "Raman Spectroscopic Studies of Hydrogen Clathrate Hydrates", *The Journal of Chemical Physics*, **130**, 014506-1–10 (2009).

[20] T.A. Strobel, C.A. Koh, E.D. Sloan, "Thermodynamic Predictions of Various Tetrahydrofuran and Hydrogen Clathrate Hydrates", *Fluid Phase Equilibria*, **280**, 61–67 (2009).

[21] T. Sugahara, J.C. Haag, P.S.R. Prasad, A.A. Warntjes, E.D. Sloan, A.K. Sum, C.A. Koh, "Increasing Hydrogen Storage Capacity Using Tetrahydrofuran", *Journal of the American Chemical Society*, **131**, 14616–14617 (2009).

[22] J. Pang, H.-J. Ng, J. Zuo, D. Zhang, Q. Ma, G. Chen, "Hydrogen Gas Hydrate—Measurements and Predictions", *Fluid Phase Equilibria*, **316**, 6–10 (2012).

[23] R.G. Grim, P.B. Kerkar, E.D. Sloan, C.A. Koh, A.K. Sum, "Rapid Hydrogen Hydrate Growth from Non-Stoichiometric Tuning Mixtures during Liquid Nitrogen Quenching", *The Journal of Chemical Physics*, **136**, 234504-1–5 (2012).

[24] R.G. Grim, P.B. Kerkar, M. Shebowich, M. Arias, E.D. Sloan, C.A. Koh, A.K. Sum, "Synthesis and Characterization of sI Clathrate Hydrates Containing Hydrogen", *The Journal of Physical Chemistry C*, **116**, 18557–18563 (2012).

[25] D.-Y. Peng, D.B. Robinson, "A New Two-Constant Equation of State", *Industrial & Engineering Chemistry Fundamentals*, **15**, 59–64 (1976).

[26] H. Knapp, R. Doring, L. Oellrich, U. Plocker, J.M. Prausnitz, "Vapor-Liquid Equilibria for Mixtures of Low Boiling Substances", *Chemistry Data Series, vol. VI*; Dechema, Frankfult, 1982.

[27] C. Dong, "PowderX: Windows-95-based Program for Powder X-Ray Diffraction Data Processing", *Journal of Applied Crystallography*, **32**, 838 (1999).

[28] Chekcell; http://www.ccp14.ac.uk. Chekcell developed by L. Laugier, B. Bochu, Laboratoire des Materiaux et du Genie Physique, Ecole Superieure de Physique de Grenoble: Grenoble, France (accessed April 28, 2011).

[29] S. Subramanian, R.A. Kini, S.F. Dec, E.D. Sloan, "Evidence of Structure II Hydrate Formation from Methane+Ethane Mixtures", *Chemical Engineering Science*, **55**, 1981–1999 (2000).

[30] S. Subramanian, A.L. Ballard, R.A. Kini, S.F. Dec, E.D. Sloan, "Structural Transitions in Methane+Ethane Gas Hydrates—Part I: Upper Transition Point and Applications", *Chemical Engineering Science*, **55**, 5763–5771 (2000).

[31] A.L. Ballard, E.D. Sloan, "Structural Transitions in Methane+Ethane Gas Hydrates—Part II: Modeling Beyond Incipient Conditions", *Chemical Engineering Science*, **55**, 5773–5782 (2000).

[32] G. Herzberg, *Molecular Spectra and Molecular Structure. I. Diatomic Molecules*; Prentice-Hall, New York, 1939.

Section 3

Isothermal Phase Equilibria for the Difluoromethane+1,1,1,2-Tetrafluoroethane Mixed-Gas Hydrate System

II.3.1. Abstract

Isothermal phase equilibria (pressure-composition relations in HL_1G) in the difluoromethane (HFC-32)+1,1,1,2-tetrafluoroethane (HFC-134a) mixed-gas hydrate system were measured at T = 274.15 K, 279.15 K, and 283.15 K. The heterogeneous azeotropic-like behavior derived from the structural phase transition of HFC-32+HFC-134a mixed-gas hydrates appears over the whole temperature range of the present study. In addition to the heterogeneous azeotropic-like behavior, the isothermal phase equilibrium curves of the HFC-32+HFC-134a mixed-gas hydrate system exhibit the negative homogeneous azeotropic-like behavior at T = 279.15 K and 283.15 K. The negative azeotropic-like behavior, which becomes more remarkable at higher temperatures, results in the lower equilibrium pressure of HFC-32+HFC-134a mixed-gas hydrates than that of both simple HFC-32 and HFC-134a hydrates. Although the simple HFC-134a hydrate is transformed from s-II hydrate to s-I hydrate at p = 65 MPa and T = 282.2 K, the present findings reveal that HFC-134a molecules occupy a part of the M-cages of the s-I mixed-gas hydrate even at pressures much lower than p = 65 MPa.

II.3.2. Introduction

Hydrates get much attention as newly refrigerant materials because gas hydrates have appropriate properties for cold energy storage [1,2]. HFCs are well-known refrigerant materials due to the thermodynamic characteristics and chemical stabilities. The hydrates prepared from HFCs have higher enthalpy than liquefied HFCs [3,4]. The phase equilibrium relations and the dissociation enthalpies for some simple HFC hydrates have been reported [5–7]. The studies on HFCs mixed-gas hydrate systems, however, are rarely reported.

In this section, isothermal phase equilibria (pressure-composition) in an HFCs mixed-gas hydrate system including typical refrigerant gases, HFC-32 and HFC-134a, were investigated. The main purpose of the present study is to reveal the three-phase equilibrium relations of HL_1G in the HFC-32+HFC-134a mixed-gas hydrate system for the improvement of refrigerant cycles. In addition, the hydrate structures and the cage occupancies of guest species are discussed, based on the Raman spectra.

II.3.3. Experimental

Materials

The materials used in the present study are summarized in **Table II-3-1**. All of them were used without further purification.

Table II-3-1. Information on the materials used in the present study.

Material name	Source	Mole fraction purity
HFC-32	Neriki Gas Co., Ltd.	> 0.999
HFC-134a	Daikin Ind., Ltd.	> 0.996
Distilled water	Wako Pure Chemicals Ind., Ltd.	> 0.9999

Apparatus

The present experimental apparatus for the isothermal phase equilibrium measurement is shown in **Figure II-3-1**. A high-pressure cell (inner volume: 150 cm^3, maximum working pressure: 10 MPa) was used. The temperature was controlled with a thermocontroller (Taitec, CL-80R). The equilibrium pressure was measured with a pressure gauge (Valcom, VPRT, maximum uncertainty: 0.004 MPa). The equilibrium temperature was measured with a thermistor thermometer (Takara, D632, reproducibility: 0.02 K). A TCD-GC (Shimadzu, GC-14B, maximum uncertainty: 0.005) was used for determination of compositions. The pressure was calibrated by a Ruska quartz Bourdon tube gauge (Ruska, Pressure Counter 3855-703-00). The temperature was calibrated with a platinum resistance thermometer (25 Ω) defined by ITS-90.

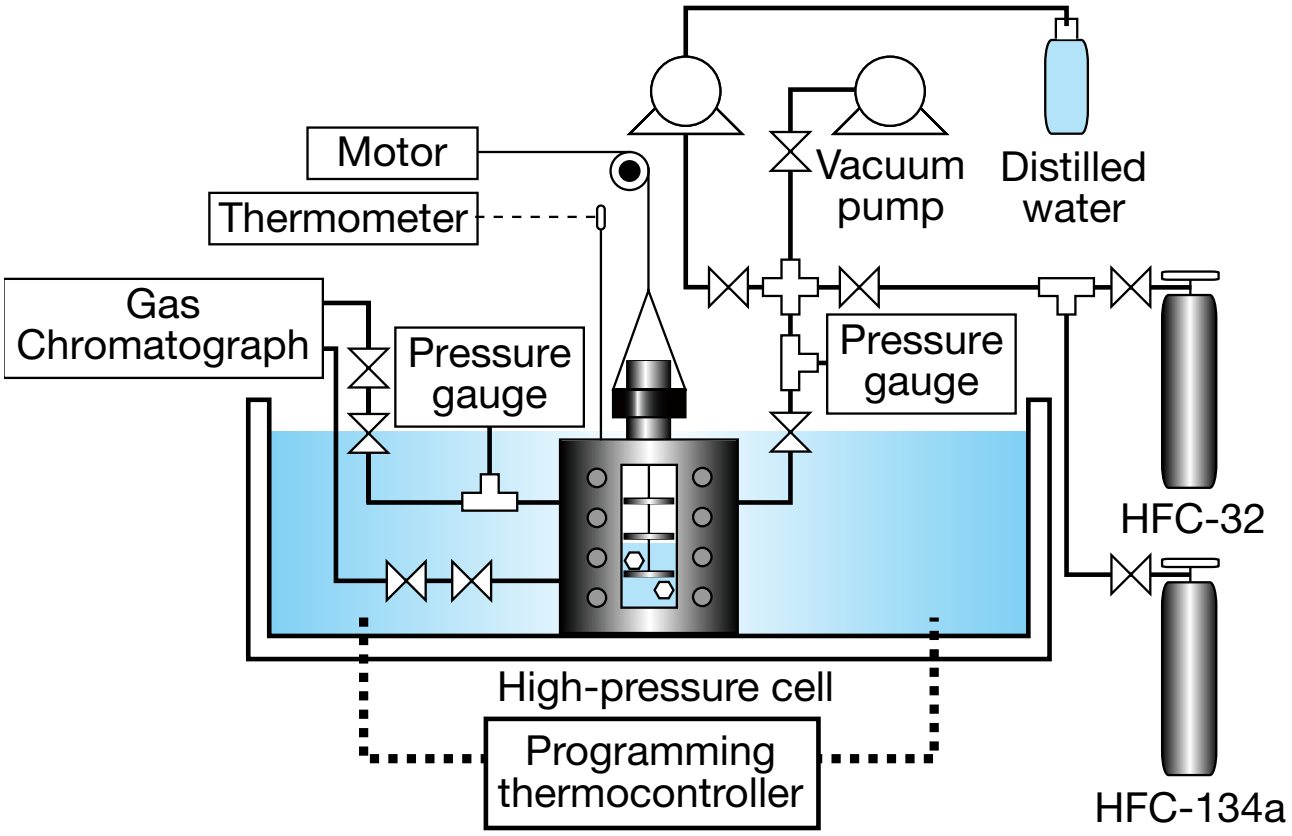

Figure II-3-1. Schematic illustration of the experimental apparatus for phase equilibrium measurement performed in the present study.

The present experimental apparatus for the Raman spectroscopic analysis is shown in **Figure II-3-2**. The high-pressure optical cell (inner volume: 0.1 cm^3, maximum working pressure: 400 MPa) was used for Raman spectroscopy. A programming thermocontroller (Taitec, CL-80R) adjusted the cell temperature. The equilibrium pressure was measured by a pressure gauge (Valcom, VPRT, maximum uncertainty: 0.02 MPa). The equilibrium temperature was measured with the thermistor thermometer (Takara, D641, reproducibility: 0.02 K). The pressure and temperature were calibrated with as the same ways as mentioned above. A laser Raman microprobe spectrometer with a multichannel CCD detector (Horiba, Jobin-Yvon T64000) and an argon ion laser beam (514.5 nm, 100 mW) condensed to 2 μm in spot diameter were used to analyze hydrate single crystals. The CCD detector was maintained at T = 140 K by LN_2 for heat-noise reduction. The spectral resolution was approximately 0.7 cm^{-1}. The Raman shift was calibrated with the neon emission lines in the air.

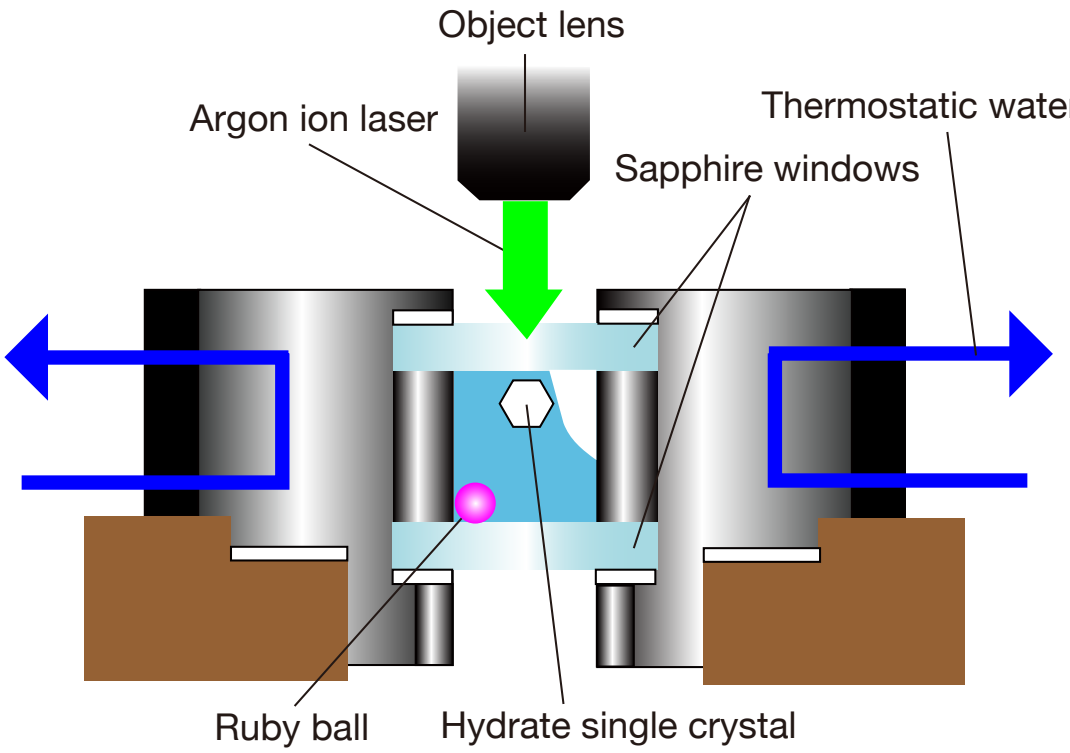

Figure II-3-2. Schematic illustration of the experimental apparatus for Raman spectroscopy performed in the present study.

Procedure

For phase equilibrium measurements, the gas mixture was introduced into an evacuated high-pressure cell. Distilled water was successively introduced into the cell to pressurize up to a desired pressure. The cell was immersed in a thermostatic bath for controlling the system temperature precisely. The content was cooled and agitated by a mixing bar that is moved up-and-down by magnetic attraction from outside of the cell. The phase behavior was directly observed through sapphire windows attached to the cell. After the formation of the mixed-gas hydrates, the temperature was kept constant for at least one day to establish the three-phase equilibrium conditions. After that, a small amount of samples separately taken from the gas and aqueous phases was analyzed by means of GC. The experimental procedure was repeated with various compositions to obtain the three-phase equilibrium (pressure-composition) relations. The equilibrium compositions of hydrate phase were measured in the following way. The mixed-gas hydrates under three-phase equilibrium conditions were prepared with the same procedure mentioned above. Then, only the excess water was sufficiently drained, and then the mixed-gas hydrates were quenched for more than 6 h at T = 263 K. The quenched mixed-gas hydrates were replaced from the formation cell to another one in the refrigerated room controlled at T = 263 K. The sample was allowed to dissociate under room temperature and atmospheric pressure conditions. The released mixed gas was analyzed by means of GC.

For Raman spectroscopy, the mixed-gas hydrates were generated in a high-pressure optical cell by the same procedure mentioned in the previous paragraph. The content was cooled and agitated by an enclosed ruby ball. The temperature was controlled by circulating thermostatic water through the jacket of the cell. After the formation of the mixed-gas hydrates, the temperature was gradually increased and decreased to prepare hydrate single crystals under three-phase coexisting conditions. Then the single crystals were annealed to avoid metastability, and the temperature was kept constant for more than one day to establish the three-phase equilibrium conditions. The phase behavior was observed with CCD camera through the sapphire window. The hydrate single crystal was analyzed by use of Raman spectrometer with multichannel CCD detector. The argon ion laser beam was irradiated from the object lens to the hydrate single crystal through the upper sapphire window.

II.3.4. Results and Discussion

Isothermal pressure (p)-composition ($x_{HFC\text{-}32}$, $y_{HFC\text{-}32}$, $z_{HFC\text{-}32}$) diagrams for the HFC-32+HFC-134a mixed-gas hydrate system at T = 274.15 K, 279.15 K, and 283.15 K under three-phase equilibrium conditions of hydrate, gas, and aqueous phases are shown in **Figures II-3-3 to 5**, respectively. The horizontal axis in **Figures II-3-3 to 5** indicates the equilibrium composition of HFC-32 on a water-free basis. **Table II-3-2** summarizes the p-$x_{HFC\text{-}32}$, $y_{HFC\text{-}32}$ relations for each isotherm obtained without the dissociation of hydrate samples. The obviously unreasonable data in the aqueous phase were removed, due to the incidental involvement of hydrate crystal in the sample of aqueous phase. **Table II-3-3** summarizes the p–$z_{HFC\text{-}32}$ relation for each isotherm. As shown in **Figures II-3-4 and 5**, the isothermal phase equilibrium relations of the HFC-32+HFC-134a mixed-gas hydrate system exhibit the negative homogeneous azeotropic-like behavior at T = 279.15 K and 283.15 K. The local pressure minima are located at p = 0.159 ± 0.004 MPa, $y_{HFC\text{-}32}$ = 0.175 ± 0.005 at T = 279.15 ± 0.02 K and p = 0.302 ± 0.004 MPa, $y_{HFC\text{-}32}$ = 0.471 ± 0.005 at T = 283.15 ± 0.02 K. Especially in the case of T = 283.15 K, a large pressure reduction from the equilibrium pressures of both the simple HFC-32 and HFC-134a hydrates is useful and effective for the refrigerant systems. The pressure reduction is getting small with the decrease in temperature, and finally, the azeotropic-like behavior disappears at T = 274.15 K. Also, the local pressure minimum moves to lower composition range with the decrease in temperature. The experimentally-observed negative azeotropic-like behavior has been already reported in the some mixed-gas hydrate systems, for example, s-II CH_4+C_3H_8 [8], s-II krypton (Kr)+C_3H_8 [8], and s-I CH_4+C_2H_4 [9] mixed-gas hydrate systems. The s-I CH_4+C_2H_4 mixed-gas hydrate system exhibits negative azeotropic behavior at T =

293 K, while the azeotropic behavior disappears at T = 284 K [9]. These results suggest that, at a relatively high temperature, the azeotropic-like behavior is clearly observed. Note that the HFC-32+HFC-134a binary system (excluding water) exhibits no azeotropic-like behavior on the vapor-liquid equilibrium relation in a temperature range of the present study [10,11].

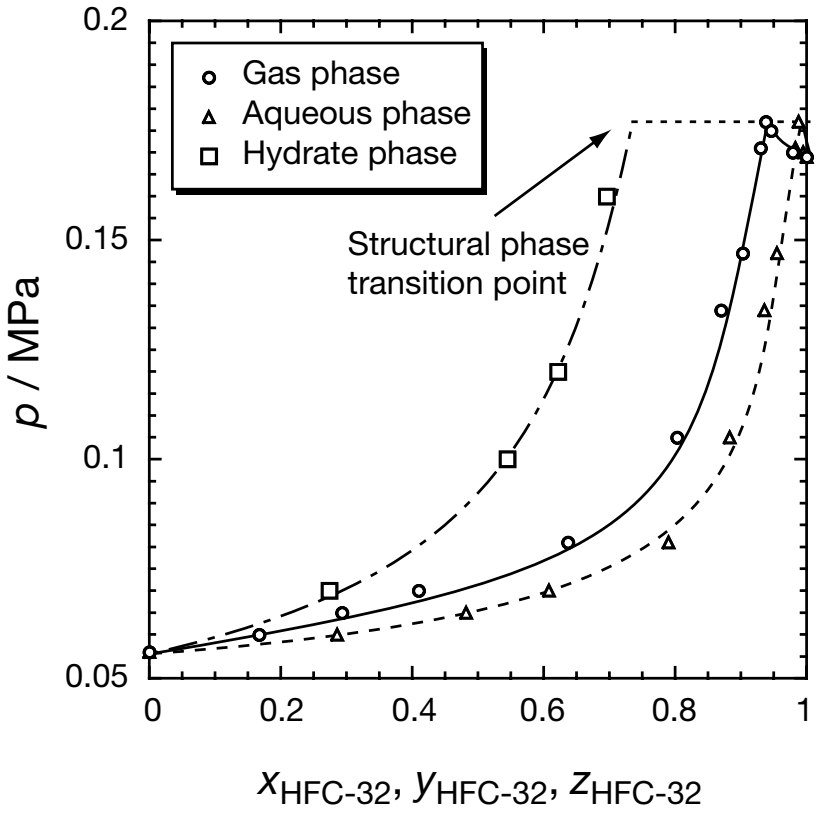

Figure II-3-3. Isothermal phase equilibria of hydrate, gas, and aqueous phases in the HFC-32+HFC-134a mixed-gas hydrate system at T = 274.15 K.

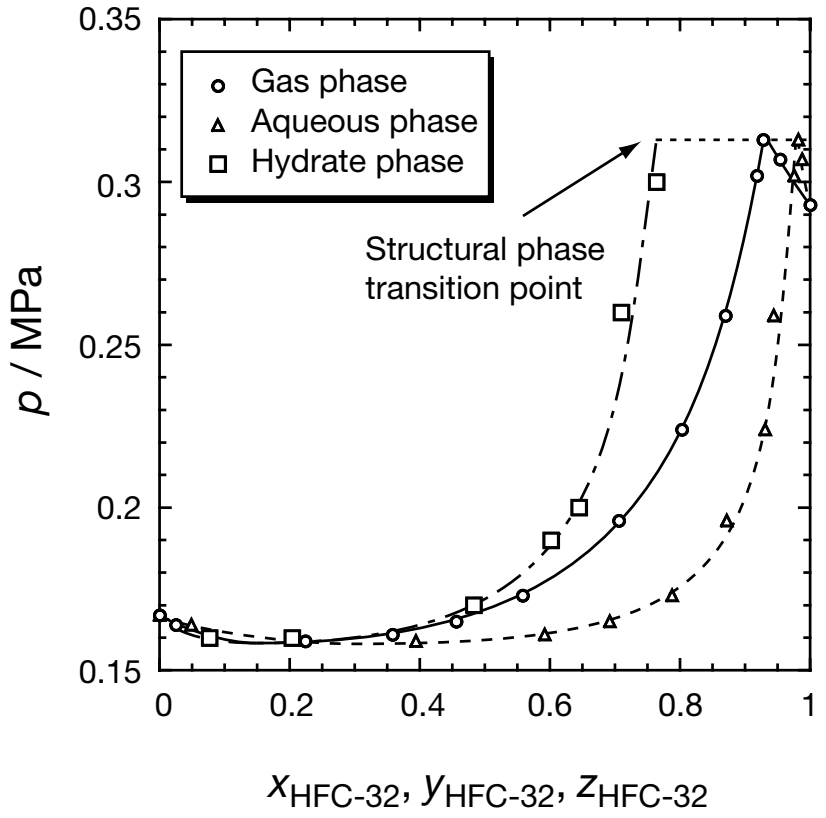

Figure II-3-4. Isothermal phase equilibria of hydrate, gas, and aqueous phases in the HFC-32+HFC-134a mixed-gas hydrate system at T = 279.15 K.

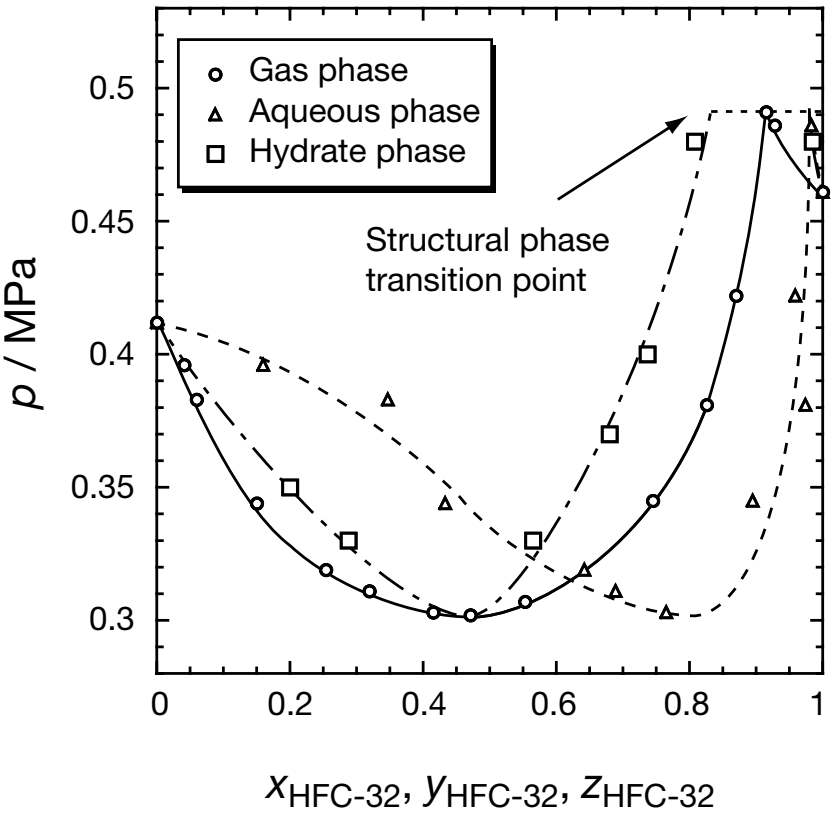

Figure II-3-5. Isothermal phase equilibria of hydrate, gas, and aqueous phases in the HFC-32+HFC-134a mixed-gas hydrate system at T = 283.15 K.

Table II-3-2. Isothermal phase equilibrium data of gas and aqueous phases coexisted with HFC-32+HFC-134a mixed-gas hydrates.

p / MPa[a]	y_{HFC-32}[a]	x_{HFC-32}[a]	p / MPa[a]	y_{HFC-32}[a]	x_{HFC-32}[a]	p / MPa[a]	y_{HFC-32}[a]	x_{HFC-32}[a]
T = 274.15 K[a]			T = 279.15 K[a]			T = 283.15 K[a]		
0.056	0.000	0.000	0.167	0.000	0.000	0.412	0.000	0.000
0.060	0.167	0.286	0.164	0.025	0.049	0.396	0.041	0.160
0.065	0.293	0.482	0.159	0.224	0.394	0.383	0.060	0.347
0.070	0.410	0.608	0.161	0.358	0.592	0.344	0.150	0.433
0.081	0.637	0.790	0.165	0.456	0.692	0.319	0.254	0.642
0.105	0.803	0.883	0.173	0.558	0.788	0.311	0.319	0.689
0.134	0.870	0.936	0.196	0.706	0.872	0.303	0.415	0.765
0.147	0.903	0.955	0.224	0.803	0.931	0.302	0.471	-[b]
0.171	0.930	0.983	0.259	0.870	0.944	0.307	0.553	-[b]
0.177	0.938	0.988	0.302	0.918	0.976	0.345	0.745	0.895
0.175	0.946	-[b]	0.313	0.928	0.982	0.381	0.826	0.974
0.170	0.979	0.995	0.307	0.954	0.988	0.422	0.870	0.959
0.169	1.000	1.000	0.293	1.000	1.000	0.491	0.915	-[b]
						0.486	0.928	0.983
						0.461	1.000	1.000

[a] $u(p)$ = 0.004 MPa, $u(T)$ = 0.02 K, and $u(y_{HFC-32}) = u(x_{HFC-32})$ = 0.005.

[b] The only p-y_{HFC-32} relation is listed in spite of the lack of x_{HFC-32} because the datum set is still meaningful for understanding the phase behavior.

Table II-3-3. Isothermal pressure-composition relations in hydrate phase for the HFC-32+HFC-134a mixed-gas hydrate system.

p / MPa[a]	z_{HFC-32}[a]	p / MPa[a]	z_{HFC-32}[a]	p / MPa[a]	z_{HFC-32}[a]
T = 274.15 K[a]		T = 279.15 K[a]		T = 283.15 K[a]	
0.06	0.00	0.17	0.00	0.41	0.00
0.07	0.27	0.16	0.08	0.35	0.20
0.10	0.55	0.16	0.20	0.33	0.29
0.12	0.62	0.17	0.48	0.33	0.57
0.16	0.70	0.19	0.60	0.37	0.68
0.17	1.00	0.20	0.65	0.40	0.74
		0.26	0.71	0.48	0.81
		0.30	0.76	0.48	0.99
		0.29	1.00	0.46	1.00

[a] $u(p)$ = 0.004 MPa, $u(T)$ = 0.02 K, and $u(z_{HFC-32})$ = 0.01.

Holder and Manganiello [12] and Thakore and Holder [8] claimed that the larger stability of hydrates with certain compositions is due to competing effect of small and large guest molecules and the hydrate structure (they claimed that no azeotropic behavior appears in s-I hydrates [8]), not a non-ideality of hydrates. The results in the present study indicate that the occurrence of the azeotropic behavior cannot be explained only by competing effect due to different sizes of both guest species. The temperature effect on the cage occupancies of both guest species has to be considered.

In addition to the homogeneous azeotropic-like behavior, the heterogeneous azeotropic-like behavior appears in the HFC-32+HFC-134a mixed-gas hydrate system. As shown in **Figures II-3-3 to 5**, a quadruple point exists at $y_{HFC-32} \approx 0.9$ in the equilibrium p-y_{HFC-32} curve and the pressures are higher than equilibrium ones of both simple HFC-32 and HFC-134a hydrates at the same temperature. In general, the structural phase transition of hydrates properly occurs in the mixed-gas hydrate when the crystal structures of the simple hydrates are different from each other. To demonstrate that the heterogeneous azeotropic-like behavior is derived from the structural phase transition, the Raman spectra corresponding to the intramolecular vibration modes of the HFC-32 and HFC-134a molecules at T = 283.15 K are shown in **Figure II-3-6**. The top spectrum at y_{HFC-32} = 0.98 is completely different from others and very similar to that of s-I simple HFC-32 hydrate [4],

while the spectra at $y_{HFC\text{-}32}$ = 0.26, 0.80, and 0.89 are similar to the bottom spectrum derived from the s-II simple HFC-134a hydrate. The Raman spectra reveal the structural phase transition occurs at the quadruple point ($H_IH_{II}L_1G$). The details of the quadruple points ($H_IH_{II}L_1G$) are summarized in **Table II-3-4**. The quadruple point ($H_IH_{II}L_1G$) is one of the most characteristics in the present mixed-gas hydrate system.

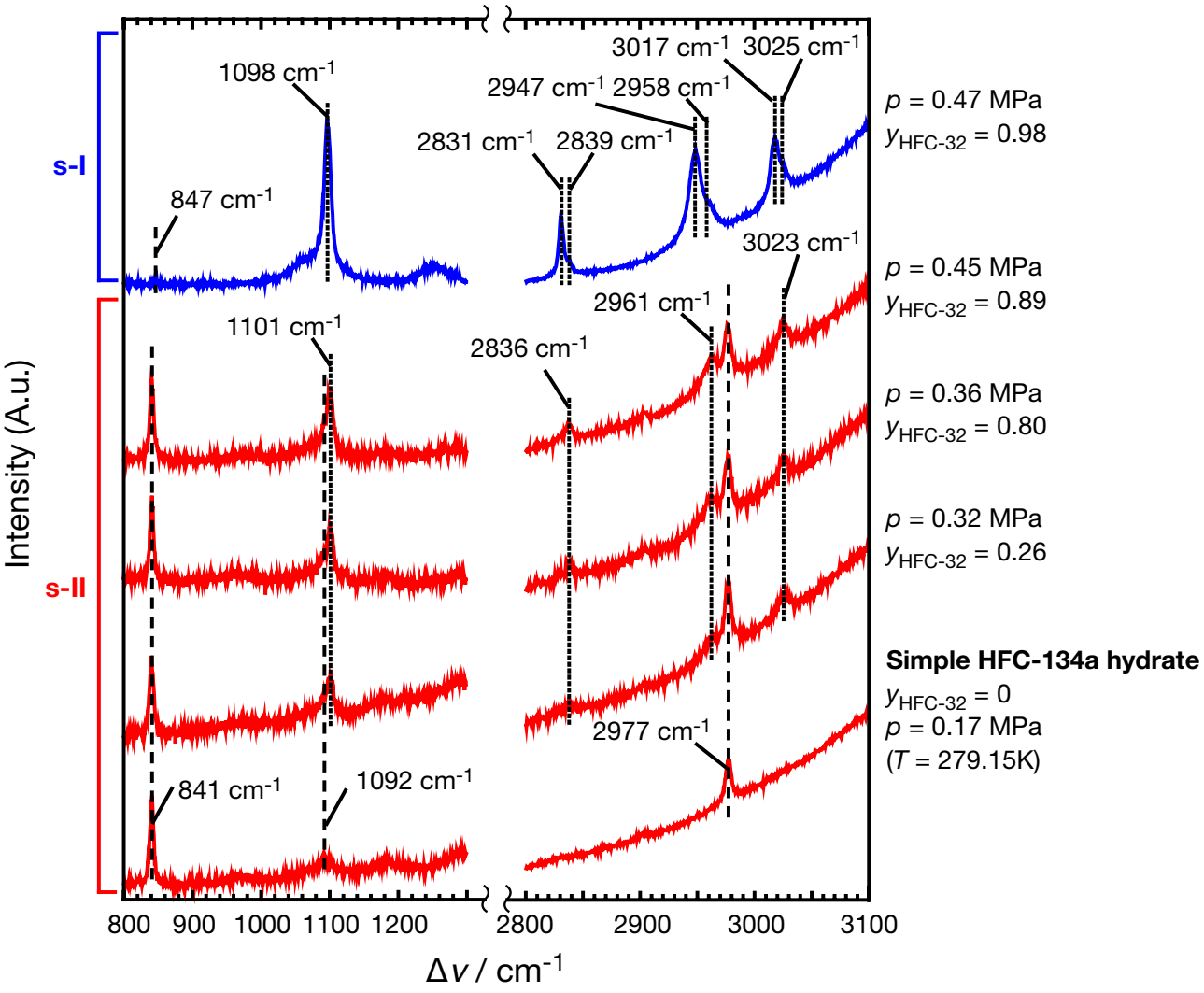

Figure II-3-6. Raman spectra of HFC-32 and HFC-134a molecules in the HFC-32+HFC-134a mixed-gas hydrates at T = 283.15 K, and Raman spectrum in the simple HFC-134a hydrate at T = 279.15 K and p = 0.17 MPa. The Raman peaks detected around $\Delta\nu$ = 840 cm^{-1}, 1090 cm^{-1}, and 2975 cm^{-1} correspond to the intramolecular vibration modes of HFC-134a molecule (broken lines). The peaks detected around $\Delta\nu$ = 1098 cm^{-1}, 2835 cm^{-1}, 2950 cm^{-1}, and 3020 cm^{-1} are the intramolecular vibration modes of HFC-32 molecule (dotted lines). The peaks of HFC-32 molecule in s-I hydrates divide into doublet except for that of $\Delta\nu$ = 1098 cm^{-1} (C–F stretching vibration mode) [4].

Table II-3-4. Summary on the structural phase transition points in the HFC-32+HFC-134a mixed-gas hydrate system. The value of $z_{HFC\text{-}32}$ in the s-I hydrate phase is speculated to be more than 0.99 on each isotherm.

T / K[a]	p / MPa[a]	$y_{HFC\text{-}32}$[a]	$x_{HFC\text{-}32}$[a]	$z_{HFC\text{-}32}$(s-II)[a]
274.15	0.177	0.938	0.988	0.73
279.15	0.313	0.928	0.982	0.77
283.15	0.491	0.915	0.982	0.83

[a] $u(p) = 0.004$ MPa, $u(T) = 0.02$ K, $u(y_{HFC\text{-}32}) = u(x_{HFC\text{-}32}) = 0.005$, and $u(z_{HFC\text{-}32}) = 0.01$.

The Raman spectra provide the additional knowledge regarding the cage occupancy of guest species. HFC-134a molecules occupy only L-cages of the s-II HFC-32+HFC-134a mixed-gas hydrates in the composition range of $y_{HFC\text{-}32}$ = 0.26–0.89, based on the single Raman peak in the simple HFC-134a hydrate shown in bottom spectrum of **Figure II-3-6**. In the hydrate equilibrated with the gas phase of $y_{HFC\text{-}32}$ = 0.98, a weak Raman peak was detected at $\Delta\nu$ = 847 cm^{-1}. This Raman shift does not correspond to the C–C stretching vibration mode of HFC-134a enclathrated into L-cages ($\Delta\nu$ = 841 cm^{-1}) of s-II hydrates. It is also different from the Raman shift of HFC-134a involved in gas phase ($\Delta\nu$ = 843 cm^{-1}) as shown in **Figure II-3-7**. At the present experimental temperatures and pressures, HFC-134a molecules occupy only the L-cages of s-II simple HFC-134a hydrate. As a supplemental experiment, phase equilibrium curve of HL_1G for the simple HFC-134a hydrate system and cage occupancy of HFC-134a were investigated by means of phase equilibrium measurement and Raman spectroscopy, respectively. Phase equilibrium relation of simple HFC-134a hydrate system is shown in **Figure II-3-8** and summarized in **Table II-3-5**. Raman spectrum obtained from the simple HFC-134a hydrate is also shown in **Figure II-3-7**. The result is that the structural phase transition point between s-I and s-II hydrates exists at p = 65 ± 1 MPa, T = 282.2 ± 0.1 K and HFC-134a occupies M-cages of s-I hydrate above the structural phase transition point. Therefore, Raman peak detected at $\Delta\nu$ = 847 cm^{-1} reveals that the coexistence of HFC-32 molecule in the hydrate crystal results in the M-cage occupancy of HFC-134a molecule. The M-cage occupancy of the HFC-134a molecule leads to the heterogeneous azeotropic-like behavior, that is, the pressure-increase from the equilibrium pressure of the simple HFC-32 hydrate.

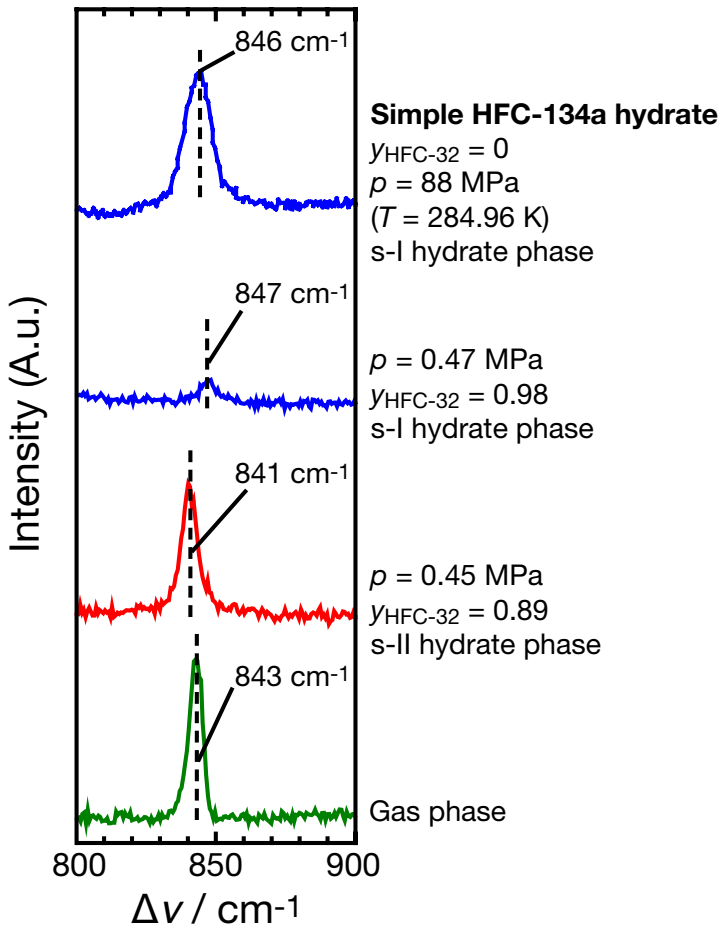

Figure II-3-7. Raman spectra of the C–C stretching vibration mode of HFC-134a molecule between hydrate at $y_{HFC\text{-}32}$ = 0.89 and 0.98 and gas phases.

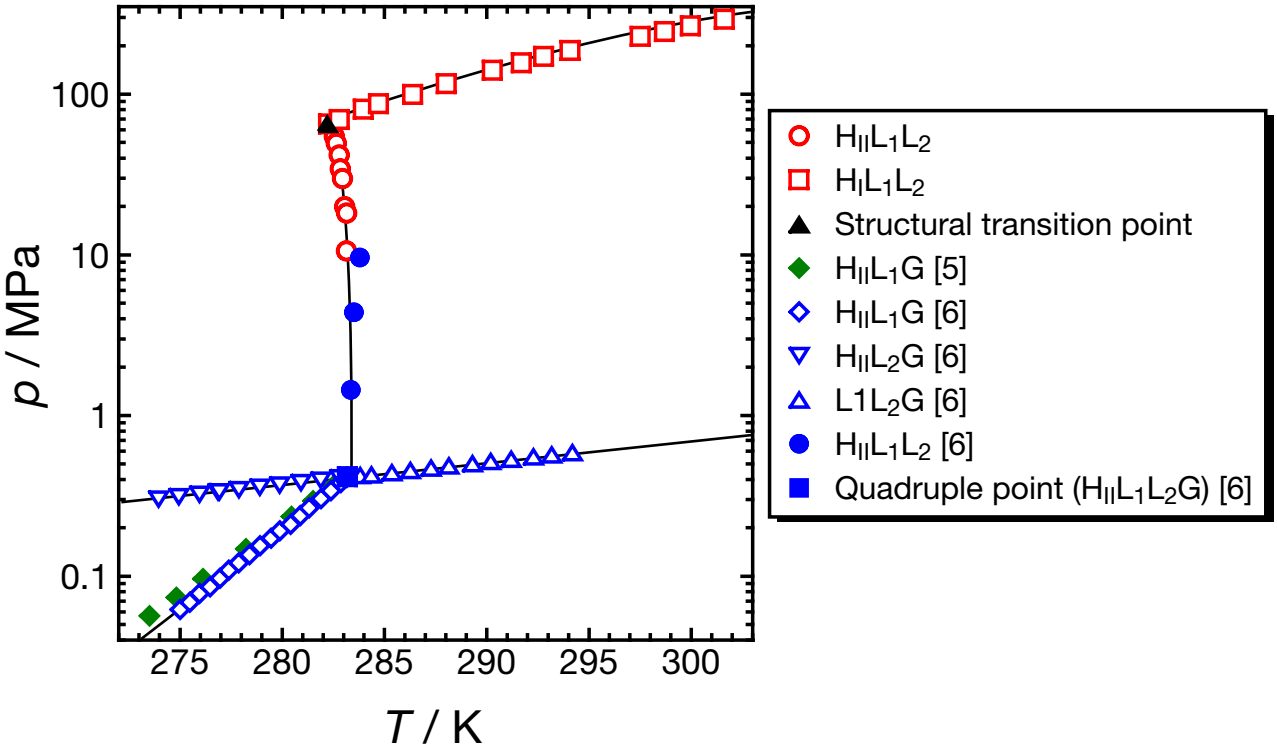

Figure II-3-8. Three-phase equilibrium relations for the HFC-134a+water binary system.

HFC-32 molecule is enclathrated in S- and M-cages of the s-I simple HFC-32 hydrate [4]. Raman spectrum in the s-I HFC-32+HFC-134a mixed-gas hydrate at $y_{HFC-32} = 0.98$ is similar to that of the simple HFC-32 hydrate [4]. At $y_{HFC-32} = 0.26$ to 0.89, Raman peaks of the HFC-32 molecules in the L-cages of the s-II HFC-32+HFC-134a mixed-gas hydrates do not seem to be detected. However, a small amount of HFC-32 molecules should occupy the L-cages of the s-II HFC-32+HFC-134a mixed-gas hydrates in the certain composition range because the mole fraction of HFC-32 in hydrate phases is beyond 2/3 (the ratio $N_S/(N_S+N_L)$ in the unit cell of s-II hydrates).

Table II-3-5. Three-phase (HL_1L_2) equilibrium data for the HFC-134a+water system.[a] The structural phase transition point is located at $p = 65 \pm 1$ MPa and $T = 282.2 \pm 0.1$ K.

T / K	p / MPa
283.12	10.63
283.14	18.32
283.04	20.02
282.93	30.03
282.82	34.75
282.77	42.04
282.63	49.73
282.53	54.77
282.27	65
282.79	70
283.97	81
284.70	87
286.37	100
288.02	116
290.28	141
291.69	156
292.78	171
294.07	187
297.51	229
298.69	245
299.96	266
301.62	293

[a] $u(p) = 0.15$ MPa at $p < 60$ MPa, $u(p) = 2$ MPa at $p > 60$ MPa, and $u(T) = 0.02$ K.

II.3.5. Conclusions

The isothermal phase equilibrium relations of the HFC-32+HFC-134a mixed-gas hydrate system were investigated under the three-phase equilibrium conditions. The remarkable characteristics in the HFC-32+HFC-134a mixed-gas hydrate system are that the isothermal phase equilibrium curves exhibit both the homogeneous and heterogeneous azeotropic-like behavior at T = 279.15 K and 283.15 K, while they exhibit only the heterogeneous azeotropic-like behavior at T = 274.15 K. This negative homogeneous azeotropic-like behavior enables the preparation of HFC-32+HFC-134a mixed-gas hydrates under low-pressure conditions. In addition, Raman spectra reveal that the HFC-134a molecule, in spite of an s-II hydrate former, occupies the M-cage of the s-I mixed-gas hydrate.

II.3.6. Nomenclatures

ν	Wavenumber [m^{-1}]
N_L	Number of L-cages in the unit cell of s-II hydrates [-]
N_S	Number of S-cages in the unit cell of s-II hydrates [-]
p	Pressure [Pa]
T	Temperature [K]
u	Standard uncertainties of pressure [Pa], temperature [K], and mole fraction [-]
x_{HFC-32}	Mole fraction of HFC-32 in aqueous phase (water free) [-]
y_{HFC-32}	Mole fraction of HFC-32 in gas phase (water free) [-]
z_{HFC-32}	Mole fraction of HFC-32 in hydrate phase (water free) [-]
G	Gas phase
H	Hydrate phase
H_I	s-I hydrate phase
H_{II}	s-II hydrate phase
L_1	Aqueous phase
L_2	HFC-134a-rich liquid phase

II.3.7. References

[1] L. Fournaison, A. Delahaya, I. Chatti, "CO_2 Hydrates in Refrigeration Processes", *Industrial & Engineering Chemistry Research*, **43**, 6521–6526 (2004).

[2] T. Ogawa, T. Ito, K. Watanabe, K. Tahara, R. Hiraoka, J. Ochiai, R. Ohmura, Y.H. Mori, "Development of a Novel Hydrate-Based Refrigeration System: A Preliminary Overview", *Applied Thermal Engineering*, **26**, 2157–2167 (2006).

[3] D.R. Defibaugh, G. Morrison, L.A. Weber, "Thermodynamic Properties of Difluoromethane", *Journal of Chemical & Engineering Data*, **39**, 333–340 (1994).

[4] S. Hashimoto, H. Miyauchi, Y. Inoue, K. Ohgaki, "Thermodynamic and Raman Spectroscopic Studies on Difluoromethane (HFC-32)+Water Binary System", *Journal of Chemical & Engineering Data*, **55**, 2764–2768 (2010).

[5] D. Liang, K. Guo, R. Wang, S. Fan, "Hydrate Equilibrium Data of 1,1,1,2-Tetrafluoroethane (HFC-134a), 1,1-Dichloro-1-fluoroethane (HCFC-141b) and 1,1-Difluoroethane (HFC-152a)", *Fluid Phase Equilibria*, **187–188**, 61–70 (2001).

[6] S. Hashimoto, T. Makino, Y. Inoue, K. Ohgaki, "Three-Phase Equilibrium Relations and Hydrate Dissociation Enthalpies for Hydrofluorocarbon Hydrate Systems: HFC-134a, -125, and -143a Hydrates", *Journal of Chemical & Engineering Data*, **55**, 4951–4955 (2010).

[7] G.K. Anderson, "A Thermodynamic Study of the (Difluoromethane + Water) System", *The Journal of Chemical Thermodynamics*, **43**, 1331–1335 (2011).

[8] J.L. Thakore, G.D. Holder, "Solid-Vapor Azeotropes in Hydrate-Forming Systems", *Industrial & Engineering Chemistry Research*, **26**, 462–469 (1987).

[9] T. Sugahara, T. Makino, K. Ohgaki, "Isothermal Phase Equilibria for the Methane+Ethylene Mixed Gas Hydrate System", *Fluid Phase Equilibria*, **206**, 117–126 (2003).

[10] J.V. Widiatmo, H. Sato, K. Watanabe, "Measurements of Liquid Densities of the Binary HFC-32+HFC-134a System", *Fluid Phase Equilibria*, **99**, 199–207 (1994).

[11] Y. Higashi, “Vapor-Liquid Equilibrium, Coexistence Curve, and Critical Locus for Binary HFC-32/HFC-134a Mixture”, *International Journal of Thermophysics*, **16**, 1175–1184 (1995).

[12] G.D. Holder, D.J. Manganiello, “Hydrate Dissociation Pressure Minima in Multicomponent Systems”, *Chemical Engineering Science*, **37**, 9–16 (1982).

Section 4

Isothermal Phase Equilibria for the Carbon Dioxide+1,1,1,2-Tetrafluoroethane and Carbon Dioxide+1,1-Difluoroethane Mixed-Gas Hydrate Systems

II.4.1. Abstract

Isothermal phase equilibrium relations of the CO_2+HFC-134a and CO_2+1,1-difluoroethane (HFC-152a) mixed-gas hydrate systems were measured at T = 279.15 K. The isothermal phase equilibria of the CO_2+HFC-134a mixed-gas hydrate system exhibit the heterogeneous azeotropic-like behavior derived from the structural phase transition of the mixed-gas hydrate. The CO_2+HFC-152a mixed-gas hydrate system shows neither a structural phase transition nor azeotropic-like behavior.

II.4.2. Introduction

Unlike simple gas hydrate systems, the particular mixed-gas hydrate system has characteristic phenomena that depend on the composition of guest mixtures, that is, the structural phase transition and the azeotropic-like behavior. In general, the structural phase transition of hydrates surely occurs in the mixed-gas hydrate when the structures of the simple gas hydrates are different from each other. In addition to the commonsensical transition, another structural phase transition has been reported, which the s-II mixed-gas hydrates emerge in a certain composition region; nevertheless each guest molecule generates an s-I hydrate. The latter type of structural phase transition has been reported only in the CO_2+*c*-C_3H_6 mixed-gas hydrate system [1] among the CO_2-containing mixed-gas hydrate systems. It does not occur in the hydrate systems of the CO_2+C_2H_6 and CO_2+trifluoromethane (CHF_3) [2].

The azeotropic-like behavior has been experimentally observed in some mixed-gas hydrate systems. For example, in the HFC-32+HFC-134a mixed-gas hydrate system as shown in **Chapter**

II Section 3, both the negative homogeneous azeotropic-like behavior and the heterogeneous azeotropic-like behavior is observed at T = 279.15 K and 283.15 K.

HFCs such as HFC-152a and HFC-134a are still key components as countermeasures against destruction of the ozone layer, although it is a temporary expedient until some reliable substitute is found in the associated industries. The mixed-gas hydrate involving HFCs is a favorable heat-conducting medium in the air-conditioning system for reducing the amount of HFCs. In addition, if the system exhibits the negative azeotropic-like behavior, the operational conditions would become mild because the minimum equilibrium pressure is depressed from those of both simple gas hydrates.

HFC-152a is as large as *c*-C_3H_6, which is one of the largest guest species forming s-I hydrates [3]. As described above, the structural phase transition occurs in the CO_2+*c*-C_3H_6 mixed-gas hydrate system [1]. If the size of guest species were the most important for the structural phase transition, a possible structural phase transition in the CO_2+HFC-152a mixed-gas hydrate system would be implied.

In this section, to clarify whether the CO_2+HFC-152a and CO_2+HFC-134a mixed-gas hydrate systems exhibit such characteristic phenomena, I have investigated isothermal phase equilibria for the mixed-gas hydrates under the three-phase (HL_1G) equilibrium conditions at T = 279.15 K. In addition, the single crystal of mixed-gas hydrates has been analyzed by *in situ* Raman spectroscopy.

II.4.3. Experimental

Materials

The materials used in the present study are summarized in **Table II-4-1**. All of them were used without further purification.

Table II-4-1. Information on the materials used in the present study.

Material name	Source	Mole fraction purity
CO_2	Neriki Gas Co., Ltd.	> 0.9999
HFC-152a	Daikin Ind., Ltd.	> 0.995
HFC-134a	Daikin Ind., Ltd.	> 0.996
Distilled water	Wako Pure Chemicals Ind., Ltd.	> 0.9999

Apparatus

The experimental apparatus for isothermal phase equilibrium measurement and Raman spectroscopy used in the present study are the same as described in **Chapter II Section 3**.

Procedure

The experimental procedures for isothermal phase equilibrium measurement and Raman spectroscopy performed in the present study are the same as described in **Chapter II Section 3**. As a typical example, a photo of the CO_2+HFC-152a mixed-gas hydrate crystals in the high-pressure cell at p = 0.23 MPa and T = 279.15 K is shown in **Figure II-4-1**.

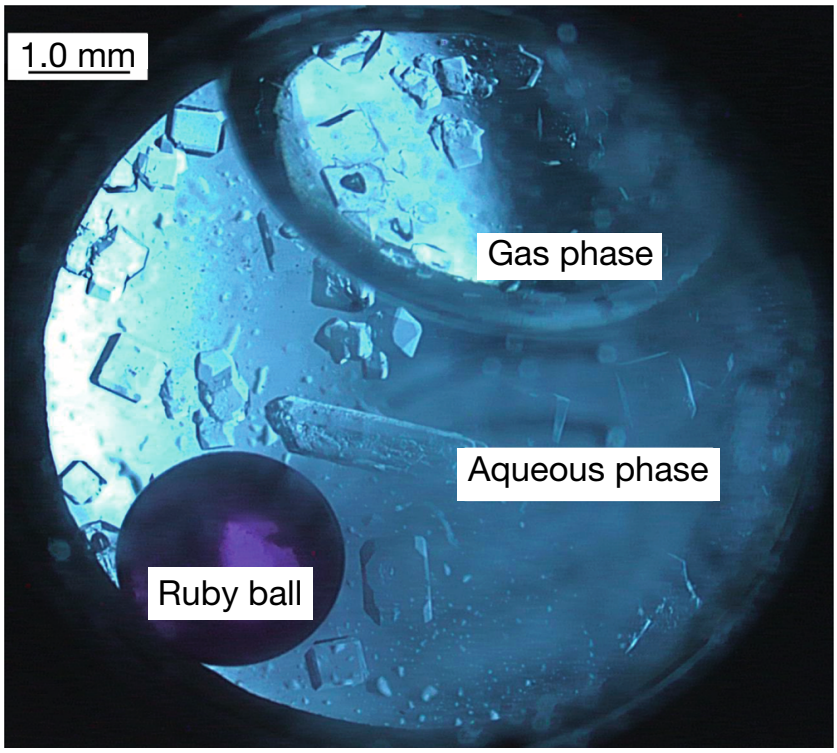

Figure II-4-1. CO_2+HFC-152a mixed-gas hydrate crystals generated under the three-phase coexisting conditions at p = 0.23 MPa and T = 279.15 K. (Many crystals are observed in the aqueous solution. A spherical ruby is trapped in the high-pressure cell for stirring the gas-liquid interface.)

II.4.4. Results and Discussion

CO_2+HFC-134a Mixed-Gas Hydrate System

Isothermal phase equilibrium relations for the CO_2+HFC-134a mixed-gas hydrate system at T = 279.15 K are shown in **Figure II-4-2** and summarized in **Table II-4-2**. The equilibrium CO_2 compositions in the gas and aqueous phases at a given pressure are comparable and larger than that of hydrate phase. The equilibrium pressure in a CO_2 composition region larger than y_{CO2} = 0.989 is higher than that of the simple CO_2 hydrate systems. The inset in **Figure II-4-2** indicates the schematic phase diagram in the high CO_2 composition region, which is deduced from the results in the HFC-32+HFC-134a mixed hydrate (**Chapter II Section 3**). Although similar behavior was observed in the HFC-32+HFC-134a mixed-gas hydrate system (**Chapter II Section 3**), the isothermal phase equilibrium relations at T = 279.15 K in the CO_2+HFC-134a mixed-gas hydrate system do not exhibit a negative azeotropic-like behavior as observed in the HFC-32+HFC-134a mixed-gas hydrate system.

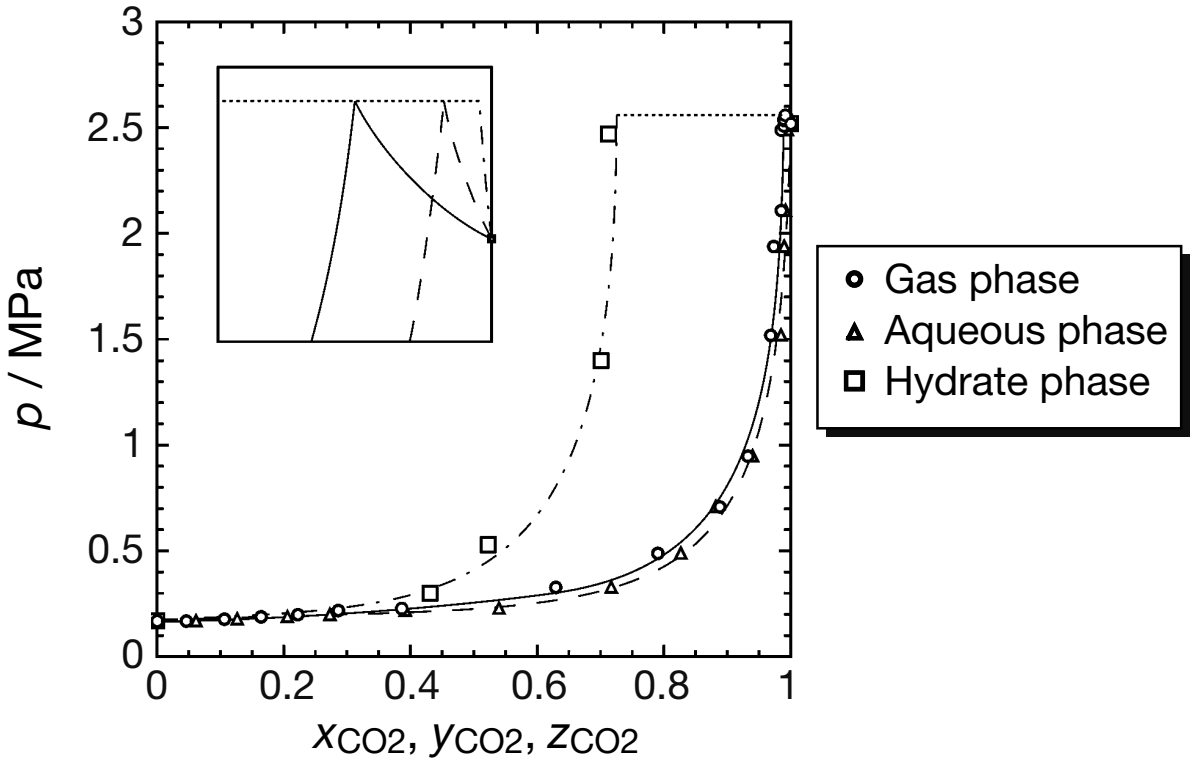

Figure II-4-2. Isothermal phase equilibria for the CO_2+HFC-134a mixed-gas hydrate system at T = 279.15 K. The inset shows the schematic magnified-diagram for the right edge around the structural phase transition point.

Table II-4-2. Isothermal phase equilibrium data in the CO_2+HFC-134a mixed-gas hydrate system at T = 279.15 K.[a]

p / MPa	x_{CO2}	y_{CO2}	z_{CO2}
0.17	0.000	0.000	0.000
0.17	0.062	0.046	
0.18	0.127	0.106	
0.19	0.206	0.164	
0.20	0.273	0.222	
0.22	0.392	0.286	
0.23	0.540	0.386	
0.30			0.431
0.33	0.717	0.629	
0.49	0.827	0.790	
0.53			0.523
0.71	0.882	0.888	
0.95	0.940	0.932	
1.40			0.701
1.52	0.985	0.968	
1.94	0.990	0.973	
2.11	0.992	0.985	
2.47			0.713
2.49	0.995	0.985	
2.51	0.994	0.989	
2.53	0.995	0.989	
2.54	0.997	0.989	
2.56	0.998	0.991	
2.52	1.000	1.000	1.000

[a] $u(p)$ = 0.01 MPa and $u(x_{CO2}) = u(y_{CO2}) = u(z_{CO2})$ = 0.005.

Figure II-4-3 shows typical Raman spectra of the CO_2+HFC-134a mixed-gas hydrate system at T = 279.15 K. The resonance peaks derived from the intramolecular vibration modes of the enclathrated CO_2 molecule were detected at $\Delta\nu$ = 1273 cm^{-1} and 1381 cm^{-1} in the composition ranges of z_{CO2} = 0.50–0.72, while the peaks were detected at $\Delta\nu$ = 1275 cm^{-1} and 1381 cm^{-1} in the composition region of $z_{CO2} \approx 0.99$. It has been reported that the Raman peak of CO_2 around $\Delta\nu$ = 1270 cm^{-1} depends on the hydrate structures of s-I and s-II. The Raman shifts of $\Delta\nu$ = 1273 cm^{-1} and 1381 cm^{-1} correspond to the CO_2 molecule encaged in the s-II hydrate [2]. The Raman shifts of $\Delta\nu$ = 1275 cm^{-1} and 1381 cm^{-1} agree well with the CO_2 molecule encaged in the s-I hydrates [1,2,4–6]. The Raman peaks derived from the intramolecular C–H symmetric and C–H antisymmetric stretching vibration modes of the enclathrated HFC-134a molecule were detected at $\Delta\nu$ = 2977 cm^{-1} and 3010 cm^{-1} in the composition ranges of z_{CO2} = 0.50–0.72. These shifts correspond to the HFC-134a molecule encaged in the L-cage of s-II hydrate (**Chapter II Section 3**). Moreover, the weak peak derived from the intramolecular C–H symmetric stretching vibration mode was detected at $\Delta\nu$ = 2985 cm^{-1}, while the peak derived from the intramolecular C–H antisymmetric stretching vibration mode was too weak to be detected at the composition of $z_{CO2} \approx 0.99$. The existence of the peak at $\Delta\nu$ = 2985 cm^{-1} reveals that HFC-134a molecule is encaged in the M-cage of s-I hydrate under the coexistence of CO_2 like the HFC-32+HFC-134a mixed-gas hydrate system (**Chapter II Section 3**).

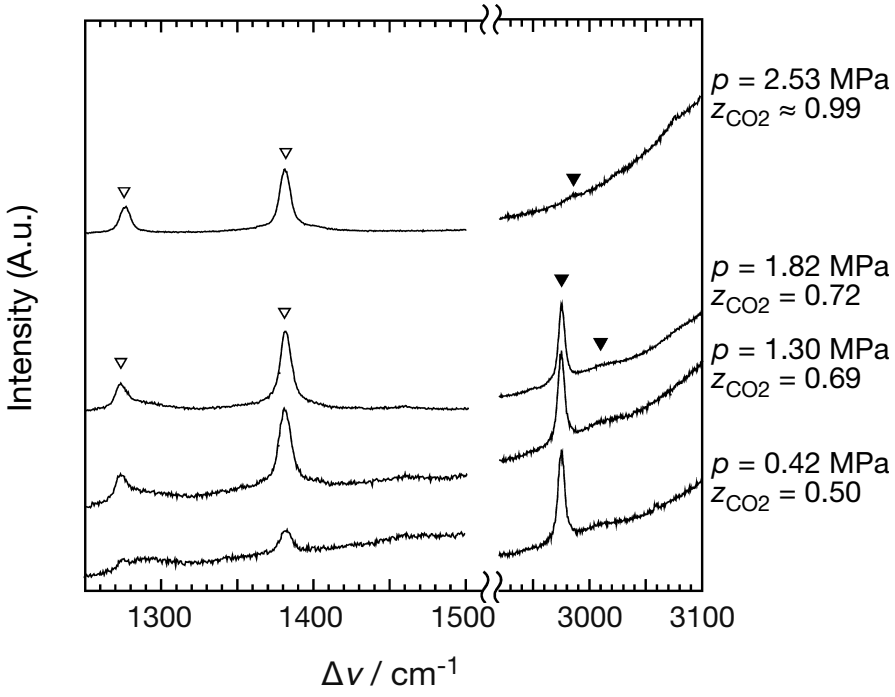

Figure II-4-3. Raman spectra of the intramolecular vibration modes of the enclathrated CO_2 (open inverse triangles) and HFC-134a (closed inverse triangles) molecules in the CO_2+HFC-134a mixed-gas hydrate system at T = 279.15 K.

These results of isothermal phase equilibrium relations and Raman spectra in the CO_2+HFC-134a mixed-gas hydrate system indicate that the structural phase transition occurs and a quadruple point ($H_IH_IIL_1G$) exists at $p \approx 2.56$ MPa and $y_{CO2} \approx 0.991$; that is, this system exhibits the heterogeneous azeotropic-like behavior like the HFC-32+HFC-134a mixed-gas hydrate system.

CO_2+HFC-152a Mixed-Gas Hydrate System

Before measuring the phase equilibria in the CO_2+HFC-152a mixed-gas hydrate system, the cage occupancy of HFC-152a in the simple HFC-152a hydrate was investigated. The structure of HFC-152a hydrate remains s-I at pressures up to p = 370 MPa. The HFC-152a molecules occupy only M-cages of s-I simple HFC-152a hydrate in the presence of completely vacant small cages at pressures up to p = 370 MPa. Pressure dependence of the Raman shifts reveals that the HFC-152a molecule would be the largest s-I hydrate former.

Isothermal phase equilibrium relations for the CO_2+HFC-152a mixed-gas hydrate system at T = 279.15 K are shown in **Figure II-4-4** and summarized in **Table II-4-3**. The equilibrium CO_2 compositions in hydrate, aqueous, and gas phases increase in that order at a given pressure. The equilibrium pressure increases monotonically with an increasing of equilibrium CO_2 composition in all phases. The continuity in each equilibrium curve reveals that, unlike the CO_2+*c*-C_3H_6 mixed-gas hydrate system, no structural phase transition occurs in the CO_2+HFC-152a mixed-gas hydrate system at T = 279.15 K.

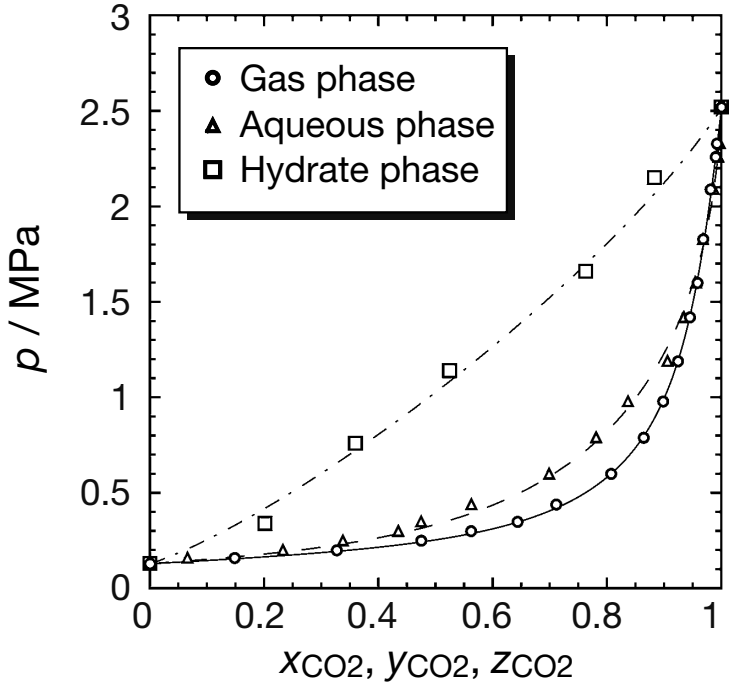

Figure II-4-4. Isothermal phase equilibria for the CO_2+HFC-152a mixed-gas hydrate system at T = 279.15 K.

Table II-4-3. Isothermal phase equilibrium data in the CO_2+HFC-152a mixed-gas hydrate system at T = 279.15 K.[a]

p / MPa	x_{CO2}	y_{CO2}	z_{CO2}
0.13	0.000	0.000	0.000
0.16	0.066	0.148	
0.20	0.233	0.327	
0.25	0.338	0.475	
0.30	0.435	0.562	
0.34			0.202
0.35	0.475	0.643	
0.44	0.563	0.711	
0.60	0.699	0.807	
0.76			0.360
0.79	0.781	0.864	
0.98	0.837	0.898	
1.14			0.525
1.19	0.906	0.924	
1.42	0.935	0.945	
1.66			0.763
1.60	0.956	0.958	
1.83	0.968	0.968	
2.09	0.987	0.981	
2.15			0.883
2.26	0.995	0.990	
2.33	0.998	0.992	
2.52	1.000	1.000	1.000

[a] $u(p)$ = 0.01 MPa and $u(x_{CO2}) = u(y_{CO2}) = u(z_{CO2})$ = 0.005.

Figure II-4-5 shows typical Raman spectra of the CO_2+HFC-152a mixed-gas hydrate system at T = 279.15 K. The double Raman peaks derived from the intramolecular vibration modes of the enclathrated CO_2 molecule were detected at $\Delta\nu$ = 1275 cm^{-1} and 1381 cm^{-1} in the whole composition range. The Raman shifts agree well with the CO_2 molecule encaged in the s-I hydrates [1,2,4–6]. The Raman peaks derived from the intramolecular CH_2 bending, C–C stretching, and CH_3 symmetric deformation vibrations of the enclathrated HFC-152a molecule were detected at $\Delta\nu$ = 1358 cm^{-1}, 1409 cm^{-1}, and 1446 cm^{-1}, respectively. The Raman shifts are in good agreement with that of the M-cage of the s-I simple HFC-152a hydrate. It is revealed that the crystal structure of the CO_2+HFC-152a mixed-gas hydrate remains s-I in the whole composition range at T = 279.15 K.

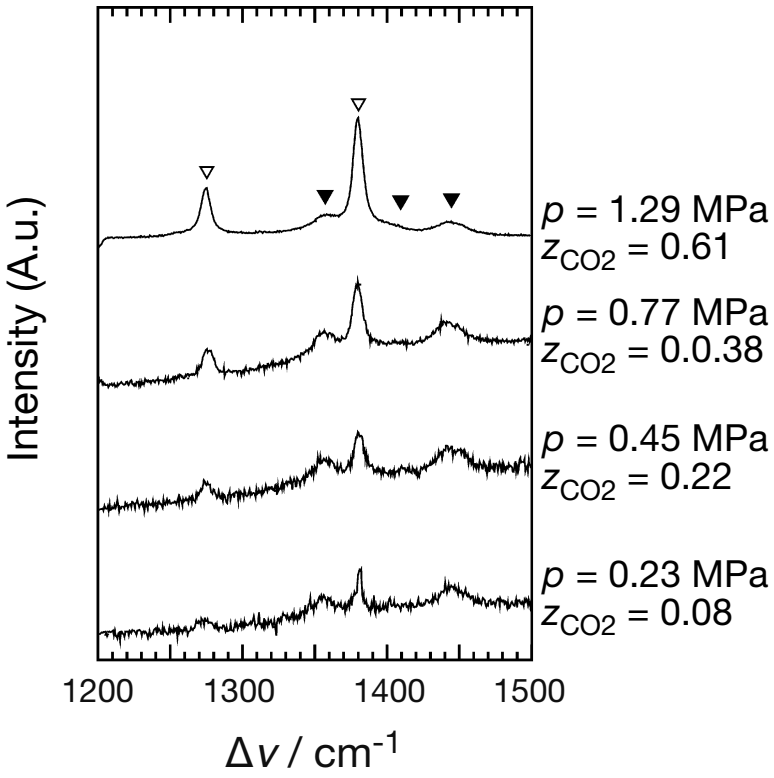

Figure II-4-5. Raman spectra of the intramolecular vibration modes of the enclathrated CO_2 (open inverse triangles) and HFC-152a (closed inverse triangles) molecules in the CO_2+HFC-152a mixed-gas hydrate system at T = 279.15 K.

II.4.5. Conclusions

The isothermal pressure-composition relations in the CO_2+HFC-134a and CO_2+HFC-152a mixed-gas hydrate systems were investigated under the three-phase equilibrium conditions at T = 279.15 K. The crystal structures of hydrates were analyzed based on the *in situ* Raman spectra. The CO_2+HFC-134a mixed-gas hydrate system exhibits the heterogeneous azeotropic-like behavior at $p \approx 2.56$ MPa and $y_{CO2} \approx 0.991$, while the CO_2+HFC-152a mixed-gas hydrate system shows straightforward equilibrium curves in the whole composition range.

II.4.6. Nomenclatures

ν	Wavenumber [m^{-1}]
p	Pressure [Pa]
T	Temperature [K]
u	Standard uncertainties of pressure [Pa], temperature [K], and mole fraction [-]
x_{CO2}	Mole fraction of CO_2 in aqueous phase (water free) [-]
y_{CO2}	Mole fraction of CO_2 in gas phase (water free) [-]
z_{CO2}	Mole fraction of CO_2 in hydrate phase (water free) [-]
G	Gas phase
H	Hydrate phase
H_I	s-I hydrate phase
H_{II}	s-II hydrate phase
L_1	Aqueous phase

II.4.7. References

[1] T. Makino, Y. Ogura, Y. Matsui, T. Sugahara, K. Ohgaki, "Isothermal Phase Equilibria and Structural Phase Transition in the Carbon Dioxide+Cyclopropane Mixed-Gas Hydrate System", *Fluid Phase Equilibria*, **284**, 19–25 (2009).

[2] Y. Matsui, Y. Ogura, H. Miyauchi, T. Makino, T. Sugahara, K. Ohgaki, "Isothermal Phase Equilibria for Binary Hydrate System of Carbon Dioxide+Ethane and Carbon Dioxide +Tetrafluoromethane", *Journal of Chemical & Engineering Data*, **55**, 3297–3301 (2010).

[3] E.D. Sloan, C.A. Koh, *Clathrate Hydrates of Natural Gases, 3rd ed*.; CRC Press, Taylor and Francis Group: Boca Raton, FL, 2008.

[4] S. Nakano, M. Moritoki, K. Ohgaki, "High-Pressure Phase Equilibrium and Raman Microprobe Spectroscopic Studies on the CO_2 Hydrate System", *Journal of Chemical & Engineering Data*, **43**, 807–810 (1998).

[5] T. Uchida, A. Takagi, S. Mae, J. Kawabata, "Dissolution Mechanisms of CO_2 Molecules in Water Containing CO_2 Hydrate", *Energy Conversion and Management*, **38**, S307–S312 (1997).

[6] T. Uchida, I.Y. Ikeda, S. Takeya, Y. Kamata, R. Ohmura, J. Nagao, O.Y. Zatsepina, B.A. Buffett, "Kinetics and Stability of CH_4-CO_2 Mixed Gas Hydrates during Formation and Long-Term Storage", *ChemPhysChem*, **6**, 646–654 (2005).

Section 5

Isothermal Phase Equilibria for the Xenon+Cyclopropane Mixed-Gas Hydrate System

II.5.1. Abstract

Isothermal three-phase equilibria of gas, aqueous, and hydrate phases for the Xe+*c*-C_3H_6 mixed-gas hydrate system were measured at T = 279.15 K and 289.15 K. The structural phase transitions from s-I to s-II and back to s-I, depending on the mole fraction of guest mixtures, occur in the Xe+*c*-C_3H_6 mixed-gas hydrate system. The isothermal pressure-composition relations have two local pressure minima. The most important characteristic in the Xe+*c*-C_3H_6 mixed-gas hydrate system is that the equilibrium pressure-composition relations exhibit the complex phase behavior involving two structural phase transitions and two homogeneous negative azeotropes. One of two structural phase transitions exhibits the heterogeneous azeotropic-like behavior.

II.5.2. Introduction

The structure of mixed-gas hydrates also depends on the composition of guest mixtures in addition to the system pressure and temperature. One of the most characteristic phenomena in the mixed-gas hydrate system is the structural phase transition from s-I to s-II and back to s-I, dependent on the composition of guest mixtures, while each guest species generates s-I hydrates. This phenomenon was first reported by Cailletet and Bordet [1] approximately 100 years ago. In 2000, Subramanian *et al*. [2] reported that the structural phase transition occurs in the CH_4+C_2H_6 mixed-gas hydrate system. The mechanism of structural phase transition is not yet clear. Therefore, it is very important to accumulate the thermodynamic properties of several mixed-gas hydrate systems such as pressure-composition relations. Our research group has reported several mixed-gas hydrate systems in which the structural phase transition exists. The structural phase transition occurs in the CH_4+C_2H_6, CH_4+*c*-C_3H_6, CH_4+CF_4, and CO_2+*c*-C_3H_6 mixed-gas hydrate systems [2–

5], while it does not occur in the CH_4+C_2H_4, CH_4+CHF_3, CO_2+C_2H_6, and CO_2+CF_4 mixed-gas hydrate systems [6–8].

The Xe-containing mixed-gas hydrate systems have a possibility of the structural phase transition because van der Waals diameter of Xe (0.43 nm) is between those of CH_4 (0.41 nm) and CO_2 (0.50 nm). However, the investigation on the structural phase transition in Xe-containing mixed-gas hydrate systems is so rare. On the other hand, there are some reports on the phase equilibria of *c*-C_3H_6-containing mixed gas hydrates. The structural phase transition occurs in both CH_4+C_2H_6 and CH_4+*c*-C_3H_6 mixed-gas hydrate systems. The CH_4+*c*-C_3H_6 mixed-gas hydrate system [3] has a wider composition range of s-II hydrate than the CH_4+C_2H_6 and CH_4+CF_4 mixed-gas hydrate systems under isothermal conditions [2,4]. A structural phase transition occurs in the CO_2+*c*-C_3H_6 mixed-gas hydrate system [5], while it does not occur in the CO_2+C_2H_6 mixed-gas hydrate system [8]. These results imply that the Xe+*c*-C_3H_6 mixed-gas hydrate has a significant possibility of a structural phase transition, which is the reason I have focused on the Xe+*c*-C_3H_6 mixed-gas hydrate system.

In this section, isothermal phase equilibria for the Xe+*c*-C_3H_6 mixed-gas hydrate system were investigated under the three-phase (HL_1G) equilibrium conditions at T = 279.15 K and 289.15 K, where Xe and *c*-C_3H_6 generate the s-I hydrate under the present experimental conditions [9]. To clarify the structure of mixed-gas hydrates, single crystals of hydrates with various compositions were analyzed by means of *in situ* Raman spectroscopy.

II.5.3. Experimental

Materials

The materials used in the present study are summarized in **Table II-5-1**. All of them were used without further purification.

Table II-5-1. Information on the materials used in the present study.

Material name	Source	Mole fraction purity
Xe	Air Water Inc.	> 0.99995
c-C_3H_6	Takachiho Trading Co., Ltd.	> 0.995
Distilled water	Wako Pure Chemicals Ind., Ltd.	> 0.9999

Apparatus

The experimental apparatus for isothermal phase equilibrium measurement and Raman spectroscopy used in the present study are the same as described in **Chapter II Section 3**.

Procedure

The experimental procedures for isothermal phase equilibrium measurement and Raman spectroscopy performed in the present study are the same as described in **Chapter II Section 3**.

II.5.4. Results and Discussion

Three-phase equilibrium relations for the Xe+*c*-C_3H_6 mixed-gas hydrate system at T = 279.15 K and 289.15 K are shown in **Figures II-5-1 and 2**, respectively. Three-phase equilibrium data for the Xe+*c*-C_3H_6 mixed-gas hydrate system are summarized in **Tables II-5-2 and 3**. **Table II-5-2** summarizes the pressure (p)-composition (x_{Xe}, y_{Xe}) relations for each isotherm obtained without the dissociation of hydrate samples. **Table II-5-3** summarizes the pressure (p)-composition (z_{Xe}) relation for each isotherm. The pressure-composition diagrams exhibit intensely curious behavior compared with those of various mixed-gas hydrate systems. At both temperatures, two discontinuous changes and two local pressure minima appear on each isotherm. The former indicate the existence of the structural phase transitions, which is supported by the Raman spectra mentioned below. One of two structural phase transitions, the structural phase transition between two local pressure minima, exhibits the heterogeneous azeotropic-like behavior. The other at the Xe-rich side exhibits the ordinary structural phase transition as reported in the CH_4+C_2H_6 mixed-gas hydrate system [2]. The local pressure minima and structural phase transition points in the Xe+*c*-C_3H_6 mixed-gas hydrate system are summarized in **Table II-5-4**. Considering the isothermal phase equilibria with the Raman spectra (mentioned below), the thermodynamically stable region of the s-II Xe+*c*-C_3H_6 mixed-gas hydrate is y_{Xe} = 0.34–0.95, z_{Xe} = 0.40–0.74 at T = 279.15 K and y_{Xe} = 0.50–0.92, z_{Xe} = 0.55–0.71 at T = 289.15 K. The s-II hydrate region becomes narrower with increase in the temperature.

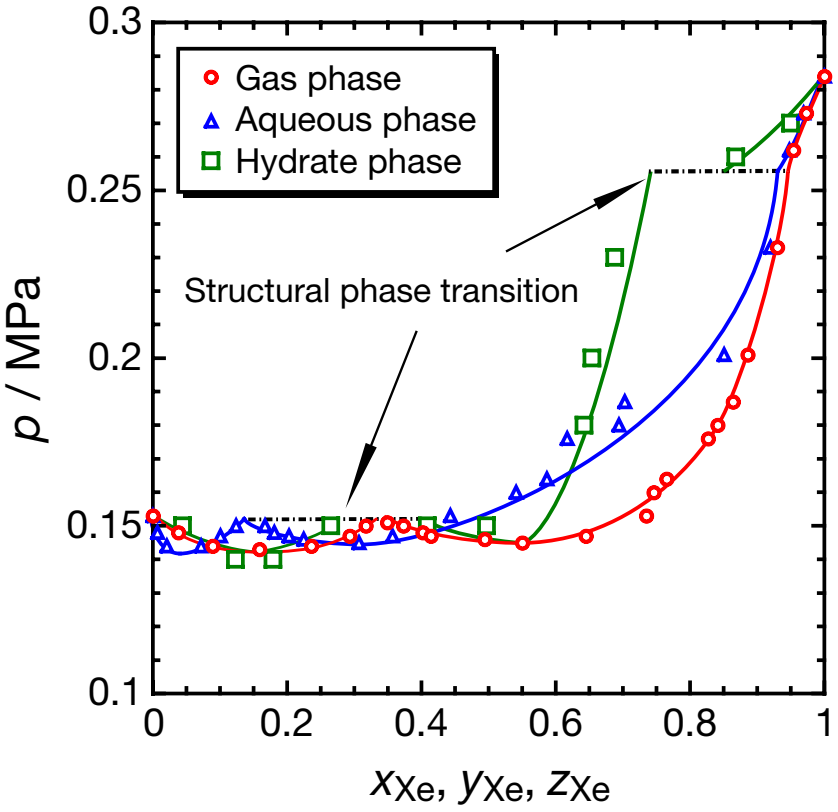

Figure II-5-1. Isothermal phase equilibria for the Xe+*c*-C_3H_6 mixed-gas hydrate system at T = 279.15 K.

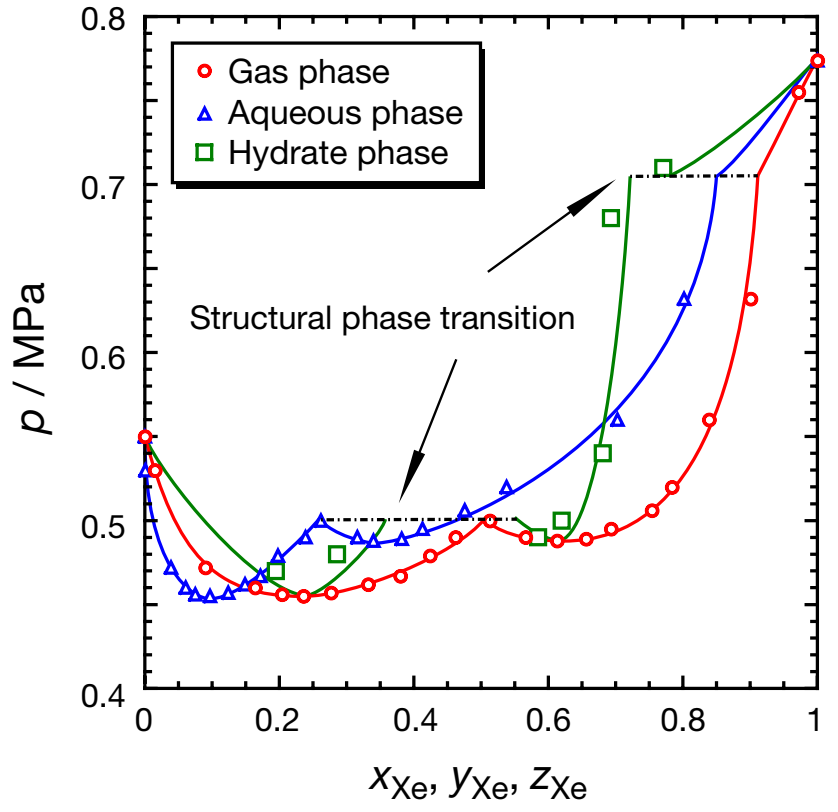

Figure II-5-2. Isothermal phase equilibria for the Xe+*c*-C_3H_6 mixed-gas hydrate system at T = 289.15 K.

Table II-5-2. Isothermal phase equilibrium data of gas and aqueous phases coexisting with Xe+*c*-C_3H_6 mixed-gas hydrates.

p / MPa[a]	y_{Xe}[a]	x_{Xe}[a]	p / MPa[a]	y_{Xe}[a]	x_{Xe}[a]
	T = 279.15 K[a]			T = 289.15 K[a]	
0.153	0.000	0.000	0.550	0.000	0.000
0.148	0.038	0.007	0.530	0.015	0.001
0.144	0.089	0.021	0.472	0.090	0.039
0.143	0.159	-[b]	0.460	0.164	0.061
0.144	0.236	0.072	0.456	0.204	0.075
0.147	0.293	0.101	0.455	0.236	0.097
0.151	0.349	-[b]	0.457	0.277	0.124
0.150	0.373	-[b]	0.462	0.332	0.149
0.148	0.402	0.181	0.467	0.380	0.172
0.147	0.414	0.203	0.479	0.424	0.198
0.146	0.494	0.225	0.490	0.462	0.239
0.145	0.550	0.307	0.500	0.513	0.262
0.147	0.645	0.357	0.490	0.566	0.316
0.153	0.735	0.443	0.488	0.613	0.340
0.160	0.746	0.541	0.489	0.656	0.382
0.164	0.765	0.587	0.495	0.693	0.413
0.176	0.827	0.617	0.506	0.754	0.476
0.180	0.841	0.694	0.520	0.784	0.538
0.187	0.864	0.703	0.560	0.839	0.703
0.201	0.886	0.851	0.632	0.901	0.802
0.233	0.930	0.920	0.755	0.972	-[b]
0.262	0.954	0.948	0.774	1.000	1.000
0.273	0.973	0.969			
0.284	1.000	1.000			

[a] $u(p)$ = 0.004 MPa, $u(T)$ = 0.02 K, and $u(y_{Xe}) = u(x_{Xe})$ = 0.005.

[b] The only p-y_{Xe} relation is listed in spite of the lack of x_{Xe} because the datum set is still meaningful for understanding the phase behavior.

Table II-5-3. Isothermal pressure-composition relations in hydrate phase for the Xe+*c*-C_3H_6 mixed-gas hydrate system at T = 279.15 K and 289.15 K.

p / MPa[a]	z_{Xe}[a]	p / MPa[a]	z_{Xe}[a]
T = 279.15 K[a]		T = 289.15 K[a]	
0.15	0.000	0.55	0.000
0.15	0.044	0.47	0.195
0.14	0.123	0.48	0.286
0.14	0.179	0.49	0.585
0.15	0.409	0.50	0.620
0.15	0.265	0.54	0.681
0.15	0.497	0.68	0.693
0.18	0.642	0.71	0.771
0.20	0.654	0.77	1.000
0.23	0.688		
0.26	0.868		
0.27	0.950		
0.28	1.000		

[a] $u(p)$ = 0.02 MPa, $u(T)$ = 0.02 K, and $u(z_{Xe})$ = 0.01.

Table II-5-4. Summary of the local pressure minima and the structural phase transition points in the Xe+*c*-C_3H_6 mixed-gas hydrate system at T = 279.15 K and 289.15 K.

T / K[a]		Local pressure minima		Structural phase transition points	
		s-I	s-II		
279.15	x_{Xe}[b]	0.05 ± 0.02	0.30 ± 0.02	0.13 ± 0.02	0.93 ± 0.02
	y_{Xe}[b]	0.16 ± 0.01	0.55 ± 0.01	0.34 ± 0.01	0.95 ± 0.01
	z_{Xe}[b]	0.16 ± 0.01	0.55 ± 0.01	0.27 ± 0.02 (s-I)	0.74 ± 0.02 (s-II)
				0.40 ± 0.02 (s-II)	0.86 ± 0.03 (s-I)
	p / MPa	0.143 ± 0.004	0.145 ± 0.004	0.152 ± 0.004	0.25 ± 0.01
289.15	x_{Xe}[b]	0.10 ± 0.02	0.34 ± 0.02	0.26 ± 0.02	0.85 ± 0.02
	y_{Xe}[b]	0.23 ± 0.01	0.61 ± 0.01	0.50 ± 0.01	0.92 ± 0.01
	z_{Xe}[b]	0.23 ± 0.01	0.61 ± 0.01	0.35 ± 0.05 (s-I)	0.71 ± 0.02 (s-II)
				0.55 ± 0.03 (s-II)	0.77 ± 0.02 (s-I)
	p / MPa	0.455 ± 0.004	0.488 ± 0.004	0.505 ± 0.004	0.70 ± 0.01

[a] $u(T)$ = 0.02 K.

[b] Due to the determinations by the extrapolation of isotherms.

The single local pressure minimum derived from the homogeneous negative azeotropic-like behavior has been reported in some mixed-gas hydrate systems [6,10,11]. The same behavior was observed in the HFC-32+HFC-134a mixed-gas hydrate system as mentioned in **Chapter II Section 3**. The existence of two local pressure minima on an isotherm is very rare. Holder and Manganiello [10] and Thakore and Holder [11] have stated that the negative azeotropic-like behavior is due to the competing effect of small and large guest molecules. The compositions at the local pressure minima of the s-I Xe+*c*-C_3H_6 mixed-gas hydrate are $y_{Xe} = z_{Xe} = 0.16 \pm 0.01$ at $T = 279.15$ K and $y_{Xe} = z_{Xe} = 0.23 \pm 0.01$ at $T = 289.15$ K. In the case of the s-II Xe+*c*-C_3H_6 mixed-gas hydrate, the compositions are $y_{Xe} = z_{Xe} = 0.55 \pm 0.01$ at $T = 279.15$ K and $y_{Xe} = z_{Xe} = 0.61 \pm 0.01$ at $T = 289.15$ K. If the Xe and *c*-C_3H_6 molecules occupy the small and large cages of both hydrate structures respectively, the ideal compositions, which are equal to the fractions of S-cage in the unit lattices, are $z_{Xe} = 0.25$ (s-I) and $z_{Xe} = 0.67$ (s-II). With increase in the temperature, the compositions at the local pressure minima are getting close to the fraction of S-cage in each hydrate structure and the negative azeotropic-like behavior becomes more remarkable. These results imply that the negative azeotropic-like behavior would result from both the compartmental occupancy of a suitable size of small and large guest species and the S-cage occupancy ratio of small guest species. Therefore, this discussion holds also in the HFC-32+HFC-134a mixed hydrate system mentioned in **Chapter II Section 3**, HFC-32 and HFC-134a could compartmentally occupy S-cages and L-cages of s-II hydrate at a pressure minimum, respectively.

As mentioned above, two discontinuous changes indicate the existence of the structural phase transitions. I confirmed this based on the Raman spectra corresponding to the intramolecular vibration modes of *c*-C_3H_6 in Xe+*c*-C_3H_6 mixed-gas hydrates with various compositions. Raman spectra corresponding to the ring-breathing and C–H stretching vibration modes of *c*-C_3H_6 in the Xe +*c*-C_3H_6 mixed-gas hydrates at $T = 279.15$ K and 289.15 K were measured. The results at $T = 289.15$ K have the same trend as those at $T = 279.15$ K. As typical spectra, the Raman spectra at $T = 279.15$ K are shown in **Figure II-5-3**. At $y_{Xe} = 0.34$ and 0.97, the Raman peak corresponding to the ring-breathing vibration mode of the *c*-C_3H_6 molecule is detected at $\Delta\nu = 1191$ cm^{-1}. On the other hand, at $y_{Xe} = 0.75$, 0.84, and 0.89, the Raman shift is $\Delta\nu = 1184$ cm^{-1}. The Raman shifts of $\Delta\nu = 1191$ cm^{-1} and 1184 cm^{-1} are in good agreement with those of *c*-C_3H_6 in the both s-I and s-II CH_4+*c*-C_3H_6 (and also CO_2+*c*-C_3H_6) mixed-gas hydrate systems, respectively [3,5]. Also, the peak shape and shift of the Raman spectra corresponding to the C–H stretching vibration mode are in good agreement with those of *c*-C_3H_6 in the both s-I and s-II hydrates [3,5]. That is, the Raman peak detected at $\Delta\nu = 3029$ cm^{-1} (shown by the dotted lines) is derived from the *c*-C_3H_6 molecule in M-cages of s-I hydrate. Those at $\Delta\nu = 3009$ cm^{-1} and 3024 cm^{-1} (shown by the broken lines) are

derived from the *c*-C_3H_6 molecule in L-cages of s-II hydrate. These results prove the existence of structural phase transitions from s-I to s-II and back to s-I.

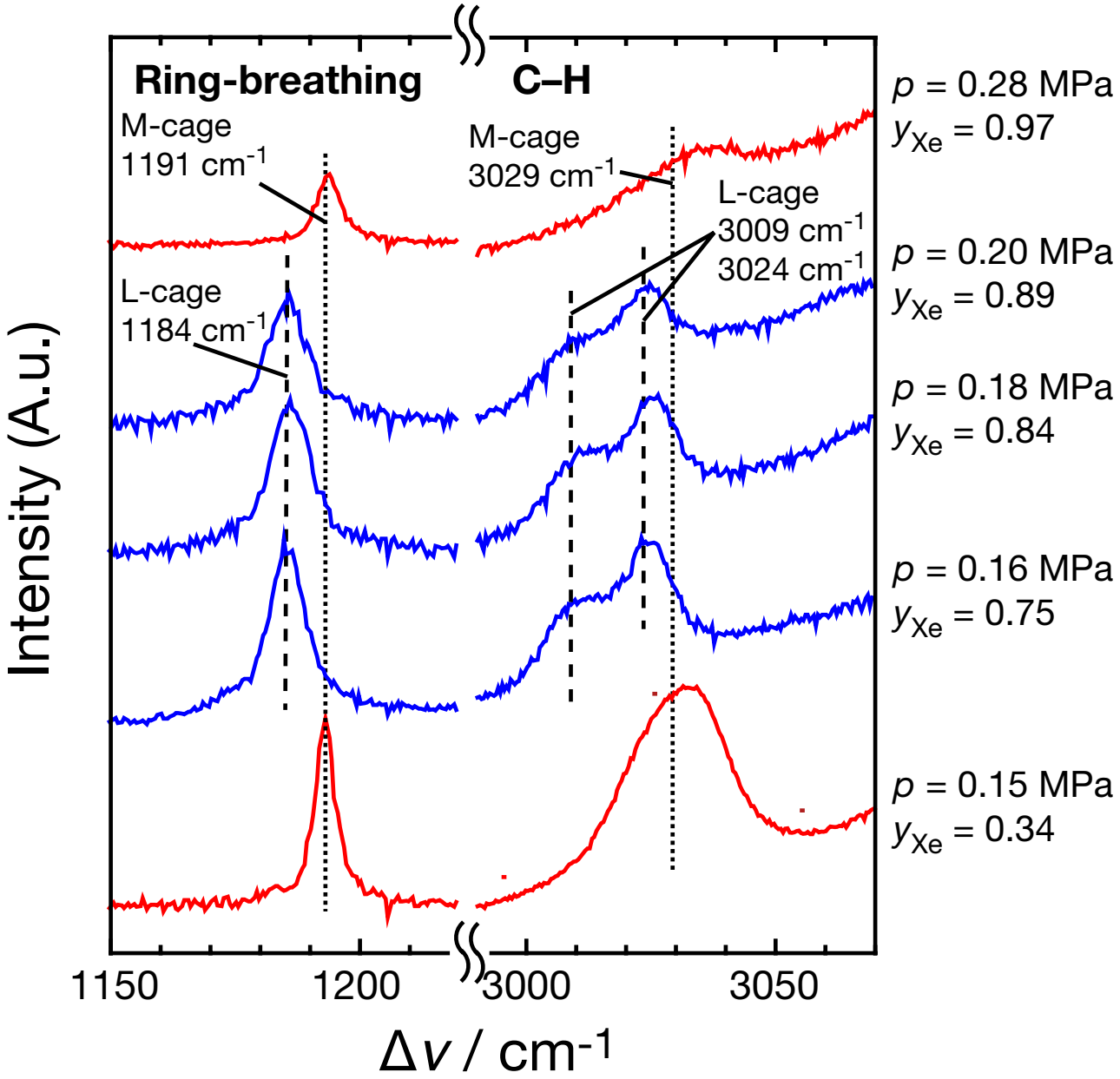

Figure II-5-3. Raman spectra corresponding to the ring-breathing ($\Delta\nu$ = 1190 cm^{-1}) and C–H stretching vibration ($\Delta\nu$ = 3000–3040 cm^{-1}) modes of *c*-C_3H_6 in the Xe+*c*-C_3H_6 mixed-gas hydrate at T = 279.15 K. The dotted and broken lines correspond to the Raman shifts in the s-I and s-II Xe +*c*-C_3H_6 mixed-gas hydrates, respectively.

II.5.5. Conclusions

Isothermal phase equilibria and Raman spectra in the Xe+*c*-C_3H_6 mixed-gas hydrate system were measured at T = 279.15 K and 289.15 K. The following important findings are obtained in the present study.

(1) Two kinds of homogeneous negative azeotropic-like behavior appear on an isotherm at the temperatures. The compositions of the local pressure minima are located at the vicinity of the cage fraction of the s-I and s-II hydrates.

(2) The phase behavior and the Raman spectra reveal the existence of two structural phase transitions from s-I to s-II and back to s-I. One of them exhibits the heterogeneous azeotropic-like behavior.

II.5.6. Nomenclatures

ν	Wavenumber [m^{-1}]
p	Pressure [Pa]
T	Temperature [K]
u	Standard uncertainties of pressure [Pa], temperature [K], and mole fraction [-]
x_{Xe}	Mole fraction of Xe in aqueous phase (water free) [-]
y_{Xe}	Mole fraction of Xe in gas phase (water free) [-]
z_{Xe}	Mole fraction of Xe in hydrate phase (water free) [-]
G	Gas phase
H	Hydrate phase
L_1	Aqueous phase

II.5.7. References

[1] L. Cailletet, R. Bordet, “Sur Divers Hydrates Qui se Forment Par la Pression et la Détente”, *Comptes Rendus*, **95**, 58–61 (1882).

[2] S. Subramanian, R.A. Kini, S.F. Dec, E.D. Sloan Jr., “Evidence of Structure II Hydrate Formation from Methane+Ethane Mixtures”, *Chemical Engineering Science*, **55**, 1981–1999 (2000).

[3] T. Makino, M. Tongu, T. Sugahara, K. Ohgaki, "Hydrate Structural Transition Depending on the Composition of Methane+Cyclopropane Mixed Gas Hydrate", *Fluid Phase Equilibria*, **233**, 129–133 (2005).

[4] Y. Kunita, T. Makino, T. Sugahara, K. Ohgaki, "Raman Spectroscopic Studies on Methane +Tetrafluoromethane Mixed-Gas Hydrate System", *Fluid Phase Equilibria*, **251**, 145–148 (2007).

[5] T. Makino, Y. Ogura, Y. Matsui, T. Sugahara, K. Ohgaki, "Isothermal Phase Equilibria and Structural Phase Transition in the Carbon Dioxide+Cyclopropane Mixed-Gas Hydrate System", *Fluid Phase Equilibria*, **284**, 19–25 (2009).

[6] T. Sugahara, T. Makino, K. Ohgaki, "Isothermal Phase Equilibria for the Methane+Ethylene Mixed Gas Hydrate System", *Fluid Phase Equilibria*, **206**, 117–126 (2003).

[7] T. Makino, Y. Kunita, T. Sugahara, K. Ohgaki, "Isothermal Phase Equilibria and Cage Occupancies for CH_4+CHF_3 Mixed-Gas Hydrate System", *The Open Thermodynamics Journal*, **2**, 17–21 (2008).

[8] Y. Matsui, Y. Ogura, H. Miyauchi, T. Makino, T. Sugahara, K. Ohgaki, "Isothermal Phase Equilibria for Binary Hydrate System of Carbon Dioxide+Ethane and Carbon Dioxide +Tetrafluoromethane", *Journal of Chemical & Engineering Data*, **55**, 3297–3301 (2010).

[9] E.D. Sloan, C.A. Koh, *Clathrate Hydrates of Natural Gases, 3rd ed.*; CRC Press, Taylor and Francis Group: Boca Raton, FL, 2008.

[10] G.D. Holder, D.J. Manganiello, "Hydrate Dissociation Pressure Minima in Multicomponent Systems", *Chemical Engineering Science*, **37**, 9–16 (1982).

[11] J.L. Thakore, G.D. Holder, "Solid-Vapor Azeotropes in Hydrate-Forming Systems", *Industrial & Engineering Chemistry Research*, **26**, 462–469 (1987).

Chapter III

Compartmental-Type Mixed Hydrates

Section 1

Phase Equilibrium Relations for Binary Mixed Hydrate Systems Composed of Carbon Dioxide and Cyclopentane Derivatives

III.1.1. Abstract

Thermodynamic stability boundaries of CO_2+*c*-C_5H_{10}, CO_2+cyclopentanone (*c*-C_5H_8O), and CO_2+fluorocyclopentane (*c*-C_5H_9F) mixed hydrates have been investigated at T = 274.19–293.72 K and up to p = 4.88 MPa. The phase equilibrium curves of the s-II mixed hydrates are located at temperatures remarkably higher than that of the s-I simple CO_2 hydrate. The highest temperature point of each four-phase (HL_1L_3G) equilibrium curve is T = 292.60 K (CO_2+*c*-C_5H_{10} mixed hydrate system), 284.78 K (CO_2+*c*-C_5H_8O mixed hydrate system), and 293.72 K (CO_2+*c*-C_5H_9F mixed hydrate system). CO_2+bromocyclopentane (*c*-C_5H_9Br)+water system has also been investigated in the similar pressure and temperature range. However, the *c*-C_5H_9Br molecule is not enclathrated into any cage in the presence of CO_2.

III.1.2. Introduction

Hydrate is suggested to be utilized for some applications such as gas storage and transportation, gas isolation, gas separation, refrigeration, and so on. However, high pressures and low temperatures are naturally required for its formation and stabilization. Wherever hydrate is operated practically, therefore, it is necessary to moderate the working conditions. A reasonable way to moderate these conditions is the addition of the second guest species which is called a thermodynamic promoter [1–6].

In this section, four five-membered cyclic hydrocarbon molecules (*c*-C_5H_{10}, *c*-C_5H_8O, *c*-C_5H_9F, and *c*-C_5H_9Br) were selected as candidates for thermodynamic promoters. Five-membered cyclic hydrocarbons have a suitable molecular size for the L-cage occupancy of s-II hydrates, and

they may work as thermodynamic promoters [2–6]. The pressure-temperature relations for CO_2+*c*-C_5H_{10} derivative+water systems were measured under four-phase equilibrium conditions (HL_1L_3G). The crystal structure of hydrate was analyzed by means of PXRD. Furthermore, the dissociation enthalpies of the CO_2+*c*-C_5H_{10} derivative mixed hydrates were roughly estimated with Clapeyron equation under the assumption of full compartmental occupancy in S- and L-cages.

III.1.3. Experimental

Materials

The materials used in the present study are summarized in **Table III-1-1**. All of them were used without further purification.

Table III-1-1. Information on the chemicals used in the present study.

Chemical name	Source	Mole fraction purity
CO_2	Neriki Gas Co., Ltd.	> 0.9999
c-C_5H_{10}	Tokyo Chemical Ind. Co., Ltd.	> 0.98
c-C_5H_8O	Merck, Ltd.	> 0.99
c-C_5H_9F	SynQuest Laboratories, Inc.	> 0.9869
c-C_5H_9Br	Merck, Ltd.	> 0.99
Distilled water	Wako Pure Chemical Ind., Ltd.	> 0.9999

Apparatus

The experimental apparatus for phase equilibrium measurement used in the present study is the same as described in **Chapter II Section 3** and shown in **Figure II-3-1**. The PXRD pattern was measured using a diffractometer (Rigaku, Ultima IV) with a Rigaku D/teX ultra high-speed position sensitive detector and CuKα X-ray (generation power: 40 kV, 50 mA).

Procedure

For phase equilibrium measurement, a desired volume of distilled water and *c*-C_5H_{10} derivative was introduced into the evacuated high-pressure cell. The contents were pressurized with CO_2 up to a desired pressure. The cell was immersed into a thermostatic cooling bath. The contents were cooled and agitated to generate mixed hydrates. A magnetic stirrer was moved up and down

for agitation. After that, the temperature was gradually increased and decreased respectively to establish four-phase coexistence condition. When the pressure change was within 0.01 MPa and four-phase coexistence was confirmed visually, I determined that the system reached a four-phase equilibrium. Phase equilibrium curves stand vertically or rather retrograde at a pressure above the maximum temperature point. Temperature was increased very gradually (0.1 K every 1 h) to allow the amount of hydrate to decrease and the system to reach equilibrium at each step. The temperature and pressure where negligible amount of gas hydrates exists were determined as a four-phase equilibrium condition.

For PXRD, the structure of the CO_2+*c*-C_5H_8O mixed hydrate has not been reported. After the CO_2+*c*-C_5H_8O mixed hydrates were prepared in the high-pressure cell, the contents were pressurized with additional CO_2 so that almost all of free water was converted to mixed hydrate. The hydrate samples were taken from the cell at T = 263 K and kept at T = 77 K. Samples were ground and put flatly on the sample stage of the diffractometer. PXRD was performed at T = 143 K. The measurements were performed in the step scan mode with scan rate of 10° min^{-1} and step size of 0.02°. The PXRD pattern indexing and cell refinement were performed with PowderX [7] and Chekcell [8] programs.

III.1.4. Results and Discussion

The four-phase (HL_1L_3G) equilibrium curves of the CO_2+*c*-C_5H_{10} derivative mixed hydrate systems are shown in **Figure III-1-1** accompanied with the three kinds of three-phase (HL_1G, HL_2G, and L_1L_2G) equilibrium curves of the simple CO_2 hydrate system [9]. **Table III-1-2** summarizes the four-phase equilibrium relations of the CO_2+*c*-C_5H_{10} derivative+water systems containing hydrates. The present four-phase (HL_1L_3G) equilibrium curve of the CO_2+*c*-C_5H_{10} mixed hydrate system below p = 3 MPa agrees well with the reported data [10,11]. The dissociation temperatures of the present mixed hydrates except for CO_2+*c*-C_5H_9Br+water system are higher than that of the simple CO_2 hydrate at a certain pressure. On the other hand, the phase equilibrium curve (HL_1L_3G) of CO_2+*c*-C_5H_9Br+water system coincides with that of simple CO_2 hydrate system (HL_1G) [9]. It means that the *c*-C_5H_{10}, *c*-C_5H_8O, and *c*-C_5H_9F are enclathrated in hydrate cages. On the other hand, *c*-C_5H_9Br is not enclathrated in the presence of CO_2. Hereafter, CO_2+*c*-C_5H_9Br +water system is not mentioned. The enclathration of the *c*-C_5H_8O molecule was revealed in the present study. The largest pressure reduction from the equilibrium pressure of the simple CO_2 hydrate is observed in the CO_2+*c*-C_5H_9F hydrate system, followed by the CO_2+*c*-C_5H_{10} and CO_2+*c*-C_5H_8O systems. Similar tendencies have been reported in the HFC-32+*c*-C_5H_{10} and HFC-32+*c*-

C_5H_9F systems [5], the Kr+*c*-C_5H_{10} and Kr+*c*-C_5H_9F systems [5], and fluoromethane (CH_3F)+*c*-C_5H_{10} and CH_3F+*c*-C_5H_9F systems [6]. It is described in the literatures that *c*-C_5H_{10} [12] and *c*-C_5H_9F [5,6] molecules occupy L-cages of s-II hydrates. PXRD pattern revealed that the crystal structure of the CO_2+*c*-C_5H_8O mixed hydrate is also s-II ($Fd3m$, a = 1.7291 ± 0.0010 nm).

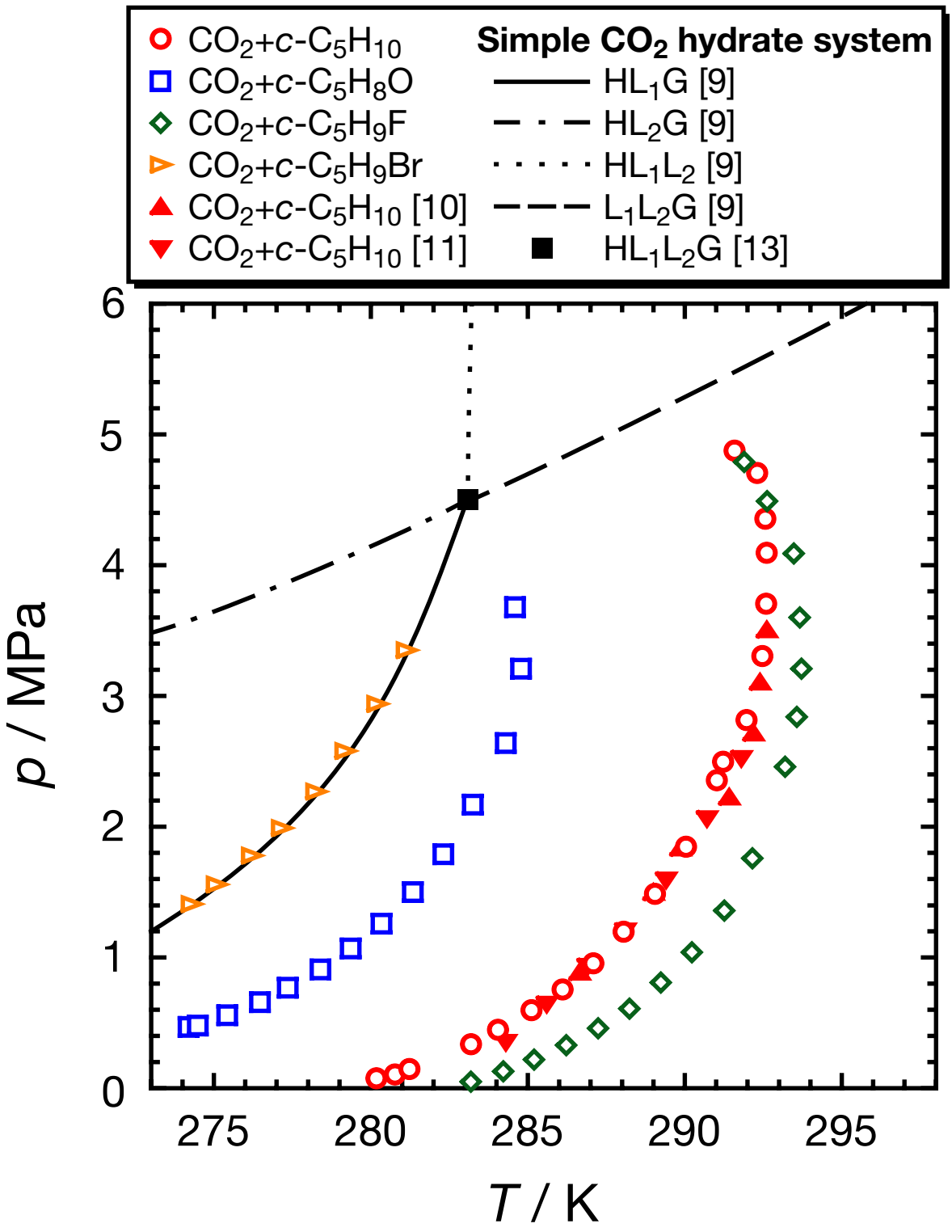

Figure III-1-1. Phase equilibrium relations of the CO_2+*c*-C_5H_{10} derivative mixed hydrate systems.

Table III-1-2. Four-phase equilibrium conditions for CO_2+*c*-C_5H_{10} derivative+water systems.

T / K[a]	p / MPa[a]	T / K[a]	p / MPa[a]	T / K[a]	p / MPa[a]	T / K[a]	p / MPa[a]
CO_2+*c*-C_5H_{10}+water system		CO_2+*c*-C_5H_8O+water system		CO_2+*c*-C_5H_9F+water system		CO_2+*c*-C_5H_9Br+water system	
280.16	0.08	274.19	0.47	283.18	0.05	274.29	1.41
280.76	0.11	274.49	0.48	284.21	0.13	275.08	1.56
281.22	0.15	275.42	0.56	285.20	0.22	276.21	1.78
283.17	0.34	276.46	0.66	286.22	0.33	277.16	1.99
284.04	0.45	277.36	0.77	287.24	0.46	278.26	2.27
285.11	0.60	278.39	0.91	288.24	0.61	279.19	2.58
286.09	0.76	279.36	1.07	289.23	0.81	280.20	2.94
287.07	0.96	280.34	1.26	290.23	1.04	281.13	3.35
288.03	1.20	281.34	1.50	291.25	1.36		
289.03	1.49	282.31	1.79	292.15	1.76		
290.03	1.85	283.24	2.17	293.19	2.46		
291.01	2.36	284.30	2.64	293.56	2.84		
291.21	2.45	284.78[b]	3.21	293.72[b]	3.21		
291.95	2.82	284.60	3.68	293.66	3.60		
292.45	3.31	293.47	4.09				
292.57	3.71	292.62	4.49				
292.60[b]	4.10	291.89	4.79				
292.55	4.36						
292.29	4.71						
291.57	4.88						

[a] $u(p)$ = 0.02 MPa and $u(T)$ = 0.02 K.

[b] The maximum equilibrium temperatures.

As the equilibrium pressure increases, the dissociation temperature monotonically increases at pressures below about 3 MPa. The equilibrium temperature scarcely changes at $p \approx 3$ MPa and the highest dissociation temperature is observed in the present mixed hydrate systems. The equilibrium temperature gradually decreases with an increase of pressure at pressures above the highest temperature point. The highest equilibrium temperature points in the CO_2+*c*-C_5H_8O, CO_2+*c*-C_5H_{10}, and CO_2+*c*-C_5H_9F mixed hydrate systems are located at p = 3.21 MPa and T = 284.78 K, p = 4.10 MPa and T = 292.60 K, and p = 3.21 MPa and T = 293.72 K, respectively. Based on Clapeyron equation (**Equation III-1-1**), the retrograde behavior was mainly caused by negative change of the molar volume (maybe derived from the partial molar volume of *c*-C_5H_{10} derivative in L_3 phase as well as the slight change of S-cage occupancy of CO_2) during hydrate dissociation.

$$\frac{dp}{dT} = \frac{\Delta_{hyd}H}{T\Delta_{hyd}v} \qquad \textbf{(Equation III-1-1)}$$

where $\Delta_{hyd}H$ and $\Delta_{hyd}v$ mean the enthalpy and molar volume changes through the hydrate dissociation, respectively.

The existence of the quintuple point ($HL_1L_2L_3G$) was reported in CO_2+tetrahydropyran, CO_2+cyclobutanone, CO_2+cyclohexane, and CO_2+methylcyclohexane mixed hydrate systems [14]. In these cases, five four-phase equilibrium curves ($HL_1L_2L_3$, HL_1L_2G, HL_1L_3G, HL_2L_3G, and $L_1L_2L_3G$) converge at the quintuple point ($HL_1L_2L_3G$) as reported elsewhere [14]. I have explored four-phase equilibrium curves other than HL_1L_3G by changing the ratio of materials. For the exploration of the HL_2L_3G or HL_1L_2G curves, the phase L_1 or L_3 needs to disappear after hydrate formation. A small amount of either water or *c*-C_5H_{10} derivative was added into the normal volume (2 cm^3) of *c*-C_5H_{10} derivative or water, respectively. However, hydrates were not formed and then the phase condition was the three-phase coexistence of L_1L_3G in both experiments. Theoretically, a quintuple point must have five four-phase equilibrium curves. However, no other curve than HL_1L_3G was observed in the present study. Extrapolating each four-phase equilibrium curve (HL_1L_3G), the coexistence point of both s-II mixed hydrate and s-I simple CO_2 hydrate would be placed near the quadruple point in simple CO_2 hydrate system (HL_1L_2G). It is because the present CO_2+*c*-C_5H_{10} derivative mixed hydrates are s-II and simple CO_2 hydrate is s-I, whereas none of the *c*-C_5H_{10} derivatives is able to occupy the M-cage of s-I hydrate.

The overall dissociation enthalpies of CO_2+*c*-C_5H_{10} derivative mixed hydrates were estimated with Clapeyron equation (**Equation III-1-1**). The partial differentials of pressure with respect to temperature were obtained from the correlated four-phase equilibrium curves obtained in the present study. IUPAC recommended equations of state [15] and the correlation of Wagner and Pruss [16] were used to calculate the molar volumes of CO_2 and H_2O, respectively. The molar volumes of *c*-C_5H_{10} derivatives were calculated from densities measured in the present study. The molar

volumes of the s-I and s-II hydrates were calculated from each lattice constant (a = 1.20 nm (s-I), a = 1.73 nm (s-II) [1]). I made some assumptions in the calculation of the overall dissociation enthalpy of the CO_2+c-C_5H_{10} derivative mixed hydrates. CO_2 and c-C_5H_{10} derivative compartmentally occupy S- and L-cages of the s-II hydrate ($2CO_2$·c-C_5H_{10} derivative·$17H_2O$), respectively. In the case of the simple CO_2 hydrate, it was assumed that CO_2 molecules completely occupy the S-cages and M-cages of s-I hydrate (CO_2·$5.75H_2O$). It was considered that the pressure dependence on the molar volume for the c-C_5H_{10} derivative was negligible and the lattice parameter of the s-II hydrate was constant. To minimize the errors caused by the pressure effect, I have estimated the dissociation enthalpy only in a low pressure range. The dissociation enthalpies per mole of hydrates were 308 ± 29 kJ mol^{-1} (p = 0.60–0.96 MPa and T = 285.11–287.07 K), 202 ± 5 kJ mol^{-1} (p = 0.66–0.91 MPa and T = 276.46–278.39 K), and 379 ± 25 kJ mol^{-1} (p = 0.46–0.81 MPa and T = 287.24–289.23 K) in the CO_2+c-C_5H_{10}, CO_2+c-C_5H_8O, and CO_2+c-C_5H_9F mixed hydrates, respectively. The dissociation enthalpy of the CO_2+c-C_5H_9F mixed hydrate is the highest, followed by the CO_2+c-C_5H_{10} and CO_2+c-C_5H_8O mixed hydrates. The dissociation enthalpy of the simple CO_2 hydrate per mole of CO_2, which is estimated with the same procedure, is approximately 68 ± 6 kJ mol^{-1} (T = 275.37–281.21 K, p = 1.54–3.28 MPa) on the three-phase equilibrium curve (HL_1G) [9]. For comparison, the estimated dissociation enthalpies per mole of CO_2 are 154 ± 15 kJ mol^{-1} (p = 0.60–0.96 MPa and T = 285.11–287.07 K), 101 ± 2 kJ mol^{-1} (p = 0.66–0.91 MPa and T = 276.46–278.39 K), and 190 ± 13 kJ mol^{-1} (p = 0.46–0.81 MPa and T = 287.24–289.23 K) in the CO_2+c-C_5H_{10}, CO_2+c-C_5H_8O, and CO_2+c-C_5H_9F mixed hydrates, respectively.

III.1.5. Conclusions

Phase equilibrium curves of the CO_2+c-C_5H_{10} derivative+water systems have been investigated. c-C_5H_9F, c-C_5H_{10}, and c-C_5H_8O form s-II mixed hydrates with CO_2 and the equilibrium pressures of the mixed hydrates are lower than those of the simple CO_2 hydrate, whereas c-C_5H_9Br does not form hydrate in the presence of CO_2. The CO_2+c-C_5H_9F hydrate has the highest dissociation temperature followed by the CO_2+c-C_5H_{10} hydrate and CO_2+c-C_5H_8O hydrate at a certain pressure. Except for the CO_2+c-C_5H_9Br hydrate system, each four-phase equilibrium curve has the maximum dissociation temperature at $p \approx 3$ MPa, and that of the CO_2+c-C_5H_9F mixed hydrate system is the highest in the present mixed hydrate systems. Except for the CO_2+c-C_5H_9Br hydrate system, four-phase equilibrium curves (HL_1L_3G) show retrograde behavior and approach to the structural transition point between s-I and s-II at pressures above the maximum dissociation

point. The dissociation enthalpies of the CO_2+*c*-C_5H_9F, CO_2+*c*-C_5H_{10}, and CO_2+*c*-C_5H_8O mixed hydrates decrease in this order.

III.1.6. Nomenclatures

a	Lattice constant [m]
H	Enthalpy [J mol^{-1}]
p	Pressure [Pa]
T	Temperature [K]
u	Standard uncertainties of pressure [Pa] and temperature [K]
v	Molar volume [m^3 mol^{-1}]
G	Gas phase
H	Hydrate phase
L_1	Aqueous phase
L_2	CO_2-rich liquid phase
L_3	*c*-C_5H_{10} derivative-rich liquid phase
Q_2	Quadruple point of hydrate, aqueous, CO_2-rich liquid, and gas phases

III.1.7. References

[1] E.D. Sloan, C.A. Koh, *Clathrate Hydrates of Natural Gases, 3rd ed.*; CRC Press, Taylor and Francis Group: Boca Raton, FL, 2008.

[2] Z.-G. Sun, S.-S. Fan, K.-H. Guo, L. Shi, Y.-K. Guo, R.-Z. Wang, "Gas Hydrate Phase Equilibrium Data of Cyclohexane and Cyclopentane", *Journal of Chemical & Engineering Data*, **47**, 313–315 (2002).

[3] L.J. Florusse, C.J. Peters, J. Schoonman, K.C. Hester, C.A. Koh, S.F. Dec, K.N. Marsh, E.D. Sloan, "Stable Low-Pressure Hydrogen Clusters Stored in a Binary Clathrate Hydrate", *Science*, **306**, 469–471 (2004).

[4] S. Imai, K. Okutani, R. Ohmura, Y.H. Mori, "Phase Equilibrium for Clathrate Hydrates Formed with Difluoromethane+either Cyclopentane or Tetra-*n*-butylammonium Bromide", *Journal of Chemical & Engineering Data*, **50**, 1783–1786 (2005).

[5] S. Imai, K. Miyake, R. Ohmura, Y.H. Mori, "Phase Equilibrium for Clathrate Hydrates Formed with Difluoromethane or Krypton, Each Coexisting with Fluorocyclopentane", *Journal of Chemical & Engineering Data*, **51**, 2222–2224 (2006).

[6] S. Takeya, K. Yasuda, R. Ohmura, "Phase Equilibrium for Structure II Hydrates Formed with Methylfluoride Coexisting with Cyclopentane, Fluorocyclopentane, Cyclopentene, or Tetrahydropyran", *Journal of Chemical & Engineering Data*, **53**, 531–534 (2008).

[7] C. Dong, "PowderX: Windows-95-based Program for Powder X-Ray Diffraction Data Processing", *Journal of Applied Crystallography*, **32**, 838 (1999).

[8] Chekcell; http://www.ccp14.ac.uk. Chekcell developed by L. Laugier, B. Bochu, Laboratoire des Materiaux et du Genie Physique, Ecole Superieure de Physique de Grenoble: Grenoble, France (accessed April 28, 2011)

[9] K. Ohgaki, Y. Makihara, K. Takano, "Formation of CO_2 Hydrate in Pure and Sea Waters", *Journal of Chemical Engineering of Japan*, **26**, 558–564 (1993).

[10] J.S. Zhang, J.W. Lee, "Equilibrium of Hydrogen+Cyclopentane and Carbon Dioxide +Cyclopentane Binary Hydrates", *Journal of Chemical & Engineering Data*, **54**, 659–661 (2009).

[11] A.H. Mohammadi, D. Richon, "Phase Equilibria of Clathrate Hydrates of Methyl Cyclopentane, Methyl Cyclohexane, Cyclopentane or Cyclohexane+Carbon Dioxide", *Chemical Engineering Science*, **64**, 5319–5322 (2009).

[12] S.S. Fan, D.Q. Liang, K.H. Guo, "Hydrate Equilibrium Conditions for Cyclopentane and a Quaternary Cyclopentane-Rich Mixture", *Journal of Chemical & Engineering Data*, **46**, 930–932 (2001).

[13] C.H. Unruh, D.L. Karz, "Gas Hydrates of Carbon Dioxide-Methane Mixtures", *Journal of Petroleum Technology*, **1**, 83–86 (1949).

[14] M.M. Mooijer-van den Heuvel, R. Witteman, C.J. Peters, "Phase Behaviour of Gas Hydrates of Carbon Dioxide in the Presence of Tetrahydropyran, Cyclobutanone, Cyclohexane and Methylcyclohexane", *Fluid Phase Equilibria*, **182**, 97–110 (2001).

[15] S. Angus, B. Armstrong, K.M. de Reuck, *International Thermodynamic Tables of the Fluid State Carbon Dioxide*; Pergamon Press, Oxford, 1976.

[16] W. Wagner, A. Pruss, "International Equations for the Saturation Properties of Ordinary Water Substance. Revised According to the International Temperature Scale of 1990", *Journal of Physical and Chemical Reference Data*, **22**, 783–787 (1993).

Section 2

Thermodynamic Stability Boundaries and Structures of Methane+Monohalogenated Cyclopentane Mixed Hydrates

III.2.1. Abstract

Thermodynamic stability boundaries of mixed hydrates composed of CH_4 and *c*-C_5H_9F, chlorocyclopentane (*c*-C_5H_9Cl), or *c*-C_5H_9Br were investigated at T = 274.17–306.19 K and pressures up to p = 9.93 MPa under four-phase (HL_1L_3G) equilibrium conditions. The each boundary is laid at pressures lower than that of simple CH_4 hydrate. Especially, the CH_4+*c*-C_5H_9F mixed hydrate system has the lowest equilibrium pressure among three mixed hydrate systems investigated in the present study. Also, crystal structure of CH_4+*c*-C_5H_9Cl and CH_4+*c*-C_5H_9Br mixed hydrates was determined by means of PXRD. The PXRD patterns reveal that there is the limit of L-cage occupancy between *c*-C_5H_9Cl and *c*-C_5H_9Br.

III.2.2. Introduction

Hydrate enclathrates large amount of gas such as H_2, CH_4, and CO_2. Therefore, hydrate is suggested to be utilized for gas storage, transportation, and separation. However, high pressures and/or low temperatures are required for the formation and stabilization of hydrates, which is one of the most serious problems to be solved. Adding large guest species as a thermodynamic promoter to a simple gas hydrate system, the gas and large guest species occupy small and large cages respectively, resulting that s-II or s-H mixed hydrate can form at thermodynamic conditions milder than simple gas hydrate (i.e. lower pressure). That is why s-II and s-H hydrates have drawn attention in the field of natural gas storage and transportation. So far, many large guest species forming s-II and s-H hydrates were reported [1]. In **Chapter III Section 1**, I stated that *c*-C_5H_{10}, *c*-C_5H_8O, and *c*-C_5H_9F form s-II hydrates with CO_2. However, the occupancy limit for the L-cage of s-II hydrate former has not been clarified yet. Which cage large guest species occupy gives

fundamentally significant information about the occupancy limits of large guest species for the L-cage of s-II hydrate.

In this section, three monohalogenated cyclopentanes (*c*-C_5H_9X, X = F, Cl, and Br) are adopted as large guest species. *c*-C_5H_{10} and *c*-C_5H_9F form s-II hydrates and they occupy only L-cages [2–4]. It has not been reported whether *c*-C_5H_9Cl forms hydrates or not. According to previous reports mentioned above and the results in **Chapter III Section 1**, *c*-C_5H_9Cl is supposed to be either s-II or s-H hydrate former because it is larger than *c*-C_5H_9F and smaller than *c*-C_5H_9Br. Additionally, taking into consideration the previous studies on Kr+*c*-C_5H_9F [3], HFC-32+*c*-C_5H_9F [3], CH_3F+*c*-C_5H_9F [4], and CO_2+*c*-C_5H_9F mixed hydrates (**Chapter III Section 1**), CH_4+*c*-C_5H_9F mixed hydrate should be formed under drastically mild conditions. The four-phase (HL_1L_3G) equilibrium curves of the CH_4+*c*-C_5H_9F, CH_4+*c*-C_5H_9Cl, and CH_4+*c*-C_5H_9Br mixed hydrate systems were measured. The structure of the CH_4+*c*-C_5H_9Cl mixed hydrate, in addition, was clarified based on PXRD pattern.

III.2.3. Experimental

Materials

The materials used in the present study are summarized in **Table III-2-1**. All of them were used without further purification.

Table III-2-1. Information on the chemicals used in the present study.

Chemical name	Source	Mole fraction purity
CH_4	Liquid Gas Co., Ltd.	> 0.9999
c-C_5H_9F	SynQuest Laboratories, Inc.	> 0.9869
c-C_5H_9Cl	Wako Pure Chemical Ind., Ltd.	> 0.98
c-C_5H_9Br	Merck Ltd.	> 0.99
Distilled water	Wako Pure Chemical Ind., Ltd.	> 0.9999

Apparatus

The experimental apparatus for phase equilibrium measurement and PXRD used in the present study are the same as described in **Chapter II Section 3** and **Chapter III Section 1**, respectively.

Procedure

The experimental procedures for phase equilibrium measurement and PXRD performed in the present study are the same as described in **Chapter III Section 1**.

III.2.4. Results and Discussion

The PXRD patterns of the CH_4+*c*-C_5H_9Cl and CH_4+*c*-C_5H_9Br mixed hydrates obtained in the present study are shown in **Figure III-2-1**. The typical pattern of s-II hydrate was observed in the CH_4+*c*-C_5H_9Cl mixed hydrate. The space group and the lattice constant of the CH_4+*c*-C_5H_9Cl mixed hydrate are *Fd*3*m* and a = 1.734 ± 0.003 nm, respectively. On the other hand, the typical pattern of s-H hydrate was detected in the CH_4+*c*-C_5H_9Br mixed hydrate. The space group and the lattice constants of the CH_4+*c*-C_5H_9Br mixed hydrate are *P*6/*mmm* and a = 1.232 ± 0.001 nm, c = 1.019 ± 0.001 nm, respectively. The present study firstly proved that *c*-C_5H_9Cl is enclathrated into the L-cages of s-II hydrate in the presence of CH_4. One of the most surprising findings is that *c*-C_5H_9Br is enclathrated into the U-cages of s-H hydrate in the presence of CH_4, while *c*-C_5H_9Br is not enclathrated in the presence of CO_2 (**Chapter III Section 1**). This result indicates that CH_4 is more helpful than CO_2 for the enclathration of large guest species. The PXRD patterns also indicate that there is the limit of L-cage occupancy between *c*-C_5H_9Cl and *c*-C_5H_9Br, the former is one of the largest guest species that occupy the L-cages of s-II hydrate and the latter is one of the smallest guest species that occupy the U-cages of s-H hydrate.

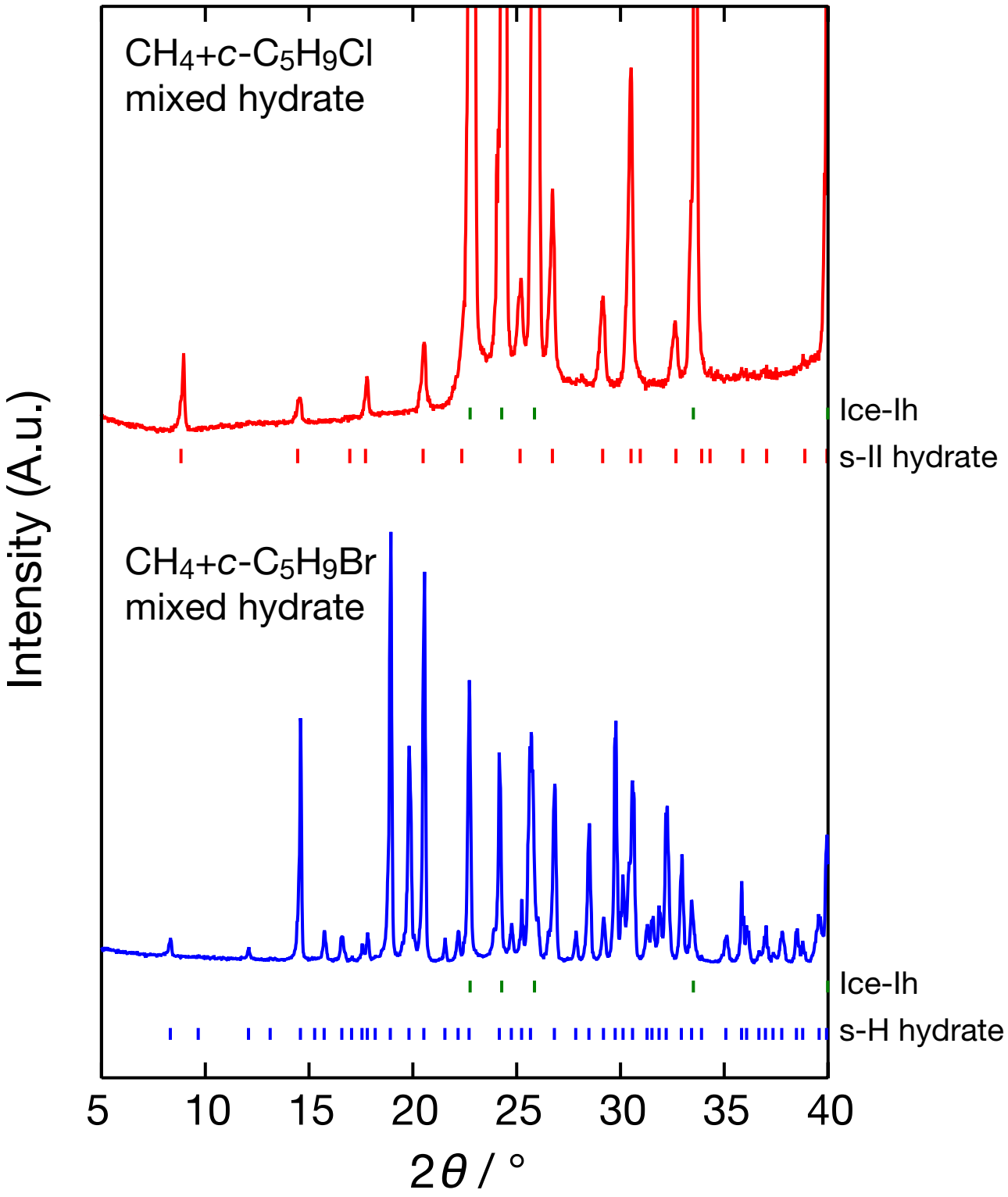

Figure III-2-1. PXRD patterns obtained from CH_4+*c*-C_5H_9Cl and CH_4+*c*-C_5H_9Br mixed hydrate samples prepared in the present study (recorded at T = 173 K).

Thermodynamic stability boundaries of CH_4+*c*-C_5H_9X (X = F, Cl, and Br) mixed hydrates measured in the present study under four-phase (HL_1L_3G) equilibrium conditions are shown in **Figure III-2-2** accompanied with those of the CH_4+*c*-C_5H_{10} mixed hydrate (s-II) [5,6] and the simple CH_4 hydrate (s-I) [7]. The obtained four-phase equilibrium data are also listed in **Table III-2-2**. The data for the CH_4+*c*-C_5H_9Br mixed hydrate agree well with the data recently reported in [8]. The four-phase equilibrium curves are located at a pressure side lower than the three-phase (HL_1G) equilibrium curve of s-I simple CH_4 hydrate system. All of the *c*-C_5H_9X adopted in the present study work as a thermodynamic promoter. CH_4+*c*-C_5H_9F mixed hydrate is the most thermodynamically stable in the present study, followed by CH_4+*c*-C_5H_9Cl and CH_4+*c*-C_5H_9Br mixed hydrates. Thermodynamic stability region of the s-II CH_4+*c*-C_5H_9F mixed hydrate is quite different from that of the s-II CH_4+*c*-C_5H_9Cl mixed hydrate. It implies that *c*-C_5H_9F has significantly appropriate molecular size and shape to occupy L-cage, whereas *c*-C_5H_9Cl may be a little bit too large for the L-cage occupancy. Especially, the CH_4+*c*-C_5H_9F hydrate is formed at thermodynamic conditions milder than CH_4+*c*-C_5H_{10} hydrate [5,6], where *c*-C_5H_{10} is a remarkable thermodynamic promoter forming s-II hydrates. The same tendency is observed in the Kr+*c*-C_5H_{10} and Kr+*c*-C_5H_9F mixed hydrates [3], HFC-32+*c*-C_5H_{10} and HFC-32+*c*-C_5H_9F mixed hydrates [3], CH_3F+*c*-C_5H_{10} and CH_3F+*c*-C_5H_9F mixed hydrate [4], and CO_2+*c*-C_5H_{10} and CO_2+*c*-C_5H_9F mixed hydrates (**Chapter III Section 1**).

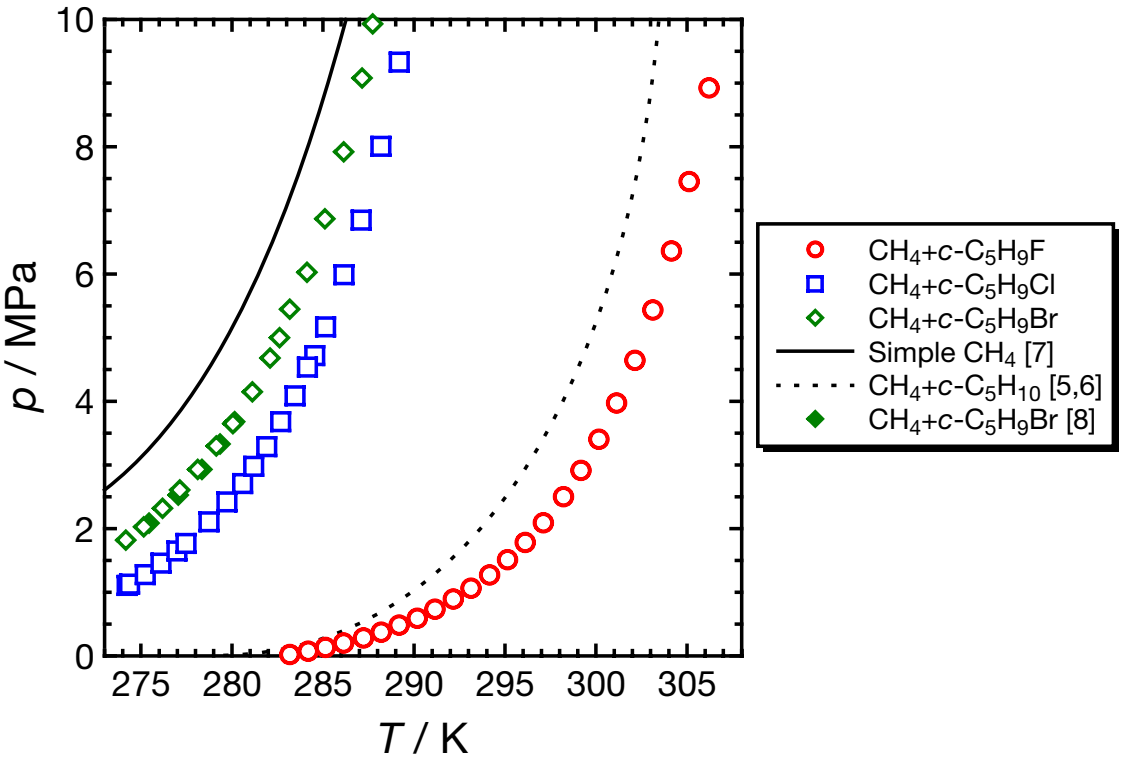

Figure III-2-2. Four-phase (HL_1L_3G) equilibrium relations in the CH_4+*c*-C_5H_9X (X = F, Cl, and Br)+water ternary systems.

Table III-2-2. Four-phase equilibrium conditions for CH_4+*c*-C_5H_9X (X = F, Cl, and Br)+water systems.

T / K[a]	p / MPa[a]	T / K[a]	p / MPa[a]	T / K[a]	p / MPa[a]
CH_4+*c*-C_5H_9F+water system		CH_4+*c*-C_5H_9Cl+water system		CH_4+*c*-C_5H_9Br+water system	
283.17	0.03	274.24	1.11	274.17	1.82
284.17	0.08	274.37	1.13	275.15	2.03
285.12	0.14	275.24	1.28	276.19	2.32
286.12	0.21	276.11	1.46	277.13	2.61
287.21	0.29	276.98	1.65	278.12	2.93
288.18	0.38	277.48	1.77	279.15	3.30
289.17	0.49	278.74	2.11	280.05	3.65
290.16	0.60	279.73	2.42	281.12	4.15
291.14	0.74	280.59	2.71	282.10	4.68
292.14	0.90	281.20	2.98	282.61	5.00
293.12	1.07	281.91	3.29	283.18	5.45
294.14	1.28	282.68	3.68	284.12	6.03
295.13	1.52	283.47	4.09	285.11	6.87
296.10	1.79	284.55	4.72	286.14	7.92
297.09	2.10	284.15	4.54	287.15	9.08
298.19	2.51	285.14	5.17	287.74	9.93
299.16	2.92	286.16	5.99		
300.14	3.41	287.10	6.85		
301.11	3.98	288.19	8.01		
302.12	4.65	289.19	9.33		
303.11	5.44				
304.12	6.37				
305.10	7.46				
306.19	8.93				

[a] $u(p)$ = 0.02 MPa and $u(T)$ = 0.02 K.

III.2.5. Conclusions

Thermodynamic stabilities of CH_4+*c*-C_5H_9F, CH_4+*c*-C_5H_9Cl, and CH_4+*c*-C_5H_9Br mixed hydrate systems were investigated. In addition, the structure of these mixed hydrates was clarified. Compared to the s-I simple CH_4 hydrate, the s-II CH_4+*c*-C_5H_9F mixed hydrate is much more thermodynamically stable, followed by s-II CH_4+*c*-C_5H_9Cl, and s-H CH_4+*c*-C_5H_9Br mixed hydrates. *c*-C_5H_9F works as a thermodynamic promoter much greater than *c*-C_5H_9Cl and *c*-C_5H_9Br. CH_4 works as a help gas for the enclathration of *c*-C_5H_9Br, whereas CO_2 does not. There is the limit of L-cage occupancy between *c*-C_5H_9Cl and *c*-C_5H_9Br. Comprehensively speaking, *c*-C_5H_9F is one of the best thermodynamic promoters, which is helpful for hydrate utilization.

III.2.6. Nomenclatures

a	Lattice constant [m]
c	Lattice constant [m]
p	Pressure [Pa]
T	Temperature [K]
u	Standard uncertainties of pressure [Pa] and temperature [K]
G	Gas phase
H	Hydrate phase
L_1	Aqueous phase
L_3	*c*-C_5H_9X-rich liquid phase

III.2.7. References

[1] E.D. Sloan, C.A. Koh, *Clathrate Hydrates of Natural Gases, 3rd ed.*; CRC Press, Taylor and Francis Group: Boca Raton, FL, 2008.

[2] S.S. Fan, D.Q. Liang, K.H. Guo, "Hydrate Equilibrium Conditions for Cyclopentane and a Quaternary Cyclopentane-Rich Mixture", *Journal of Chemical & Engineering Data*, **46**, 930–932 (2001).

[3] S. Imai, K. Miyake, R. Ohmura, Y.H. Mori, "Phase Equilibrium for Clathrate Hydrates Formed with Difluoromethane or Krypton, Each Coexisting with Fluorocyclopentane", *Journal of Chemical & Engineering Data*, **51**, 2222–2224 (2006).

[4] S. Takeya, K. Yasuda, R. Ohmura, "Phase Equilibrium for Structure II Hydrates Formed with Methylfluoride Coexisting with Cyclopentane, Fluorocyclopentane, Cyclopentene, or Tetrahydropyran", *Journal of Chemical & Engineering Data*, **53**, 531–534 (2008).

[5] B. Tohidi, A. Danesh, A.C. Todd, R.W. Burgass, K.K. Østergaard, "Equilibrium Data and Thermodynamic Modelling of Cyclopentane and Neopentane Hydrates", *Fluid Phase Equilibria*, **138**, 241–250 (1997).

[6] Z.-G. Sun, S.-S. Fan, K.-H. Guo, L. Shi, Y.-K. Guo, R.-Z. Wang, "Gas Hydrate Phase Equilibrium Data of Cyclohexane and Cyclopentane", *Journal of Chemical & Engineering Data*, **47**, 313–315 (2002).

[7] T. Nakamura, T. Makino, T. Sugahara, K. Ohgaki, "Stability Boundaries of Gas Hydrates Helped by Methane—Structure-H Hydrates of Methylcyclohexane and *cis*-1,2-Dimethylcyclohexane", *Chemical Engineering Science*, **58**, 269–273 (2003).

[8] Y. Jin, M. Kida, J. Nagao, "Structure H (sH) Clathrate Hydrate with New Large Molecule Guest Substances", *The Journal of Physical Chemistry C*, **117**, 23469–23475 (2013).

Section 3

Extraordinary Stability of Structure-H Methane+1,1,2,2,3,3,4-Heptafluorocyclopentane Mixed Hydrate at Pressures up to 373 MPa

III.3.1. Abstract

Thermodynamic stability boundary of s-H hydrates with large guest species (thermodynamic promoters) and CH_4 at extremely high pressures has been almost unclear. In the present study, the four-phase equilibrium relations in the s-H CH_4+1,1,2,2,3,3,4-heptafluorocyclopentane (1,1,2,2,3,3,4-HFCP) mixed hydrate system were investigated at T = 281.05–330.12 K and pressures up to p = 373 MPa. The difference between equilibrium pressures in the s-H CH_4+1,1,2,2,3,3,4-HFCP mixed hydrate system and the s-I simple CH_4 hydrate system gets larger with increase in temperature. The s-H CH_4+1,1,2,2,3,3,4-HFCP mixed hydrate survives even at p = 373 MPa and T = 330 K without any structural phase transition. The maximum temperature where the s-H CH_4+1,1,2,2,3,3,4-HFCP mixed hydrate is thermodynamically stable is likely to be beyond that of the s-H simple CH_4 hydrate.

III.3.2. Introduction

In general, simple gas hydrate belongs to either s-I or s-II hydrate, except at extremely high pressures [1–3]. In a part of s-II and s-H hydrates, small and large guest species occupy small and large cages, compartmentally. If the large guest species does not form hydrates without small guest species, the small guest species is called a help gas.

Recently, s-H hydrates have drawn much attention as a new medium for the natural gas transportation system [4]. The equilibrium pressure of an s-H hydrate formed by the addition of a small amount of large guest species is smaller than that of a simple gas hydrate (s-I or s-II, dependent on help gases). Furthermore, a larger amount of help gas can be stored because s-H

hydrates have the largest storage potential in small cage(s) among s-I, s-II, and s-H hydrates by stabilizing large cage with large guest species [4]. The thermodynamic properties and storage abilities of s-H hydrates depend on the chemical and physical properties of large guest species [5–7], for example, the molecular volume, the molar mass, the shape of large guest species, and so on.

One of the characteristic phenomena in an s-H hydrate system is the existence of the structural phase transition point, where an s-H mixed hydrate is collapsed and instead a simple gas hydrate, which contains only a help gas without large guest species, is formed. For example, in the case of the utilization of CH_4 as help gas, phase equilibrium curve in the s-H mixed hydrate systems comes close to that of the simple CH_4 hydrate system as pressures and temperatures rise. Finally, the curve of the s-H mixed hydrate systems crosses that of the simple CH_4 hydrate system at the structural phase transition point. For example, CH_4+*cis*-4-methylcyclohexanol [6], Xe+1,1-dimethylcyclohexane (1,1-DMCH) [7], CO_2+2,2-dimethylbutane [8], and CH_3F +methylcyclohexane [9] mixed hydrate systems exhibit such behavior. In other s-H mixed hydrate systems where such structural phase transition has not been reported, in addition, it has been considered that the s-H mixed hydrate is collapsed and changed to simple CH_4 hydrate at pressures higher than tens of MPa. It is because the slope (dp/dT) of phase equilibrium curve of the typical s-H mixed hydrate is larger than that of the simple gas hydrate containing only the once-help gas.

There are some important studies on the phase equilibria for the simple CH_4 hydrate system at extremely high pressures. Dyadin *et al*. [1] have reported that the simple CH_4 hydrate has the structural phase transition point at p = 620 MPa and T = 320 K on the three-phase (HL_1G) equilibrium curve. They have claimed that phase equilibrium curve after the phase transition intersects the melting curve of ice-VI at p = 1.62–1.65 GPa and T = 331 K, while the new crystal lattice was not identified definitely. Loveday *et al*. [2] have reported that the simple CH_4 hydrate above p = 620 MPa is very similar to s-H hydrate based on the X-ray and neutron diffraction analyses. Moreover, Kumazaki *et al*. [3] have reported the Raman spectra in a single crystal of the s-H CH_4 hydrate formed under three-phase equilibrium conditions (p = 1.0 GPa, T = 323 K).

In order to elucidate the characteristics of s-H hydrates, it is very important to investigate the phase equilibrium relations in s-H CH_4+large guest species mixed hydrate systems at higher pressures than ever, especially several hundred MPa. In this section, CH_4 and 1,1,2,2,3,3,4-HFCP are adopted as a help gas and a large guest species, respectively. First, I identified the structure of CH_4+1,1,2,2,3,3,4-HFCP mixed hydrate because it has not been reported whether 1,1,2,2,3,3,4-HFCP forms hydrates. Thermodynamic stability of the CH_4+1,1,2,2,3,3,4-HFCP mixed hydrate was investigated at pressures up to p = 373 MPa.

III.3.3. Experimental

Materials

The materials used in the present study are summarized in **Table III-3-1**. All of them were used without further purification.

Table III-3-1. Information on the chemicals used in the present study.

Chemical name	Source	Mole fraction purity
CH_4	Liquid Gas Co., Ltd.	> 0.9999
1,1,2,2,3,3,4-HFCP	Zeon Corp.	> 0.98
Distilled water	Wako Pure Chemical Ind., Ltd.	> 0.9999

Apparatus

The experimental apparatus for phase equilibrium measurement and PXRD used in the present study are the same as described in **Chapter II Section 3** and **Chapter III Section 1**, respectively.

Procedure

The experimental procedures for phase equilibrium measurement and PXRD performed in the present study are the same as described in **Chapter III Section 1**. The experimental procedure for Raman spectroscopy done in the present study is the same as described in **Chapter II Section 3**.

III.3.4. Results and Discussion

The PXRD pattern of the CH_4+1,1,2,2,3,3,4-HFCP mixed hydrate prepared at p = 3.31 MPa and T = 282.44 K is shown in **Figure III-3-1**. The typical pattern derived from s-H hydrate (hexagonal, *P*6/*mmm*) was detected in the CH_4+1,1,2,2,3,3,4-HFCP mixed hydrate. The lattice constants are a = 1.221 ± 0.002 nm and c = 1.002 ± 0.001 nm at T = 173 K.

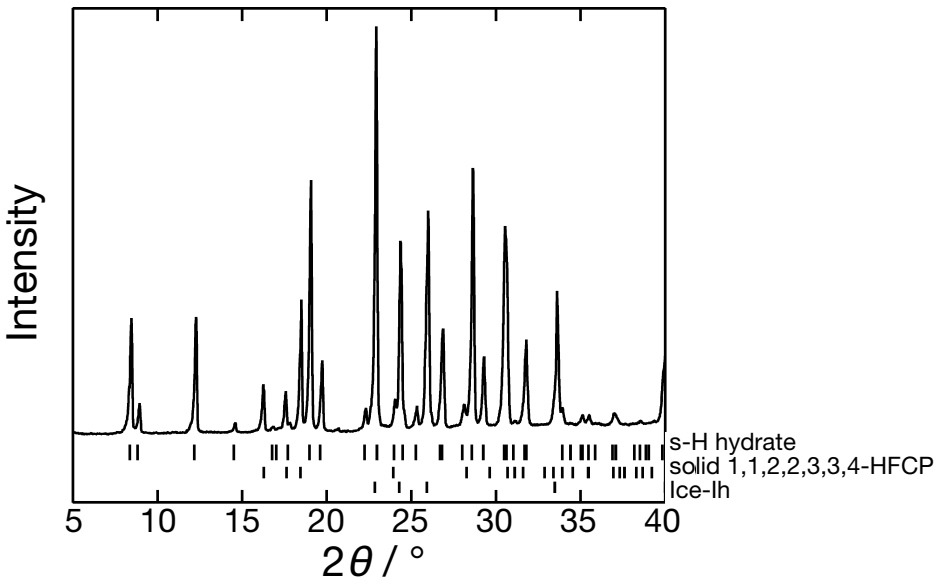

Figure III-3-1. PXRD pattern of CH_4+1,1,2,2,3,3,4-HFCP mixed hydrate prepared at p = 3.31 MPa and T = 282.44 K (recorded at T = 173 K).

Four-phase equilibrium relations of HL_1L_3G and $S_3L_1L_3G$ in the CH_4+1,1,2,2,3,3,4-HFCP +water ternary system are shown in **Figure III-3-2** and summarized in **Table III-3-2**. In the whole pressure and temperature range of the present study, the four-phase equilibrium curve (HL_1L_3G) is laid at a lower pressure side than the three-phase equilibrium curve (HL_1G) in simple CH_4 hydrate system. Until now, it had been believed that the s-H mixed hydrate is collapsed at the intersection between the four-phase equilibrium curve of s-H hydrates and the three-phase equilibrium curve of simple gas hydrates containing only the once-help gas in s-H hydrate system. In fact, such phase behavior has been reported in some s-H hydrates helped by CH_4 [6] and Xe [7]. Surprisingly, the four-phase equilibrium curve (HL_1L_3G) in the CH_4+1,1,2,2,3,3,4-HFCP mixed hydrate system does not intersect with the three-phase equilibrium curve (HL_1G) in the simple CH_4 hydrate system up to p = 373 MPa and T = 330.12 K. Rather, the difference between both equilibrium curves gets larger with increases in temperature and pressure. The four-phase equilibrium curve of HL_1L_3G exhibits no structural phase transition up to p = 373 MPa and T = 330.12 K. In addition, there is no significant difference in Raman shifts of the intramolecular vibration modes of the CH_4 and 1,1,2,2,3,3,4-HFCP molecules except for the weak pressure and temperature dependences, as shown in **Figure III-3-3**. On the other hand, the structure of simple CH_4 hydrate changes from s-I to s-H at p = 620 MPa and T = 320 K on the three-phase equilibrium curve (HL_1G) [1–3]. In the s-H simple CH_4 hydrate system, multiple CH_4 molecules surely occupy U-cage [2,3,10]. Directly comparing the stability boundary of the s-H CH_4+1,1,2,2,3,3,4-HFCP mixed hydrate with that of the s-H simple CH_4 hydrate, it is suggested that the contribution of large guest species to the stability of s-H hydrates is crucially significant.

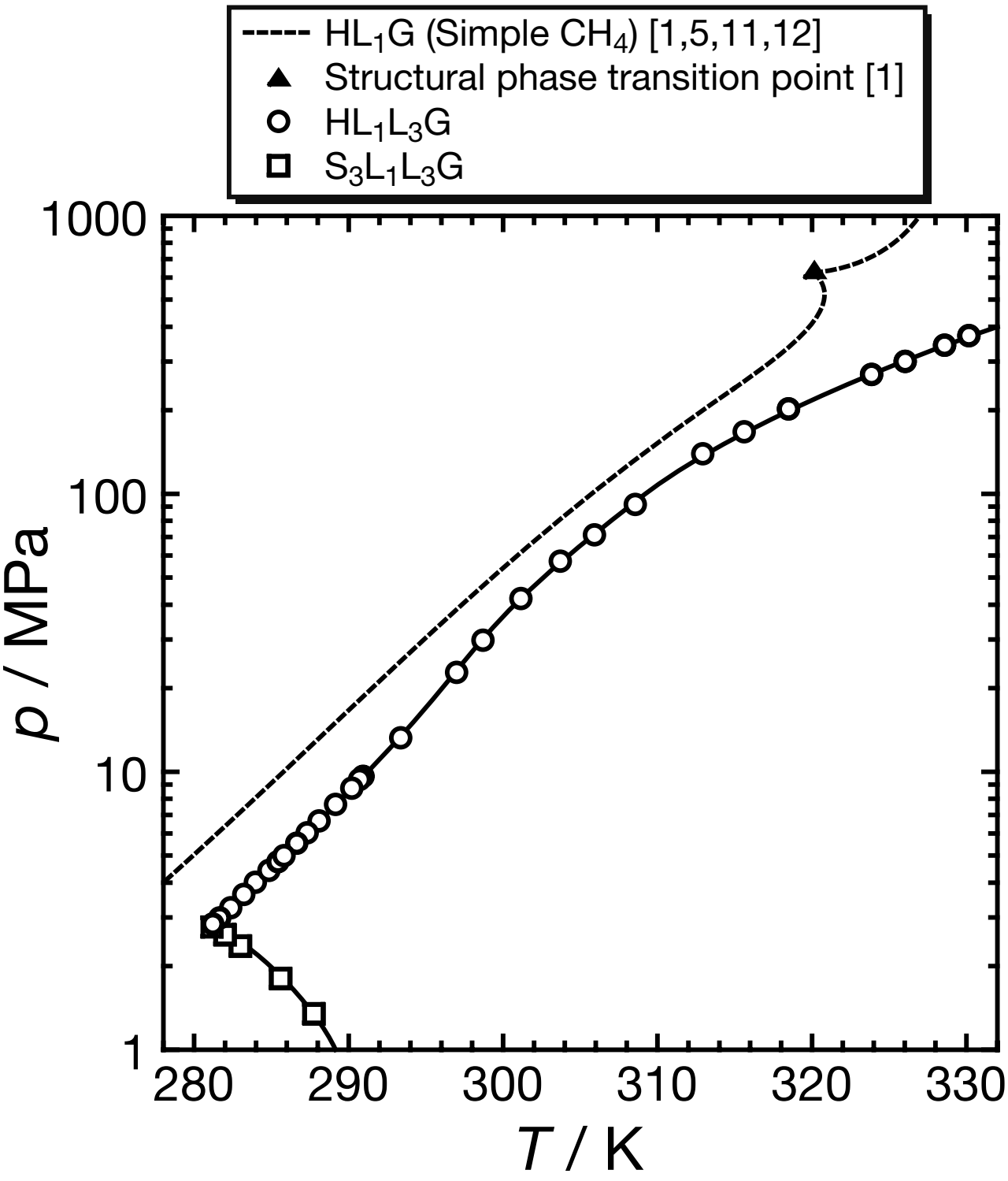

Figure III-3-2. Four-phase (HL_1L_3G and $S_3L_1L_3G$) equilibrium relations in the CH_4+1,1,2,2,3,3,4-HFCP+water ternary system.

Table III-3-2. Four-phase equilibrium data in the CH_4+1,1,2,2,3,3,4-HFCP+water ternary system.

T / K[a]	p / MPa[a]	T / K[a]	p / MPa[a]
HL_1L_3G		$S_3L_1L_3G$	
281.19	2.85	287.73	1.35
281.61	3.00	285.58	1.81
282.34	3.26	282.98	2.37
283.17	3.64	281.99	2.60
283.94	4.02	281.16	2.77
284.81	4.44		
285.12	4.63		
285.40	4.77		
285.78	5.02		
286.61	5.56		
287.30	6.06		
288.06	6.69		
289.12	7.68		
290.16	8.76		
290.69	9.41		
290.90	9.68		
293.35	13.3		
296.96	22.9		
298.67	29.9		
301.13	42.2		
303.69	57.6		
305.89	71.6		
308.53	92.0		
312.90	140		
315.59	168		
318.45	203		
323.83	270		
326.00	301		
328.56	344		
330.12	373		

[a] $u(p)$ = 0.02 MPa at p < 10 MPa, $u(p)$ = 0.2 MPa at p = 10–100 MPa, $u(p)$ = 2 MPa at p > 100 MPa, and $u(T)$ = 0.02 K.

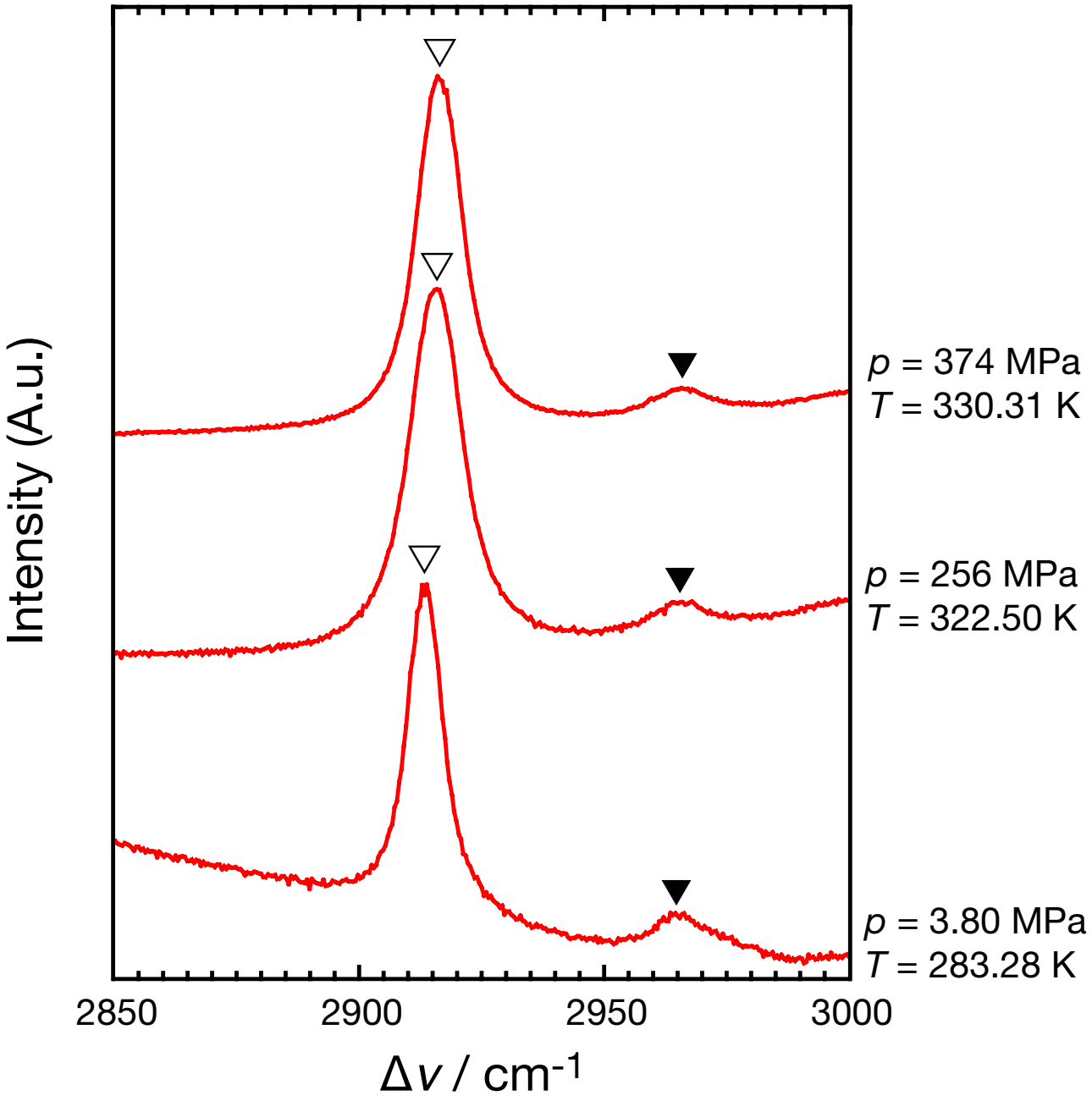

Figure III-3-3. Raman spectra of the intramolecular vibrations of the enclathrated CH_4 (open inverse triangle) and 1,1,2,2,3,3,4-HFCP (closed inverse triangle) molecules in the CH_4+1,1,2,2,3,3,4-HFCP mixed hydrates.

Among the large guest species forming s-H hydrates, 1,1-DMCH has been considered to be the most suitable for the s-H hydrate generation (that is, as a thermodynamic promoter) from the viewpoint of the equilibrium pressure reduction [13,14]. The equilibrium pressure of the CH_4+1,1,2,2,3,3,4-HFCP mixed hydrate is slightly higher than that of CH_4+1,1-DMCH mixed hydrate at pressures up to p = 10 MPa. Therefore, 1,1,2,2,3,3,4-HFCP would also be one of the suitable large guest species for the s-H hydrate generation.

III.3.5. Conclusions

1,1,2,2,3,3,4-HFCP generates an s-H hydrate in the presence of CH_4. Thermodynamic stability of the s-H CH_4+1,1,2,2,3,3,4-HFCP mixed hydrate was investigated at pressures up to p = 373 MPa. The most important finding is that the s-H CH_4+1,1,2,2,3,3,4-HFCP mixed hydrate remains thermodynamically stable even at p = 373 MPa and T = 330 K without any structural phase transition, although it had been believed that s-H hydrates with help gases would be collapsed and transformed to the simple hydrates enclathrating only help gases. Moreover, the stability boundary of the s-H CH_4+1,1,2,2,3,3,4-HFCP mixed hydrate is located beside that of the s-H CH_4+1,1-DMCH mixed hydrate. 1,1,2,2,3,3,4-HFCP would be one of the most suitable large guest species for the equilibrium pressure reduction derived from s-H hydrate formation.

III.3.6. Nomenclatures

θ	Diffraction angle [°]
ν	Wavenumber [m^{-1}]
a	Lattice constant [m]
c	Lattice constant [m]
p	Pressure [Pa]
T	Temperature [K]
u	Standard uncertainties of pressure [Pa] and temperature [K]
G	Gas phase
H	Hydrate phase
L_1	Aqueous phase
L_3	1,1,2,2,3,3,4-HFCP-rich liquid phase
S_3	Solid 1,1,2,2,3,3,4-HFCP phase

III.3.7. References

[1] Y.A. Dyadin, E.Y. Aladko, E.G. Larionov, “Decomposition of Methane Hydrates up to 15 kbar”, *Mendeleev Communications*, **7**, 34–35 (1997).

[2] J.S. Loveday, R.J. Nelmes, M. Guthrie, S.A. Belmonte, D.R. Allan, D.D. Klug, J.S. Tse, Y.P. Handa, "Stable Methane Hydrate above 2 GPa and the Source of Titan's Atmospheric Methane", *Nature*, **410**, 661–663 (2001).

[3] T. Kumazaki, Y. Kito, S. Sasaki, T. Kume, H. Shimizu, "Single-Crystal Growth of the High-Pressure Phase II of Methane Hydrate and Its Raman Scattering Study", *Chemical Physics Letters*, **388**, 18–22 (2004).

[4] A.A. Khokhar, J.S. Gudmundsson, E.D. Sloan, "Gas Storage in Structure H Hydrates", *Fluid Phase Equilibria*, **150–151**, 383–392 (1998).

[5] T. Nakamura, T. Makino, T. Sugahara, K. Ohgaki, "Stability Boundaries of Gas Hydrates Helped by Methane—Structure-H Hydrates of Methylcyclohexane and *cis*-1,2-Dimethylcyclohexane", *Chemical Engineering Science*, **58**, 269–273 (2003).

[6] T. Makino, M. Mori, Y. Mutou, T. Sugahara, K. Ohgaki, "Four-Phase Equilibrium Relations of Methane+Methylcyclohexanol Stereoisomer+Water Systems Containing Gas Hydrate", *Journal of Chemical & Engineering Data*, **54**, 996–999 (2009).

[7] T. Sugahara, T. Hara, S. Hashimoto, K. Ohgaki, "Icosahedron Cage Occupancy of Structure-H Hydrate Helped by Xe-1,1-, *cis*-1,2-, *trans*-1,2-, and *cis*-1,4-Dimethylcyclohexanes", *Chemical Engineering Science*, **60**, 1783–1786 (2005).

[8] R. Shen, K. Tezuka, T. Uchida, R. Ohmura, "Hydrate Phase Equilibrium in the System of (Carbon Dioxide+2,2-Dimethylbutane+Water) at Temperatures below Freezing Point of Water", *The Journal of Chemical Thermodynamics*, **53**, 27–29 (2012).

[9] S. Takeya, R. Ohmura, "Phase Equilibrium for Structure I and Structure H Hydrates Formed with Methylfluoride and Methylcyclohexane", *Journal of Chemical & Engineering Data*, **52**, 635–638 (2007).

[10] C.A. Tulk, D.D. Klug, A.M. dos Santos, G. Karotis, M. Guthrie, J.J. Molaison, N. Pradhan, "Cage Occupancies in the High Pressure Structure H Methane Hydrate: A Neutron Diffraction Study", *The Journal of Chemical Physics*, **136**, 054502-1–6 (2012).

[11] A.H. Mohammadi, R. Anderson, B. Tohidi, "Carbon Monoxide Clathrate Hydrates: Equilibrium Data and Thermodynamic Modeling", *AIChE Journal*, **51**, 2825–2833 (2005).

[12] S. Nakano, M. Moritoki, K. Ohgaki, "High-Pressure Phase Equilibrium and Raman Microprobe Spectroscopic Studies on the Methane Hydrate System", *Journal of Chemical & Engineering Data*, **44**, 254–257 (1999).

[13] T. Hara, S. Hashimoto, T. Sugahara, K. Ohgaki, "Large Pressure Depression of Methane Hydrate by Adding 1,1-Dimethylcyclohexane", *Chemical Engineering Science*, **60**, 3117–3119 (2005).

[14] M. Thomas, E. Behar, "Structure H Hydrate Equilibria of Methane and Intermediate Hydrocarbon Molecules", *Proceedings of 73rd Gas Processors Association Convention*, New Orleans, March 7–9, 1994.

Section 4

Structural Phase Transitions of Methane+Ethane Mixed-Gas Hydrate Induced by 1,1-Dimethylcyclohexane

III.4.1. Abstract

With the combination of natural gases and thermodynamic promoters in mind, CH_4+C_2H_6+1,1-DMCH+water system was investigated by means of Raman spectroscopy and isothermal phase equilibrium measurements under four-phase (HL_1L_3G) equilibrium conditions at T = 288.15 K. The results suggest that three kinds of hydrate structures emerge at T = 288.15 K in the CH_4+C_2H_6+1,1-DMCH+water system. The hydrate structure for this system changed from s-H to s-I via s-II with increase in the mole ratio of C_2H_6 to CH_4.

III.4.2. Introduction

The s-H hydrate formation needs both small guest species in the S-, S'-cages and large guest species in the U-cage, respectively (except for a hexagonal structure of simple hydrates at extreme pressures [1,2]). The former is called as a help-gas.

It has been reported that many kinds of molecules are encaged in hydrates, from small one (e.g. H_2) to large one (e.g. methylcyclohexane [3–6]). Gas hydrates have a large amount of potential for many fields. For example, H_2, CO_2, and CH_4 hydrates have drawn much attention to be used as gas storage medium [7]. However, these hydrates are generated at relatively high pressure and low temperature conditions, so it is necessary to moderate the conditions of hydrate formation for practical applications of gas hydrates. Generally speaking, the equilibrium pressure of the s-H hydrate containing help-gas and large guest species is lower than that of the simple hydrate (s-I or s-II) containing only a help-gas. The degree of the pressure drop depends on large guest species [8]. The s-H CH_4+1,1-DMCH hydrate exhibits quite large depression of the equilibrium pressure in the s-H hydrates containing CH_4 as help-gas [9].

In addition, the crystal structure depends on the guest concentration as reported in the CH_4+C_2H_6 [10–13], CH_4+*c*-C_3H_6 [14], CH_4+CF_4 [15] mixed-gas hydrate systems. Although each simple hydrate constructs s-I, the crystal structure of the mixed-gas hydrates changes between s-I and s-II depending on the mole fraction of guest species (water free). The transition to s-II hydrates draws much attention to increase storage capacity of CH_4 in s-II hydrates compared with that of s-I hydrates.

In this section, I adopted CH_4+C_2H_6 mixed-gas as a simple model of natural gas and 1,1-DMCH as a thermodynamic promoter. I measured the four-phase (HL_1L_3G) equilibrium relation in the CH_4+C_2H_6+1,1-DMCH+water system at T = 288.15 K. In addition, the hydrate structures and the cage occupancies of guest species were investigated by means of Raman spectroscopy.

III.4.3. Experimental

Materials

The materials used in the present study are summarized in **Table III-4-1**. All of them were used without further purification.

Table III-4-1. Information on the chemicals used in the present study.

Chemical name	Source	Mole fraction purity
CH_4	Liquid Gas Co., Ltd.	> 0.9999
C_2H_6	Takachiho Trading Co., Ltd.	> 0.999
1,1-DMCH	Sigma-Aldrich Co. LLC.	> 0.99
Distilled water	Wako Pure Chemical Ind., Ltd.	> 0.9999

Apparatus

The experimental apparatus for isothermal phase equilibrium measurement and Raman spectroscopy used in the present study are the same as described in **Chapter II Section 3**.

Procedures

The experimental procedures for isothermal phase equilibrium measurement and Raman spectroscopy performed in the present study are the same as described in **Chapter II Section 3**.

III.4.4. Results and Discussion

Figure III-4-1 shows Raman spectra of the C–H stretching, C–C stretching, and ring-breathing vibration modes of guest species in hydrate phase. These spectra were obtained under the four-phase (HL_1L_3G) equilibrium conditions for the CH_4+C_2H_6+1,1-DMCH+water system at T = 288.15 K. The Raman peaks indicated by closed inverse triangles are derived from the intramolecular vibration mode of 1,1-DMCH in the U-cage. The single peak detected at $\Delta\nu$ = 751 cm^{-1} is derived from the sapphire window.

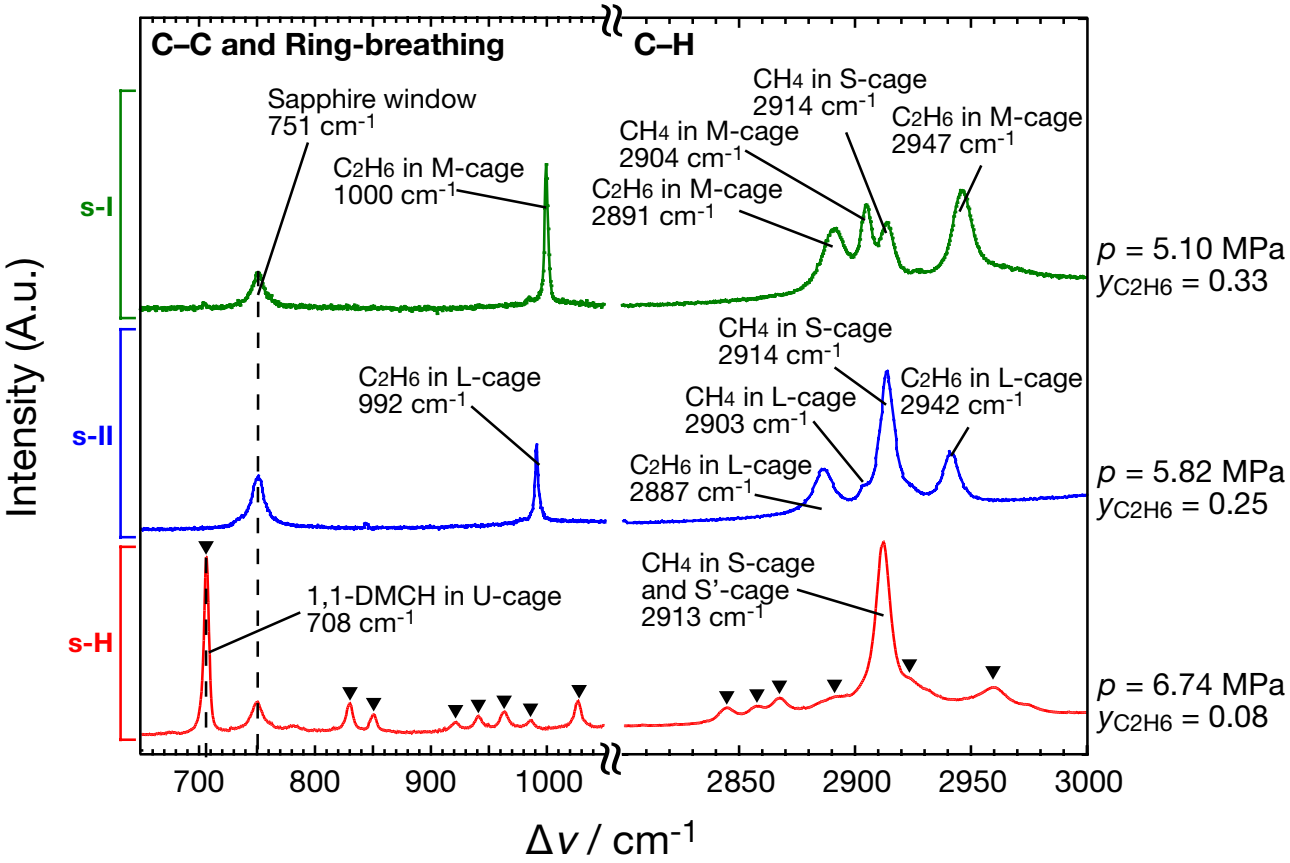

Figure III-4-1. Raman spectra of the C–H stretching, C–C stretching, and ring-breathing vibration modes of guest species in hydrate phase for CH_4+C_2H_6+1,1-DMCH+water system under four-phase (HL_1L_3G) equilibrium conditions at T = 288.15 K. Closed inverse triangles stand for the peaks derived from 1,1-DMCH in U-cage. The broken line stands for the contribution ($\Delta\nu$ = 751 cm^{-1}) from sapphire window.

At p = 6.74 MPa and y_{C2H6} = 0.08, a peak derived from the ring-breathing vibration mode of 1,1-DMCH was observed at $\Delta\nu$ = 708 cm^{-1}, which indicates that 1,1-DMCH is enclathrated in U-cages of s-H hydrates, while at $\Delta\nu$ = 705 cm^{-1} in the 1,1-DMCH-rich liquid phase [16]. The Raman shifts of 1,1-DMCH are consistent with the values reported in the previous study [16]. No remarkable Raman peak originated from the C–C stretching vibration mode of C_2H_6 was detected. A single peak was detected at $\Delta\nu$ = 2913 cm^{-1}, which corresponds to the C–H stretching vibration mode of the CH_4 in the S- and S'-cages [6,16,17]. Other peaks at p = 6.74 MPa and y_{C2H6} = 0.08 are derived from the intramolecular vibration modes of 1,1-DMCH. The Raman shifts and spectral shapes are similar to those obtained from the CH_4+1,1-DMCH hydrate crystal [16].

In the composition range over y_{C2H6} = 0.25, a single peak derived from C_2H_6 got remarkable instead of 1,1-DMCH. At p = 5.82 MPa and y_{C2H6} = 0.25, the spectral shape of the hydrate phase is completely different from that of the s-H hydrate at p = 6.74 MPa and y_{C2H6} = 0.08. The Raman peak observed at $\Delta\nu$ = 992 cm^{-1} corresponds to that of C_2H_6 encaged in the L-cages of s-II hydrates [10,13]. The peaks detected at $\Delta\nu$ = 2903 cm^{-1} and 2914 cm^{-1} are derived from CH_4 in the L- and S-cages of s-II hydrates, respectively. The peaks detected at $\Delta\nu$ = 2887 cm^{-1} and 2942 cm^{-1} are Fermi resonance peaks originated from C_2H_6 in L-cages. The Raman shifts are similar to those obtained from the s-II CH_4+C_2H_6 hydrate [10,13].

With further increase in y_{C2H6}, the single peak derived from the C_2H_6 molecule encaged in the M-cage of s-I hydrate [10,13,18] was detected at $\Delta\nu$ = 1000 cm^{-1} and the crystal structure of the mixed-gas hydrate transformed from s-II to s-I. Furthermore, there is no peak around $\Delta\nu$ = 1022 cm^{-1} of C_2H_6 forced to be enclathrated in the S-cage [18]. Therefore, the C_2H_6 molecule occupies only the large cages of s-I and s-II hydrates under the present experimental conditions. The CH_4 molecules are encaged in both the large (M-, L-cages) and small cages as shown in **Figure III-4-1**. The Raman peaks detected at $\Delta\nu$ = 2904 cm^{-1} and 2915 cm^{-1} are derived from CH_4 in the M- and S-cages of s-I hydrates [6,10,11,13,17,19]. The peaks detected at $\Delta\nu$ = 2891 cm^{-1} and 2947 cm^{-1} are the Fermi resonance peaks of C_2H_6 in the M-cages [10,11,13]. It is concluded that the crystal structure of the mixed-gas hydrates in the CH_4+C_2H_6+1,1-DMCH+water quaternary system changes from s-H to s-II, then to s-I with increase in C_2H_6 composition, while that in the CH_4+C_2H_6+water ternary system changes from s-I to s-II and back to s-I [10–13].

The pressure-composition projection for the CH_4+C_2H_6+1,1-DMCH+water system containing gas hydrates at T = 288.15 K is shown in **Figure III-4-2**. **Table III-4-2** summarizes the relation of equilibrium pressure and composition of gas phase. The three-phase equilibrium conditions for the CH_4+C_2H_6 mixed-gas hydrate system [13] are also shown in **Figure III-4-2** to compare with those of the present system. The equilibrium pressure at y_{C2H6} = 0 (i.e. the s-H CH_4+1,1-DMCH hydrate) agrees well with that reported in the previous study [9].

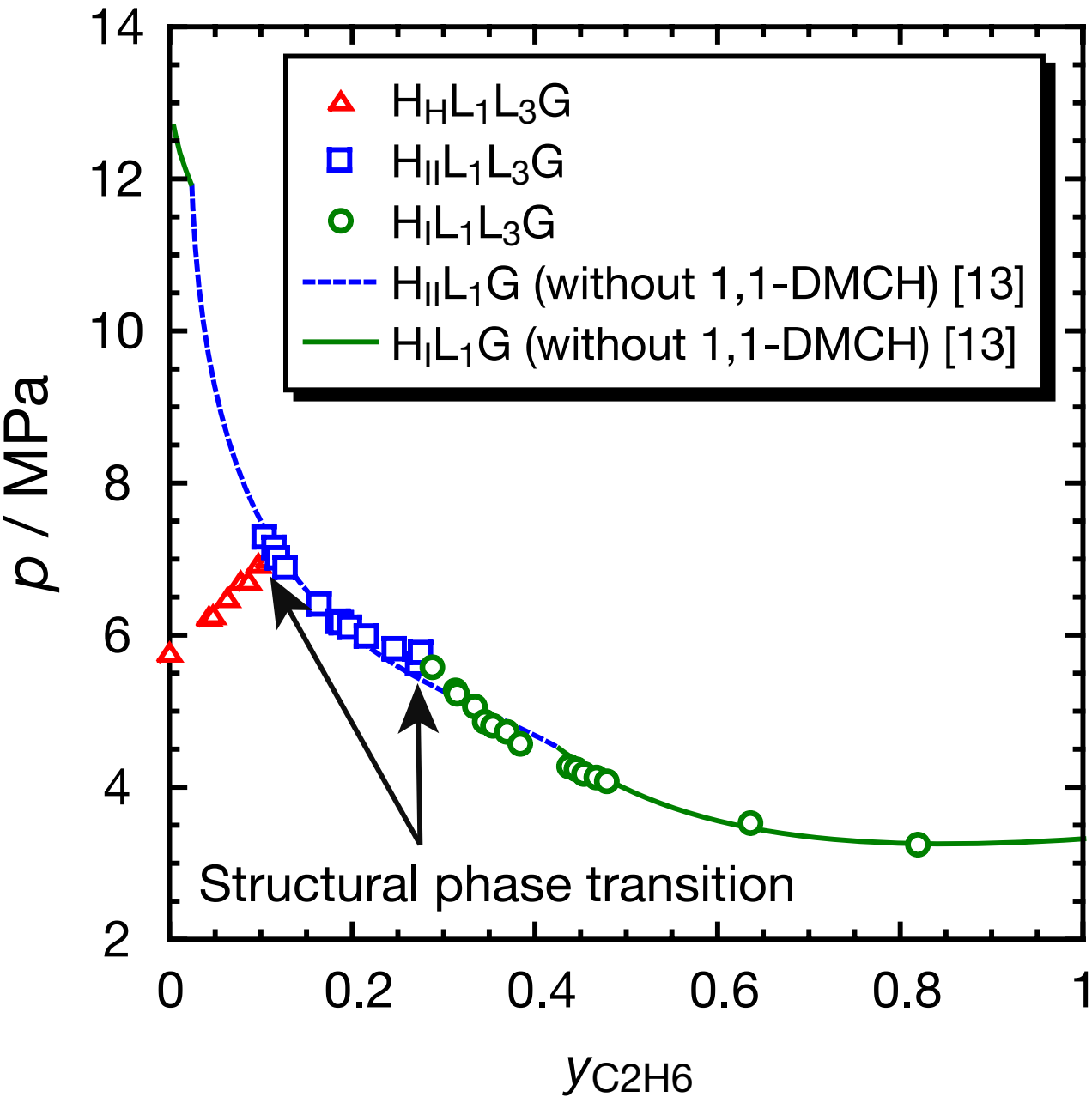

Figure III-4-2. Four-phase (HL_1L_3G) equilibrium pressure-composition projection for the CH_4+C_2H_6+1,1-DMCH+water system and three-phase (HL_1G) equilibrium pressure-composition projection for the CH_4+C_2H_6+water system [13] at T = 288.15 K.

Table III-4-2. Four-phase (HL_1L_3G) equilibrium data for CH_4+C_2H_6+1,1-DMCH+water system at T = 288.15 K.

p / MPa[a]	y_{C2H6}[a]	p / MPa[a]	y_{C2H6}[a]	p / MPa[a]	y_{C2H6}[a]
$H_HL_1L_3G$		$H_{II}L_1L_3G$		$H_IL_1L_3G$	
5.78	0	7.30	0.10	5.59	0.29
6.25	0.04	7.16	0.11	5.29	0.31
6.27	0.05	7.02	0.12	5.24	0.31
6.49	0.06	6.89	0.13	5.07	0.33
6.71	0.08	6.41	0.16	4.87	0.34
6.72	0.09	6.19	0.18	4.82	0.35
6.94	0.10	6.17	0.19	4.74	0.37
7.01	0.11	6.11	0.20	4.58	0.38
		5.99	0.22	4.29	0.44
		5.83	0.25	4.25	0.44
		5.63	0.27	4.19	0.45
		5.78	0.27	4.14	0.47
				4.09	0.48
				3.54	0.64
				3.26	0.82

[a] $u(p)$ = 0.04 MPa, $u(T)$ = 0.02 K, and $u(y_{C2H6})$ = 0.005.

Large pressure reduction from the CH_4+C_2H_6+water ternary system was observed in the composition range of y_{C2H6} = 0–0.10, which results from the formation of the s-H hydrate. The equilibrium pressure increases with a rise in the mole fraction of C_2H_6. If the C_2H_6 molecule occupies none of cages in the s-H hydrate, C_2H_6 would behave a diluent gas toward s-H CH_4+1,1-DMCH hydrate formation in the composition range of y_{C2H6} = 0–0.10. To evaluate cage occupancy of C_2H_6 in the s-H hydrate, the following thermodynamic prediction [20,21] based on the fugacity of CH_4 was performed.

In the CH_4+1,1-DMCH+water ternary system without C_2H_6, the equilibrium fugacity of CH_4 in the gas phase can be evaluated at a given temperature as:

$$f_{CH4}^{o} = \phi_{CH4}^{o} p^{o} \qquad \textbf{(Equation III-4-1)}$$

where f_{CH4}^{o} and ϕ_{CH4}^{o} are the fugacity and fugacity coefficient of CH_4 at four-phase (HL_1L_3G) equilibrium pressure p^{o}, respectively. Superscript o represents the absence of C_2H_6. In the present study, the fugacity coefficient was calculated by use of the Soave-Redlich-Kwong equation of state [22].

In the CH_4+C_2H_6+1,1-DMCH+water quaternary system, the equilibrium fugacity of CH_4 in the gas phase can be evaluated as:

$$f_{CH4} = y_{CH4} \phi_{CH4} p \qquad \textbf{(Equation III-4-2)}$$

where y_{CH4} is the equilibrium composition of CH_4 in the gas phase and p stands for the four-phase (HL_1L_3G) equilibrium pressure (total pressure).

Supposing that the gas hydrate generated from the CH_4+C_2H_6+1,1-DMCH+water quaternary system is the s-H CH_4+1,1-DMCH hydrate and the cage occupancies of CH_4 (in S- and S'-cages) and 1,1-DMCH (in U-cage) remain stationary, the fugacity of CH_4 calculated from **Equations III-4-1 and 2** should coincide with each other. In other words, the CH_4+1,1-DMCH hydrate is supposed to be generated when the fugacity of CH_4 in the gas mixture exceeds the equilibrium fugacity of CH_4+1,1-DMCH hydrate system.

Equation III-4-3 is derived from **Equations III-4-1 and 2** as:

$$p = \frac{\phi_{CH4}^{o}}{\phi_{CH4}} \frac{p^{o}}{y_{CH4}} \qquad \textbf{(Equation III-4-3)}$$

At a given gas phase composition, the equilibrium pressure is obtained by the trial and error method from **Equation III-4-3** on the assumption that the equilibrium fugacity of CH_4 in gas mixture is equal to that (f_{CH4} = 5.19 MPa) of CH_4+1,1-DMCH hydrate system in the whole composition range. The fugacity coefficient of CH_4 in the gas mixture was calculated by the Soave-Redlich-Kwong equation of state [22] with the ordinary mixing rule (k = -0.0078 for CH_4+C_2H_6) [23]. The critical constants of CH_4 and C_2H_6 were obtained from the reference [24].

Figure III-4-3 shows the comparison of experimental data with the predicted iso-fugacity curve in s-H hydrate region. The experimental pressures shift to the high-pressure side of the predicted pressures in this region. This result implies that the hydrate phase would be changed from the CH_4+1,1-DMCH hydrate to CH_4+C_2H_6+1,1-DMCH hydrate. In other words, there is a possibility that C_2H_6 is encaged in any cages of the s-H hydrate.

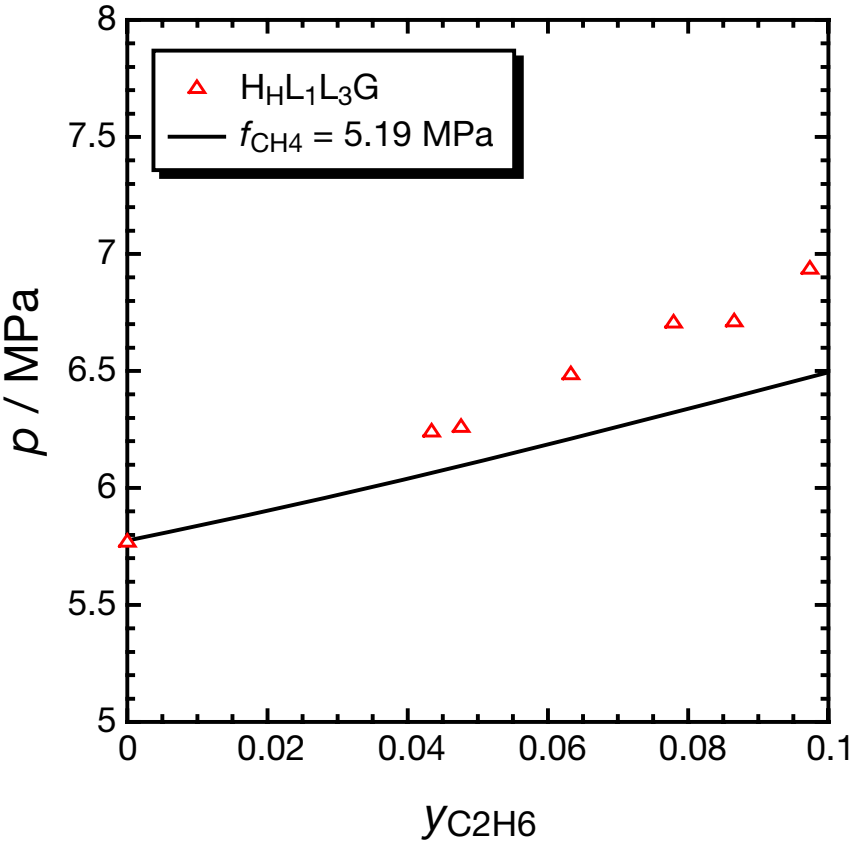

Figure III-4-3. Experimental data and predicted iso-fugacity curve in s-H hydrate region.

The four-phase equilibrium curve shows a discontinuous change in gradient at around y_{C2H6} = 0.10. Based on the results of Raman spectroscopic analysis, the crystal structure of the mixed-gas hydrates transforms from s-H to s-II at the composition. Beyond the composition of y_{C2H6} = 0.10, the equilibrium pressures are close to those for the CH_4+C_2H_6 mixed-gas hydrate system [13]. The equilibrium curve represented in **Figure III-4-2** shows a discontinuous change in gradient again at the composition of y_{C2H6} = 0.29 ± 0.04. The Raman spectrum obtained at p = 5.82 MPa and y_{C2H6} = 0.25 indicates the formation of the s-II hydrate, while that obtained at p = 5.10 MPa and y_{C2H6} = 0.33 indicates the formation of the s-I hydrate. Therefore, the discontinuous point corresponds to the hydrate structural phase transition point from s-II to s-I. In the case without 1,1-DMCH (i.e. the CH_4+C_2H_6 mixed-gas hydrate system), it is reported that the transition point from s-II to s-I exists at around y_{C2H6} = 0.40 at T = 288.15 K [13]. The shift of transition point may be caused by the existence of 1,1-DMCH, but is not clear at this stage.

The crystal structure of the mixed-gas hydrate is s-I in the composition range from y_{C2H6} = 0.29–1. The equilibrium pressures are almost consistent with those of the CH_4+C_2H_6 mixed-gas hydrate system [13]. Therefore, it is suggested that the addition of 1,1-DMCH hardly affects on the equilibrium pressure of s-I CH_4+C_2H_6 mixed-gas hydrate at $y_{C2H6} > 0.29$ except liquid C_2H_6 phase appears instead of gas phase under the conditions of y_{C2H6} = 0.82–1.0.

III.4.5. Conclusions

Isothermal phase equilibria have been investigated for the CH_4+C_2H_6+1,1-DMCH hydrate system at T = 288.15 K. In addition, crystal structures of the mixed-gas hydrates have been identified by means of Raman spectroscopy. The most important finding is that the existence of 1,1-DMCH results in a different phase behavior from the CH_4+C_2H_6 mixed-gas hydrate system. The thermodynamically stable phase in the CH_4+C_2H_6+1,1-DMCH+water quaternary system is transformed from s-H to s-I via s-II with increase in C_2H_6 concentration, while from s-I to s-II and back to s-I without 1,1-DMCH. In the present system, CH_4 and C_2H_6 are enclathrated in the s-I and s-II hydrates. On the other hand, CH_4 and 1,1-DMCH are mainly enclathrated in the s-H hydrate. In the s-H hydrate, there is a possibility that C_2H_6 can be enclathrated in hydrate cages.

III.4.6. Nomenclatures

ν	Wavenumber [m^{-1}]
ϕ_{CH4}	Fugacity coefficient of CH_4 [-]
f_{CH4}	Fugacity of CH_4 [Pa]
k	Binary parameter between CH_4 and C_2H_6 [-]
p	Pressure [Pa]
T	Temperature [K]
u	Standard uncertainties of pressure [Pa], temperature [K], and mole fraction [-]
y_{CH4}	Mole fraction of CH_4 in gas phase (water and 1,1-DMCH free) [-]
y_{C2H6}	Mole fraction of C_2H_6 in gas phase (water and 1,1-DMCH free) [-]
G	Gas phase
H	Hydrate phase
H_I	s-I hydrate phase
H_{II}	s-II hydrate phase
H_H	s-H hydrate phase
L_1	Aqueous phase
L_3	1,1-DMCH-rich liquid phase

III.4.7. References

[1] H. Hirai, Y. Uchihara, H. Fujihisa, M. Sakashita, E. Katoh, K. Aoki, K. Nagashima, Y. Yamamoto, T. Yagi, "High-Pressure Structures of Methane Hydrate Observed up to 8 GPa at Room Temperature", *The Journal of Chemical Physics*, **115**, 7066–7070 (2001).

[2] A.Y. Manakov, V.I. Voronon, A.V. Kurnosov, A.E. Teplykh, V.Y. Komarov, Y.A. Dyadin, "Structural Investigations of Argon Hydrates at Pressures up to 10 kbar", *Journal of Inclusion Phenomena and Macrocyclic Chemistry*, **48**, 11–18 (2004).

[3] A.P. Mehta, E.D. Sloan, "Structure H Hydrate Phase Equilibria of Methane+Liquid Hydrocarbon Mixtures", *Journal of Chemical & Engineering Data*, **38**, 580–582 (1993).

[4] T. Nakamura, T. Makino, T. Sugahara, K. Ohgaki, "Stability Boundaries of Gas Hydrates Helped by Methane—Structure-H Hydrates of Methylcyclohexane and *cis*-1,2-Dimethylcyclohexane", *Chemical Engineering Science*, **58**, 269–273 (2003).

[5] N. Shimada, K. Sugahara, T. Sugahara, K. Ohgaki, "Phase Transition from Structure-H to Structure-I in the Methylcyclohexane+Xenon Hydrate System", *Fluid Phase Equilibria*, **205**, 17–23 (2003).

[6] R. Susilo, J.A. Ripmeester, P. Englezos, "Characterization of Gas Hydrates with PXRD, DSC, NMR, and Raman Spectroscopy", *Chemical Engineering Science*, **62**, 3930–3939 (2007).

[7] J.S. Gudmundsson, A. Borrehaug, "Frozen Hydrate for Transport of Natural Gas", *Proceedings of the 2nd International Conference of Natural Gas Hydrate*, Toulouse, France, 1996.

[8] E.D. Sloan, C.A. Koh, *Clathrate Hydrates of Natural Gases, 3rd ed.*; CRC Press, Taylor and Francis Group: Boca Raton, FL, 2008.

[9] T. Hara, S. Hashimoto, T. Sugahara, K. Ohgaki, "Large Pressure Depression of Methane Hydrate by Adding 1,1-Dimethylcyclohexane", *Chemical Engineering Science*, **60**, 3117–3119 (2005).

[10] S. Subramanian, R.A. Kini, S.F. Dec, E.D. Sloan, "Evidence of Structure II Hydrate Formation from Methane+Ethane Mixtures", *Chemical Engineering Science*, **55**, 1981–1999 (2000).

[11] S. Subramanian, A.L. Ballard, R.A. Kini, S.F. Dec, E.D. Sloan, "Structural Transitions in Methane+Ethane Gas Hydrates—Part I: Upper Transition Point and Applications", *Chemical Engineering Science*, **55**, 5763–5771 (2000).

[12] A.L. Ballard, E.D. Sloan, "Structural Transitions in Methane+Ethane Gas Hydrates—Part II: Modeling Beyond Incipient Conditions", *Chemical Engineering Science*, **55**, 5773–5782 (2000).

[13] S. Hashimoto, A. Sasatani, Y. Matsui, T. Sugahara, K. Ohgaki, "Isothermal Phase Equilibria for Methane+Ethane+Water Ternary System Containing Gas Hydrates", *The Open Thermodynamics Journal*, **2**, 100–105 (2008).

[14] T. Makino, M. Tongu, T. Sugahara, K. Ohgaki, "Hydrate Structural Transition Depending on the Composition of Methane+Cyclopropane Mixed Gas Hydrate", *Fluid Phase Equilibria*, **233**, 129–133 (2005).

[15] Y. Kunita, T. Makino, T. Sugahara, K. Ohgaki, "Raman Spectroscopic Studies on Methane +Tetrafluoromethane Mixed-Gas Hydrate System", *Fluid Phase Equilibria*, **251**, 145–148 (2007).

[16] T. Makino, T. Sugahara, K. Ohgaki, "Effects of Large Guest Species on Thermodynamic Properties of Structure-H Hydrates", *Proceedings of the 11th International Conference on the Physics and Chemistry of Ice*, 363–370 (2007).

[17] A.K. Sum, R.C. Burruss, E.D. Sloan, Jr., "Measurement of Clathrate Hydrates via Raman Spectroscopy", *The Journal of Physical Chemistry B*, **38**, 7371–7377 (1997).

[18] K. Morita, S. Nakano, K. Ohgaki, "Structure and Stability of Ethane Hydrate Crystal", *Fluid Phase Equilibria*, **169**, 167–175 (2000).

[19] S. Nakano, M. Moritoki, K. Ohgaki, "High-Pressure Phase Equilibrium and Raman Microprobe Spectroscopic Studies on the Methane Hydrate System", *Journal of Chemical & Engineering Data*, **44**, 254–257 (1999).

[20] T. Sugahara, S. Murayama, S. Hashimoto, K. Ohgaki, "Phase Equilibria for H_2+CO_2+H_2O System Containing Gas Hydrates", *Fluid Phase Equilibria*, **233**, 190–193 (2005).

[21] T. Sugahara, H. Mori, J. Sakamoto, S. Hashimoto, K. Ogata, K. Ohgaki, "Cage Occupancy of Hydorogen in Carbon Dioxide, Ethane, Cyclopropane and Propane Hydrates", *The Open Thermodynamics Journal*, **2**, 1–6 (2008).

[22] G. Soave, "Equilibrium Constants from a Modified Redlich-Kwong Equation of State" *Chemical Engineering Science*, **27**, 1197–1203 (1972).

[23] H. Knapp, R. Doring, L. Oellrich, U. Plocker, J.M. Prausnitz, "Vapor-Liquid Equilibria for Mixtures of Low Boiling Substances", *Chemistry Data Series, vol. VI*; Dechema, Frankfult, 1982.

[24] R.C. Reid, J.M. Prausnitz, B.E. Poling, *The Properties of Gasses and Liquids, 4th ed.*; McGraw-Hill, New York, 1986.

Chapter IV

General Conclusions

IV.1. Conclusions in the Thesis

Many kinds of mixed hydrate systems were investigated as described in **Chapters II and III**. Crystal structures of mixed hydrates were directly analyzed with PXRD. Thermodynamic stability boundaries of the mixed hydrates and cage occupancies of guest species were also clarified. In this thesis, mixed hydrates were classified into two types according to the cage occupancy of guest species; competitive cage occupancy and compartmental cage occupancy.

Competitive-Type Mixed Hydrates

Structural phase transitions were observed in the isotherms of some mixed hydrate systems, which indicates that a mixed hydrate belongs to thermodynamically stable structure at a given pressure, temperature, and composition. In some cases, a structural phase transition causes heterogeneous azeotropic-like behavior where equilibrium curve of hydrate phase changes discontinuously. Local pressure minima, observed in the isotherms of some mixed hydrate systems, are due to negative azeotropic-like behavior where equilibrium composition of gas phase coincides with that of hydrate phase. Besides, the higher the temperature is, the more remarkable the negative azeotropic-like behavior is. From the relation between temperature and equilibrium composition at the local pressure minima in s-I and s-II hydrate regions, small and large guest species in the certain mixed gas hydrate systems almost compartmentally occupy small and large cages of s-I and s-II hydrates at the local pressure minima. At this point, the mixed hydrate can be treated as if it is the simple hydrate and can form at relatively low pressure. Therefore, it is significantly valuable for utilization.

Compartmental-Type Mixed Hydrates

Thermodynamic stabilities of s-II and s-H hydrates remarkably depend on the large guest species. In this study, it was clarified that small guest species also dominates whether large guest species is enclathrated in large cage or not. CH_4 is more helpful than CO_2 for the enclathration of large guest species in s-H hydrate. It can be commonly stated that *c*-C_5H_{10} derivatives work as effective thermodynamic promoters, especially *c*-C_5H_9F is superior. The extraordinary stability of s-H mixed hydrate at high pressures and temperatures was firstly proved. The isotherm in the quaternary mixed hydrate system, including natural gases and large guest species, showed the phase transitions among s-I, s-II, and s-H hydrates depending on the composition of gas phase. Based on the results on the s-H hydrates in this chapter, I found out the possibility that small and large guest species may competitively occupy U-cage at a certain thermodynamic condition, besides, some

small guest species multiply occupy a U-cage as shown in **Figure IV-1**. This is significantly interesting from the viewpoint of properties of s-H hydrates.

IV.2. Suggestion for the Future Works

In this thesis, the mixed hydrates composed of target gas and thermodynamic promoter were classified into two types, competitive cage occupancy and compartmental cage occupancy. Competitive and compartmental-type mixed hydrates are controlled for each application. However, the competitive cage occupancy appears in some compartmental-type mixed hydrate system and vice versa. The findings in this thesis reveal that the cage occupancy of guest species in mixed hydrates is complicated and dependent on pressure, temperature, and the combination of small and large guest species. Further investigation of the thermodynamic properties of unclarified mixed hydrate is really important for its utilization. Moreover, only experimental results on the thermodynamic properties are not sufficient at all. It is necessary to collect other properties, for instance, kinetic and rheological properties of hydrate such as formation or dissociation rates, viscosities, and cohesion. I deeply wish that, digesting the knowledge obtained from these studies, the investigation on hydrate is developed with many kinds of approach and hydrate is utilized practically in chemical and physical processes.

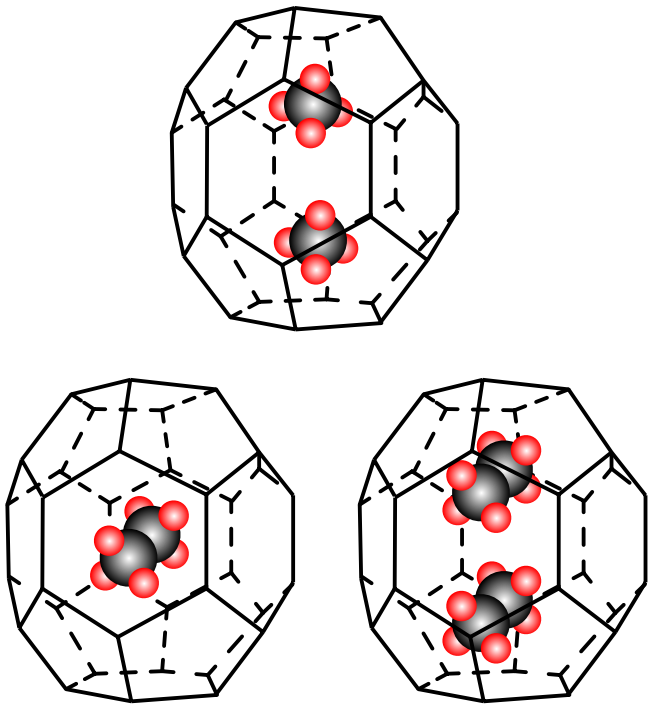

Figure IV-1. Schematic illustration of competitive and multiple U-cage occupancy by small guest species.

List of Publications

[1] Yuuki Matsumoto, Hiroshi Miyauchi, Takashi Makino, Takeshi Sugahara, Kazunari Ohgaki, "Structural Phase Transitions of Methane+Ethane Mixed-Gas Hydrate Induced by 1,1-Dimethylcyclohexane", *Chemical Engineering Science*, **66**, 2672–2676 (2011).

[2] Takeshi Sugahara, Aki Endo, Hiroshi Miyauchi, Seung An Choi, Yuuki Matsumoto, Kenjiro Yasuda, Shunsuke Hashimoto, Kazunari Ohgaki, "High-Pressure Phase Equilibrium and Raman Spectroscopic Studies on the 1,1-Difluoroethane (HFC-152a) Hydrate System", *Journal of Chemical & Engineering Data*, **56**, 4592–4596 (2011).

[3] Hiroshi Miyauchi, Kenjiro Yasuda, Yuuki Matsumoto, Shunsuke Hashimoto, Takeshi Sugahara, Kazunari Ohgaki, "Isothermal Phase Equilibria for the (HFC-32+HFC-134a) Mixed-Gas Hydrate System", *The Journal of Chemical Thermodynamics*, **47**, 1–5 (2012).

[4] Takeshi Sugahara, Hiroshi Miyauchi, Sumihiro Suzuki, Yuuki Matsumoto, Kenjiro Yasuda, Takashi Makino, Kazunari Ohgaki, "Isothermal Phase Equilibria for the (Xenon+Cyclopropane) Mixed-Gas Hydrate System", *The Journal of Chemical Thermodynamics*, **47**, 13–16 (2012).

[5] Sumihiro Suzuki, Kenjiro Yasuda, Yoshito Katsuta, Yuuki Matsumoto, Shunsuke Hashimoto, Takeshi Sugahara, Kazunari Ohgaki, "Isothermal Phase Equilibria for the CO_2+1,1-Difluoroethane and CO_2+1,1,1,2-Tetrafluoroethane Mixed-Gas Hydrate Systems", *Journal of Chemical & Engineering Data*, **58**, 780–784 (2013).

[6] Yoshito Katsuta, Sumihiro Suzuki, Yuuki Matsumoto, Shunsuke Hashimoto, Takeshi Sugahara, Kazunari Ohgaki, "Phase Equilibrium Relations and Structural Transition in the 1,1,1,2-Tetrafluoroethane Hydrate System", *Journal of Chemical & Engineering Data*, **58**, 1378–1381 (2013).

[7] Sumihiro Suzuki, Yuuki Matsumoto, Yoshito Katsuta, Shunsuke Hashimoto, Takeshi Sugahara, Kazunari Ohgaki, "Structure-H Methane+1,1,2,2,3,3,4-Heptafluorocyclopentane Mixed Hydrate at Pressures up to 373 MPa", *The Journal of Physical Chemistry A*, **117**, 4338–4341 (2013).

[8] Akio Nishikawa, Tomohiro Tanabe, Kazuma Kitamura, Yuuki Matsumoto, Kazunari Ohgaki, Takeshi Sugahara, "*In Situ* Raman Spectra of Hydrogen in Large Cages of Hydrogen +Tetrahydrofuran Mixed Hydrates", *Chemical Engineering Science*, **101**, 1–4 (2013).

[9] Yuuki Matsumoto, Takashi Makino, Takeshi Sugahara, Kazunari Ohgaki, "Phase Equilibrium Relations for Binary Mixed Hydrate Systems Composed of Carbon Dioxide and Cyclopentane Derivatives", *Fluid Phase Equilibria*, **362**, 379–382 (2014).

[10] Yuuki Matsumoto, R. Gary Grim, Takeshi Sugahara, Kazunari Ohgaki, E. Dendy Sloan, Carolyn A. Koh, Amadeu K. Sum, "Investigating the Thermodynamic Stabilities of Hydrogen and Methane Binary Gas Hydrates", *The Journal of Physical Chemistry C*, **118**, 3783–3788 (2014).

List of Presentations

[1] ○Yuuki Matsumoto, Hiroshi Miyauchi, Takashi Makino, Takeshi Sugahara, Kazunari Ohgaki, "Structural Phase Transitions of Methane+Ethane Mixed-Gas Hydrate Induced by 1,1-Dimethylcyclohexane", *7th International Conference on Gas Hydrate*, 428.00, Edinburgh, Scotland, United Kingdom, July 17–21, 2011, Oral Presentation.

[2] ○Takashi Makino, Yuuki Matsumoto, Hiroki Masuda, Takeshi Sugahara, Kazunari Ohgaki, "Effect of Ionic Liquid on Hydrate Formation Rate in Carbon Dioxide Hydrates", *7th International Conference on Gas Hydrate*, 554.00, Edinburgh, Scotland, United Kingdom, July 17–21, 2011, Poster Presentation.

[3] ○Yuuki Matsumoto, "Thermodynamic Properties of Mixed-Gas Hydrate -Systems of Carbon Dioxide+Cyclopentane Derivatives-", *The 11th Global COE International Symposium: Bio-Environmental Chemistry*, P-22, Suita, Osaka, Japan, December 19–21, 2011, Poster Presentation.

[4] Gary Grim, Yuki Matsumoto, Dendy Sloan, Amadeu K. Sum, ○Carolyn A. Koh, "Synthesis, Structure, and Property Relations of Hydrogen Clathrate Hydrates", *Invited Talk for ACS New Orleans Symposium on Hydrogen Production, Storage, and Utilization*, April 7–11, 2013, Oral Presentation.

[5] ○Yuuki Matsumoto, Takashi Makino, Takeshi Sugahara, Kazunari Ohgaki, "Phase Behavior for Carbon Dioxide+Cyclopentane Derivative Mixed Hydrate Systems", *Properties and Phase Equilibria for Product and Process Design 2013*, I-47, Puelto Iguazu, Argentina, May 26–30, 2013, Poster Presentation.

[6] ○Yuuki Matsumoto, R. Gary Grim, Takeshi Sugahara, Kazunari Ohgaki, E. Dendy Sloan, Carolyn A. Koh, Amadeu K. Sum, "Increasing the Energy Storage Capacity of Clathrate Hydrates with Hydrogen and Methane", *Properties and Phase Equilibria for Product and Process Design 2013*, I-108, Puelto Iguazu, Argentina, May 26–30, 2013, Poster Presentation.

[7] ○Yuuki Matsumoto, Yoshito Katsuta, Tatsuya Bando, Fumitaka Kamo, Sumihiro Suzuki, Takashi Makino, Takeshi Sugahara, Kazunari Ohgaki, "High-Pressure Phase Equilibria of Structure-H Hydrate Systems Enclathrating Methane and Large Guest Species", *13th International Conference on the Physics and Chemistry of Ice 2014*, Hanover, New Hampshire, United States of America, March 17–20, 2014, Oral Presentation.

[8] ○Takeshi Sugahara, Yuuya Fujisawa, Akio Nishikawa, Kazuma Kitamura, Takahiro Yamazaki, Yuuki Matsumoto, Kazunari Ohgaki, "Experimental Observation of Competitive Occupancy into the Cages of Structure-II Hydrates during H_2 Enclathration", *13th International Conference on the Physics and Chemistry of Ice 2014*, Hanover, New Hampshire, United States of America, March 17–20, 2014, Poster Presentation.

[9] Yuki Matsumoto, ○R. Gary Grim, Naveed M. Khan, Takeshi Sugahara, Kazunari Ohgaki, E. Dendy Sloan, Carolyn A. Koh, Amadeu K. Sum, "Investigating the Thermodynamic Properties of Gas Hydrates Including Hydrogen and Methane", *8th International Conference on Gas Hydrate*, Beijing, China, July 28–August 1, 2014, Poster Presentation.

Acknowledgements

First of all, I really appreciate Professor Yasunori Okano (Division of Chemical Engineering, Department of Materials Engineering Science, Graduate School of Engineering Science, Osaka University) for my studies. Unless his helpful advice and precise guidance, this thesis could not be completed. I would like to express my gratitude to Professor Michio Matsumura (Research Center for Solar Energy Chemistry, Osaka University) and Professor Norikazu Nishiyama (Division of Chemical Engineering, Department of Materials Engineering Science, Graduate School of Engineering Science, Osaka University) for their helpful suggestions and comments.

I express heartily my special thanks to Emeritus Professor Kazunari Ohgaki, Associate Professor Hiroshi Sato, and Assistant Professor Takeshi Sugahara (Division of Chemical Engineering, Department of Materials Engineering Science, Graduate School of Engineering Science, Osaka University) for their supervisions. They have given numerous advice, and a great deal of warm encouragements, which were enormous helps to my student and private life, and indispensable to complete the present studies and this thesis.

I would like to take this opportunity to express my thanks to Associate Professor Daisuke Kodama (College of Engineering, Nihon University), Dr. Takashi Makino (National Institute of Advanced Industrial Science and Technology), Dr. Shunsuke Hashimoto (Toyota Central R&D Labs., Inc.), Dr. Keisuke Sugahara (Research Center for Solar Energy Chemistry, Osaka University), Assistant Professor Kei Takeya (Department of Electrical Engineering and Computer Science, Graduate School of Engineering, Nagoya University), and Assistant Professor Atsushi Tani (Department of Earth and Space Science, Graduate School of Science, Osaka University) for their valuable advice and supports.

I express my thanks to Dr. Masato Moritoki, Dr. Masamitsu Matsumoto, and Mr. Makoto Nagasawa for their technical support concerning experimental apparatus. I am thankful to Mr. Masao Kawashima for his kind assistance in the GHAS (Gas Hydrate Analyzing System) room.

Thanks are made to all of colleagues in Environmental Physical Chemistry Group. They are Dr. Takaaki Tsuda, Mr. Khanh Quoc Nguyen, Mr. Naohiro Kobayashi, Ms. Ayumi Sakai, Mr. Shingo Amano, Mr. Takahiro Kinoshita, Mr. Yasuhiro Joden, Mr. Kenji Takato, Mr. Tatsuya Inoue, Mr. Naoto Ohtsubo, Ms. Yume Takahashi, Mr. Yuuya Fujisawa, Mr. Shin-ichiro Asahara, Mr. Sunn Ki Kim, Ms. Yukiko Koumoto, Mr. Hiroya Sakamoto, Mr. Akio Nishikawa, Mr. Shotaro Ogino, Mr. Takashi Kitajima, Mr. Tomohiro Tanabe, Mr. Yusuke Urabe, Mr. Kazuma Kitamura, Mr. Takahiro Yamazaki, Mr. Yuta Hirosaki, Ms. Hiroko Suzuki, Mr. Atsushi Date, Mr. Takashi Fujimoto, and Mr.

Yoshito Washino. Especially, I express my special thanks to the members of Phase Equilibrium Group, Mr. Yuuki Matsui, Mr. Hiroshi Miyauchi, Mr. Kenjiro Yasuda, Ms. Aki Endo, Mr. Seung An Choi, Mr. Sumihiro Suzuki, Mr. Yoshito Katsuta, Mr. Tatsuya Bando, Mr. Hiroaki Matsukawa, and Mr. Fumitaka Kamo for their insightful comments and suggestions, kind supports and encouragements.

I really appreciate Emeritus Professor E. Dendy Sloan, Professor Carolyn A. Koh, and Associate Professor Amadeu K. Sum (Center for Hydrate Research, Chemical Engineering Department, Colorado School of Mines) for much helpful support when I stayed in U.S. Mr. R. Gary Grim and many other students in Colorado School of Mines were really kind and helped my life and research in U.S.

The present study was partially supported by KAKENHI, Grant-in-Aid for JSPS Fellows (25·1430). I also acknowledge financial support "Osaka University Scholarship for Short-Term Overseas Research Activities" and Global COE (center of excellence) Program "Global Education and Research Center for Bio-Environmental Chemistry" of Osaka University.

Finally, I wish to express my gratitude to my parents, Yoshitada Matsumoto and Hisako Matsumoto, to my sister, Wakako Matsumoto, to my grandparents, Kazuo Matsumoto, Asako Matsumoto, Yukio Miura, and Yoshiko Miura for their hearty encouragements and continuous supports.

March 2014

Yuuki Matsumoto

Environmental Physical Chemistry Group,
Division of Chemical Engineering,
Department of Materials Engineering Science,
Graduate School of Engineering Science,
Osaka University